Bibliography

Solomon L. *Elasticité linéaire.* Masson, Paris (1966).
Schreiber E. & Anderson O. *Elastic constants and their measurements.* McGraw Hill, New York (1973).
Tsai S. W. & Thomas Han. *Introduction to composite materials.* Technomic (1980).
Massonet C. & Cescotto S. *Mécanique des matériaux.* Sciences et lettres, Liège (1982).
Courbon J. *Calcul des structures.* Dunod, Paris (1972).
Zienkiewicz O. C. The finite element method in engineering science, McGraw Hill, New York, 1st edn (1967)–3rd edn (1977).
Dhatt G. & Touzot G. *Une présentation de la méthode des éléments finis.* Maloine, Paris (1981).
Salençon J. *Viscoélasticité.* Presses de l'Ecole Nationale des Ponts et Chaussées, Paris (1983).
Findley W. N., Lai J. S. & Onaran K. *Creep and relaxation of non linear visco-elastic materials.* North Holland Publishing Company, Amsterdam (1976).

5

PLASTICITY

Un modèle devient une loi ... ou, sombre dans l'oubli!

This chapter deals with the phenomenological and mathematical modelling of plastic solids according to the schematic classification of Chapter 3: rigid, perfectly plastic solid; elastic, perfectly plastic solid; elastoplastic solid. It can be said that the first scientific work concerning plasticity goes back to Tresca's memoir in 1864 on the maximum shear stress criterion. Although the isotropic flow law was formulated as early as 1871 by St. Venant and Levy, its applications to structures had to wait until about 1950 when limit theorems were discovered. Since 1970 the availability of fast and large computers has led to application of the theory to practical problems. Proportional loading (where principal stresses do not rotate at any point of a structure) provides a large field of application for theories based on isotropic hardening.

Hardening, as we have seen in Chapter 1, is almost always anisotropic. This aspect of plasticity must be considered as soon as the loading is no longer proportional and especially under cyclic loads. Prager, around 1950, gave the first simple formulation of anisotropy, namely kinematic hardening, on which most of the present theories are based.

5.1 Domain of validity and use

The theory of plasticity is the mathematical theory of time-independent irreversible deformations; some comments on its physical nature were given in Chapter 1.

> For metals and alloys it involves mainly the movement of dislocations without the influence of viscous phenomena or the presence of decohesion which damages the matter. Its domain of validity is therefore restricted by the following two limitations:

low temperature usage: a very rough convention is to limit the temperature of usage to one-quarter of the absolute melting temperature of the material under consideration,
nondamaging loads: for monotonic loads the strains must remain lower than approximately half of those at fracture. For alternating loads the limit depends on the condition of stabilization. Cyclic plasticity is applicable without modification as long as the number of cycles remains below the number which corresponds to stabilization (half life).

For soils the limitation is essentially due to the occurrence of slip surfaces caused by instability.

For polymers and wood, the irreversible deformations are more appropriately accounted for by viscoplasticity.

For concrete, the irreversible deformations are mainly due to microcracks, and hence a model based on coupling between elasticity and damage may be preferable.

These limitations only give indications. In a viscoplasticity problem for example, if it is known *a priori* that the deformation process takes place with a quasi-uniform strain rate field $\dot{\varepsilon}(M)$, it is possible to solve this problem by the theory of time-independent plasticity provided that the constitutive equation is identified by hardening experiments conducted at the considered strain rate $\dot{\varepsilon}$ (and at the considered temperature). In contrast, the relaxation of steel at room temperature (evolving as a function of time) can only be accounted for by an elastoviscoplastic theory.

The theory of plasticity is used to calculate permanent deformations of structures, to predict the plastic collapse of structures, to investigate stability (of a land-fill for example), to calculate forces required in metal forming operations, etc. We can also use the scheme of time-independent plasticity for metals at high temperature to discover asymptotic states which correspond to fixed loads or very high speeds. Another aspect of plasticity consists in its coupling with damage. This is studied in Chapter 7.

5.2 Phenomenological aspects

In this section we have collected the main results directly originating from experiments supposedly conducted on the considered material in the reference state of its use. To interpret these experiments, elementary models are used. Experimental results concerning particular effects (like cyclic hardening or softening, ratchetting, relaxation of mean stress) are mentioned in Chapter 3.

5.2.1 *Uniaxial behaviour*

The hardening curve in tension–compression completely characterizes the uniaxial behaviour. Two possible types of curves (with discontinuous and continuous tangent moduli) are shown in Fig. 5.1.

Elastic limit

This is the stress above which irreversible deformations appear. Detection of this limit presents an experimental problem since it depends on the precision of the strain measuring device used. In the interest of an objective measure, we adopt a conventional definition of this limit.

The conventional elastic limit is the stress which corresponds to the occurrence of a specified amount of permanent strain.

For quality control of materials, a conventional value of permanent strain equal to 0.2% is commonly used.

If the above value of permanent strain is too high (of the same order of magnitude as the accompanying elastic strain) a more refined conventional value of 0.02% permanent strain is sometimes adopted.

Another method consists in applying the convention to the ratio of the acceptable permanent strain to the accompanying elastic strain. For example

$$\sigma_{Y0,1e} = \sigma_Y(\varepsilon_p/\varepsilon_e = 10\%)$$

corresponds to a permanent strain which is ten times smaller than the elastic strain.

Except for mild steel (with a plateau), the practical determination of the elastic limit is always conventional. Even if the concept of elastic domain is perfectly justifiable at the theoretical level, it is essential to bear in mind the fact that its measure depends on some adopted convention.

Plastic flow, hardening and threshold

The decoupling of elastic and plastic effects can be justified on the basis of the physics and chemistry of solids, thermodynamics, and phenomenological experiments as follows:

The total strain may be partitioned or separated into the reversible or elastic strain ε_e and the irreversible or inelastic strain ε_p without prejudging the nature of the latter strain which can be further

Fig. 5.1. Hardening curves: (*a*) mild steel; (*b*) A316 stainless steel.

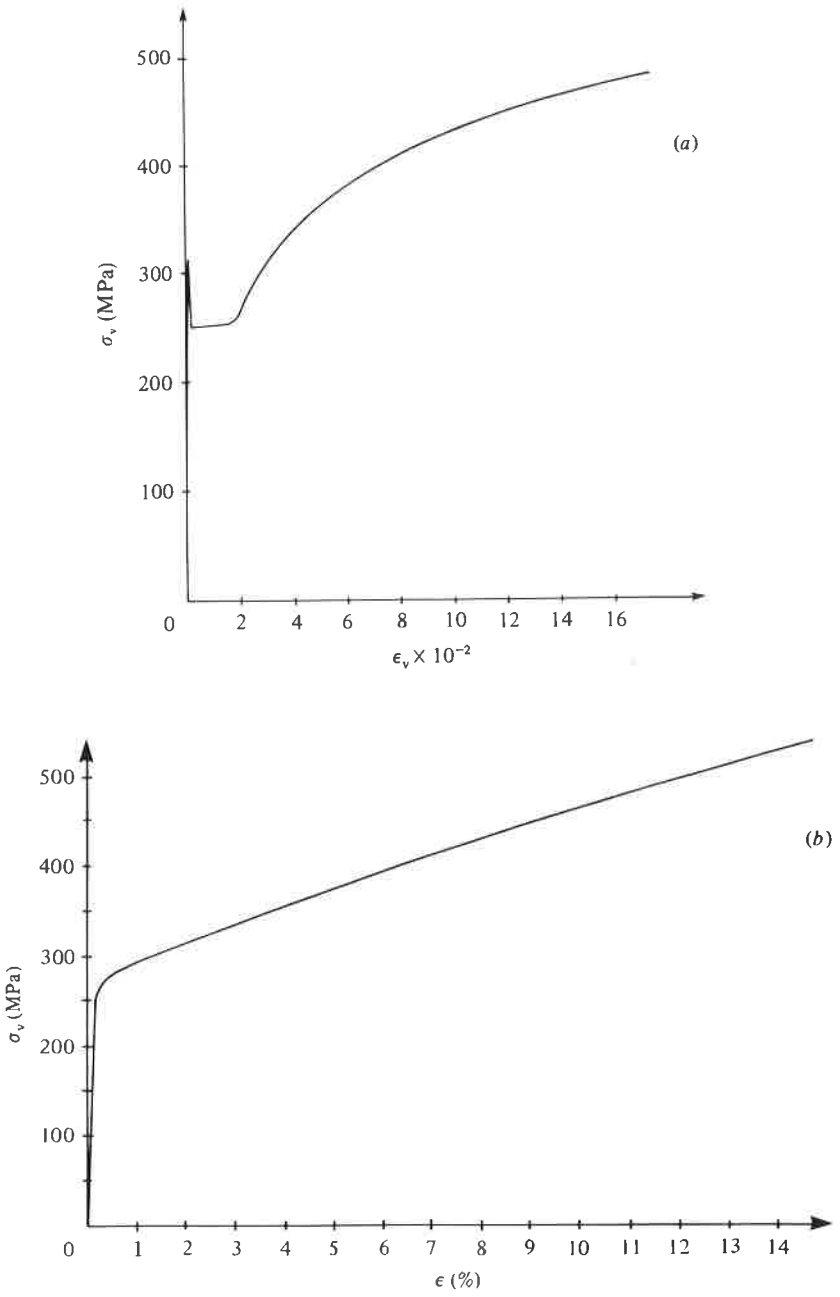

separated into anelastic, plastic, viscoplastic, etc. This partition is justified by the physics of the phenomena (cf. Chapter 3) as elastic deformation schematically corresponds to a variation in the interatomic distances without changes of place, while plastic (or inelastic) deformation implies 'slip' movements with modification of interatomic bonds. Within the framework of elastoplasticity we will therefore use

$$\varepsilon = \varepsilon_e + \varepsilon_p.$$

There exist decoupled constitutive relations for ε_e and ε_p

$$\begin{cases} \varepsilon_e = A(\sigma) & \forall \sigma \\ \varepsilon_p = g(\sigma) & \text{for} \quad |\sigma| \geqslant \sigma_Y \\ \varepsilon_p = 0 & \text{if} \quad |\sigma| < \sigma_Y \end{cases}$$

with the latter relation being valid only in the case of continuous plastic flow (without unloading). Fig. 5.2 illustrates these two properties and shows in particular that even within a large range of

Fig. 5.2. Hardening curves with unloading/reloading: 2024 age-hardened aluminium alloy, $T = 20\,^{\circ}\mathrm{C}$.

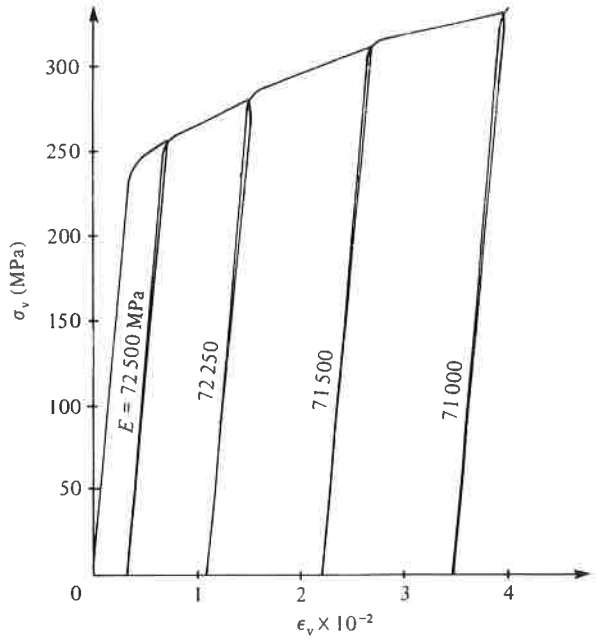

plastic strains the elastic modulus is little affected by the plastic flow.

Perfect plastic flow without hardening corresponds to the case in which the stress remains constant during the flow; this is exhibited by mild steel in the flat (plateau) zone. The hardening effect due to plastic flow manifests itself in two ways:

the flow occurs only if the stress increases, and
the elastic limit increases during the flow; this is verified by unloading and then reloading as in the examples of Fig. 5.2.

On the physical level, hardening is due to an increase in the dislocation density: the dislocations have a tendency to interlock and to block each other. In the first approximation, the increase in the elastic limit follows the increase in the stress, and it is this approximation which constitutes the theoretical basis of classical plasticity. Thus, for monotonic loading, the current limit of elasticity, also called the plasticity threshold or the yield stress, is equal to the highest value of the stress previously attained. For a material with positive hardening, $d\sigma/d\varepsilon_p > 0$, the 'natural' elastic limit σ_Y is the smallest value of the yield stress (which is a function of the history of plastic deformations).

Any point on a monotonic hardening curve can therefore be considered as a representative point of the plasticity threshold, and the characteristic hardening law may be written as

$$\sigma_s = g^{-1}(\varepsilon_p).$$

The plastic flow occurs only if $\sigma = \sigma_s$, i.e.

$$\sigma < \sigma_s \rightarrow \dot{\varepsilon}_p = 0$$
$$\sigma = \sigma_s \rightarrow \exists\, \dot{\varepsilon}_p \neq 0.$$

A number of analytic expressions have been proposed to model the hardening function g; we will use the one resulting from a calculation which is based on dislocation theory and which shows that the yield stress is proportional to the square root of the density of dislocations ρ_d:

$$\sigma_s = \kappa b \rho_d^{1/2}.$$

In reality, the density of dislocations is never zero. Hence, letting ρ_{d_0} be the dislocation density in the initial state corresponding to the elastic limit σ_Y, we may write

$$\sigma_s = \sigma_Y + \kappa b(\rho_d - \rho_{d_0})^{1/2}.$$

In terms of macroscopic strains, we may, in analogy with the above relation, write

$$\sigma_s = \sigma_Y + K_Y \varepsilon_p^{1/M_Y}.$$

This last relation, generally called the Ramberg–Osgood equation, can be

Fig. 5.3. Identification of the characteristic hardening coefficients of 316 L steel at room temperature.

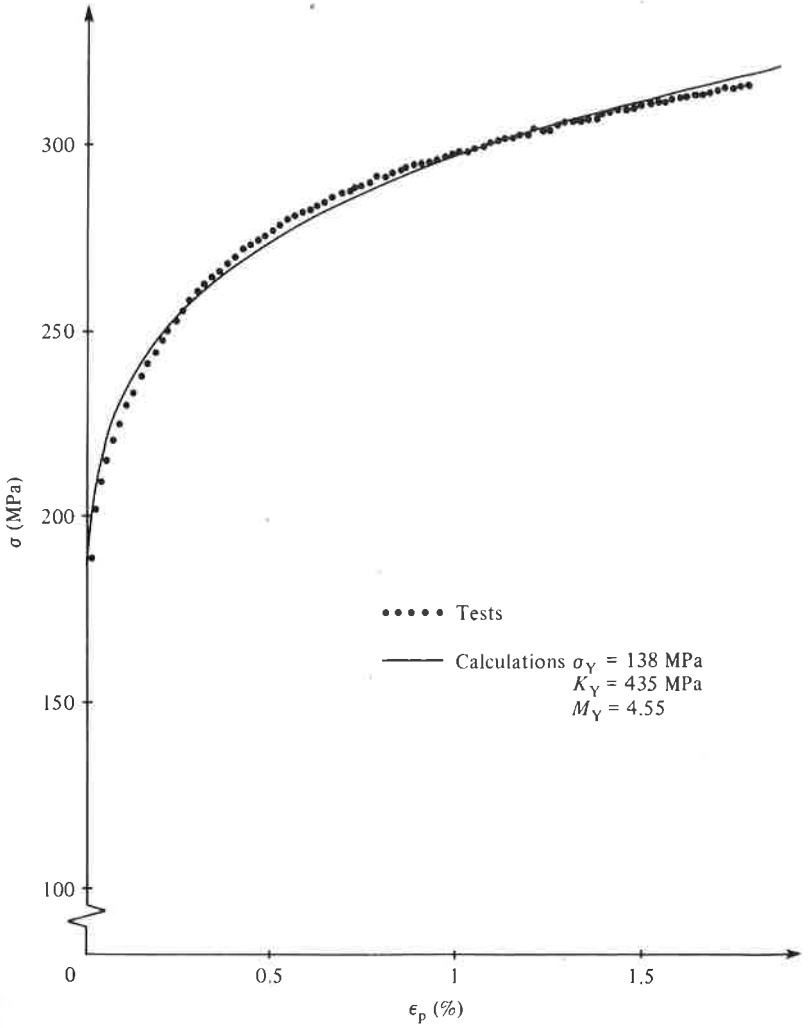

easily inverted to give†

$$\varepsilon_p = g(\sigma_s) = \left\langle \frac{\sigma_s - \sigma_Y}{K_Y} \right\rangle^{M_Y}$$

where σ_Y is the elastic limit, K_Y is the coefficient of plastic resistance, M_Y is the hardening exponent and the angular brackets have the following meaning: $\langle x \rangle = x$ if $x > 0$ and $\langle x \rangle = 0$ if $x \leqslant 0$. The identification of this expression, i.e., the determination of the values of the coefficient σ_Y, K_Y and M_Y for a particular material is done through hardening test results. After determining σ_Y from the hardening curve, the straight line closest to the experimental points, plotted as $\ln(\sigma_s - \sigma_Y)$ versus ε_p, gives K_Y and M_Y according to the following straight line equation:

$$\ln(\sigma_s - \sigma_Y) = \ln K_Y + \frac{1}{M_Y} \ln \varepsilon_p.$$

An example is given in Fig. 5.3. Chapter 3 provides an outline of numerical identification methods for non-linear equations such as this one.

The hardening law $\varepsilon_p = g(\sigma_s)$ is written in terms of nominal values of the variables if it is to be used for small strains, but should be written in terms of their true values ($\sigma_v = \sigma(1 + \varepsilon)$, $\varepsilon_v = \ln(1 + \varepsilon)$) if used for 'large strains'.

Constitutive equations

Perfectly plastic solids

In this case the threshold σ_s is constant and is equal in tension and compression. Depending on whether the model has to be used to calculate

Fig. 5.4. Elastic limit and ultimate stress.

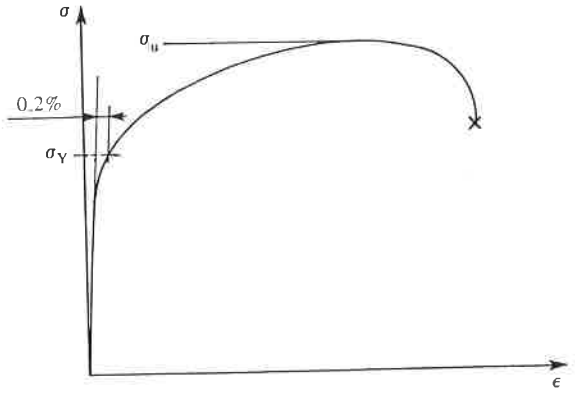

the lower or upper bounds (see Section 6.2), the threshold is chosen as equal to the conventional elastic limit σ_Y or the ultimate stress σ_u – the maximum stress attained in a hardening test (Fig. 5.4). The constitutive model is the following:

- $|\sigma| < \sigma_s \rightarrow \varepsilon = \varepsilon_e = \begin{cases} 0 & \text{(rigid body case)} \\ \sigma/E & \text{(perfect elastic body case)} \end{cases}$
- $|\sigma| = \sigma_s \rightarrow \varepsilon = \varepsilon_e +$ arbitrary ε_p of the same sign as σ.

Hardening plastic solids

The complete model of an initially isotropic elastoplastic solid subjected to monotonic uniaxial loading is the following:

- $\varepsilon = \varepsilon_e + \varepsilon_p$,
- $\varepsilon_e = \sigma/E$,
- $\varepsilon_p = \left\langle \frac{|\sigma| - \sigma_Y}{K_Y} \right\rangle^{M_Y} \mathrm{Sgn}(\sigma)$ with $\sigma = \sigma_s$.

In the case of a rigid-plastic hardening solid, two consistent hypotheses consist in neglecting the elastic strains altogether and taking the elastic limit to be equal to zero. The model is then reduced to

- $\varepsilon = \varepsilon_p = (|\sigma|/K)^M \mathrm{Sgn}(\sigma)$.

The above expressions constitute the practical ways to represent the hardening law, but other expressions, or the tension curve itself, defined point by point, can be used. Typical values of the coefficients σ_Y, K_Y, M_Y and K and M for different materials are given in Table 5.1 together with the range of their validity.

Cyclic loadings

It is interesting to relate the (peak to peak) strain range $\Delta\varepsilon$ directly to the (peak to peak) stress range $\Delta\sigma$ of stabilized cycles as defined in Chapter 3 for periodic loads.

Taking the example of a cycle symmetric with respect to the origin, such as that shown in Fig. 5.5, it is easy to express $\Delta\varepsilon_p$ as function of $\Delta\sigma$ according to the monotonic hardening law $\varepsilon_p = g(\sigma)$:

$$\Delta\varepsilon_p/2 = g(\Delta\sigma/2).$$

This corresponds to Masing's rule which assumes a homothetic transformation of ratio 2 between the initial tension curve OA and the alternating half

Table 5.1. *Plasticity characteristics*

Material	T°C	Monotonic loading σ_Y MPa	σ_u MPa	M	K	M_Y	K_Y	Cyclic loading M_c	K_c
35 NCD 16 steel	20	1200	2000	10.5	2990	3.1	3340	6.8	6230
IN 100 alloy	20	650	875	33	960	5.6	655		
IN 100 alloy	700	600	925	18	1150	6.8	354	3.25	9925
316 L steel	20	133				4.5	435	10.50	811
UDIMET 700 alloy	20	700	1250	17	1374	4.8	900		
TA 6 V alloy	350	300	690	10.2	940	4.3	884	11.00	1583
INCO 718 alloy	550	500	1180	12.2	1657	5.2	1658	11.7	2585
COTAC 744	1000			4.2	2206				
X20 CrV 12.1	350			9.6	853			7.25	951
X20 CrV 12.1	600							7.9	554
IMI 550	20			28.2	1176			11.8	1366
COBALT VO 795	20							2.4	5850
Structural steel (0.14% C–0.35 Si; 1.36 Mn–0.24 Cr)	20							5.7	2360
NIMONIC 90	20							7.3	3940

The values of the coefficients listed in Table 5.1 are with reference to the simple model studied in Section 5.2.1.

BA which corresponds to the positive flow (homothetic of ratio -2 for the alternate AB).

In fact the hardening function in the cyclic behaviour model is different from that in the monotonic model because of the consolidation effects induced by the cyclic loading. It is therefore preferable to identify this relation between the ranges from the cyclic tension–compression tests directly:

$$\Delta\varepsilon_p = g_c(\Delta\sigma)$$

where the function g_c may be modelled by

$$\Delta\varepsilon_p = (\Delta\sigma/K_c)^{M_c}.$$

This expression defines the 'stabilized cyclic hardening curve', i.e., the peaks of stabilized cycles ($\sigma_{Max}, \varepsilon_{pMax}$) on the ($\sigma, \varepsilon_p$) graph for centred cycles such as those of Fig. 5.6(a) and (b).

This cyclic hardening curve can be located 'above' (cyclic hardening) or 'below' (cyclic softening) the monotonic hardening curve. The identification of its expression in terms of stress and strain variables presents a problem linked to the history of deformation. As a matter of fact the curve may not be exactly the same if it were obtained by continuous variation as it would be if it were obtained by imposing finite increments in stress or strain ranges, or if one or several specimens are used.

To identify a simple relation between the stress and strain ranges and to verify the uniqueness of the cyclic hardening curve, several methods can be used:

Fig. 5.5. Stabilized cycle.

Fig. 5.6. Cyclic hardening curve: 30 NCD 16 nickel–chromium steel (after Lieurade).

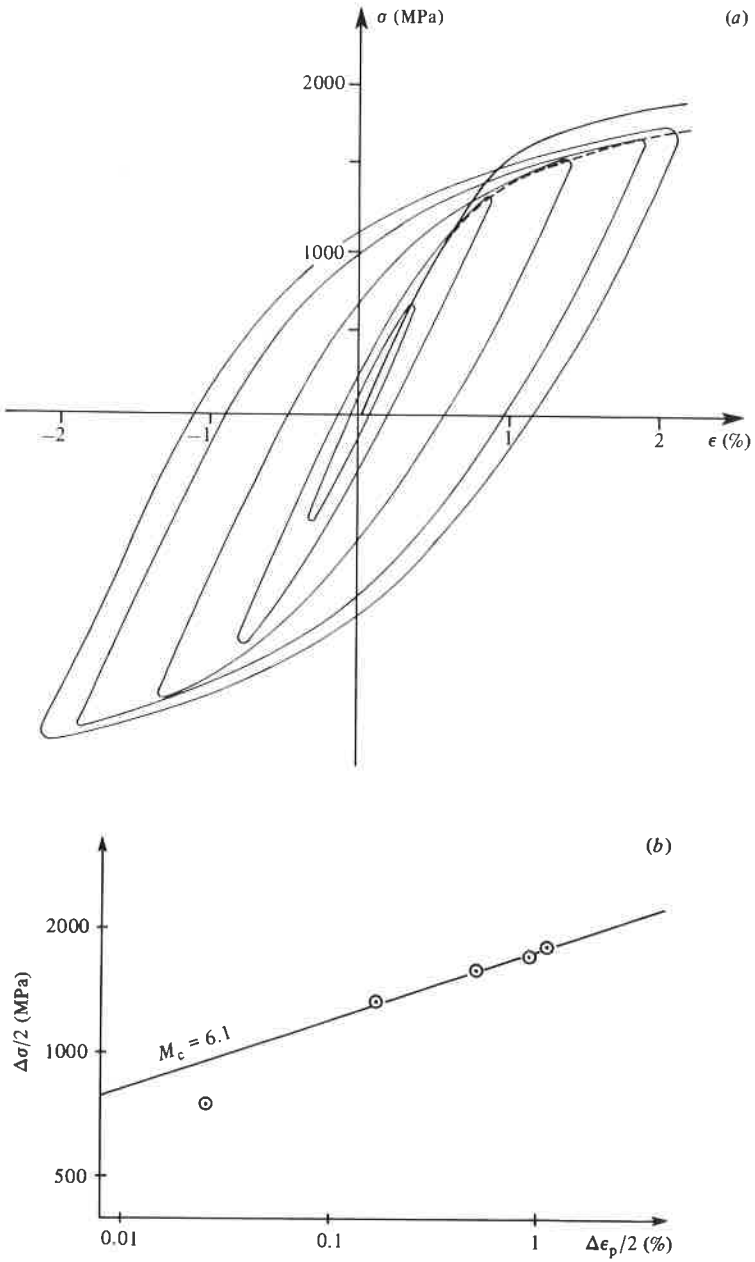

We may compare the curves of amplitudes $(\Delta\sigma, \Delta\varepsilon)$ with each of the hysterisis loops adjusted to the lower peak $(\sigma - \sigma_m, \varepsilon - \varepsilon_m)$. If all these curves approximately coincide (Masing's rule), we may conclude that there are no parasitic effects (e.g., Fig. 5.7).

We may compare the cyclic hardening curves obtained by using one specimen per level with those obtained by the incremental test method which consists in subjecting one specimen only to deformation cycles of successively increasing and then decreasing amplitudes until stabilization is achieved (e.g., Fig. 5.8).

We may perform tests in which the strains are varied stepwise, first increasing and then decreasing (e.g., Fig. 5.9 for 316 L steel at 20 °C). After stabilization of hardening at the lowest level, a resumption of hardening at a higher level is an indication of the dependence between the cyclic hardening and the strain amplitude. During decreasing levels the memory effect of the previous load is clearly established by comparison of loops obtained for the same strain level ($\pm 1\%$ and $\pm 1.5\%$ in the example under consideration).

For the identification of the cyclic hardening curve, we recommend this last type of test where the strain is varied in steps; it generally provides sufficiently detailed indications of the uniqueness of this curve with only

Fig. 5.7. Verification of Masing's rule – $TiAl_6V_4$ titanium alloy.

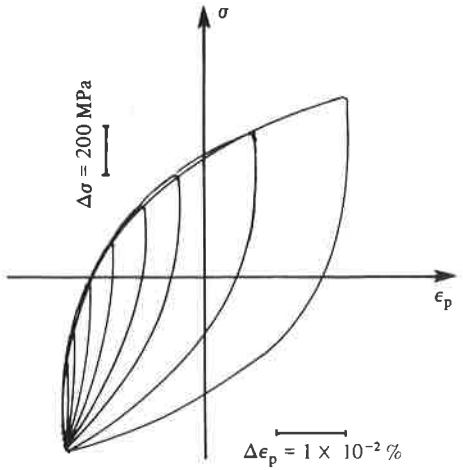

Fig. 5.8. Cyclic hardening curves obtained by different methods: (*a*) evolution of stress and imposed strain; (*b*) NIMONIC 90 alloy; (*c*) 35 CD 4 chromium steel, (*d*) 316 steel (after Lieurade).

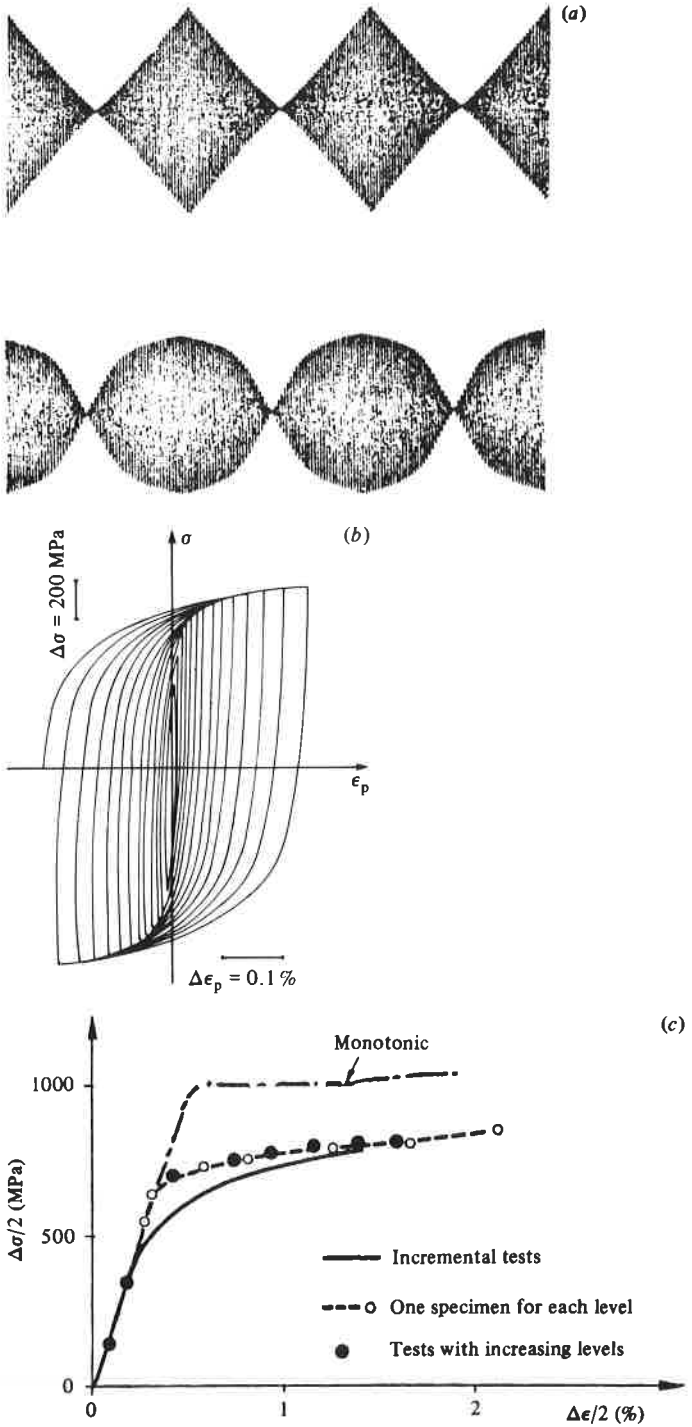

Fig. 5.9. Test with increasing and then decreasing steps, 316 L steel; successive strain ranges (2%, 3%, 4%, 5%, 6%, 2%, 3%).

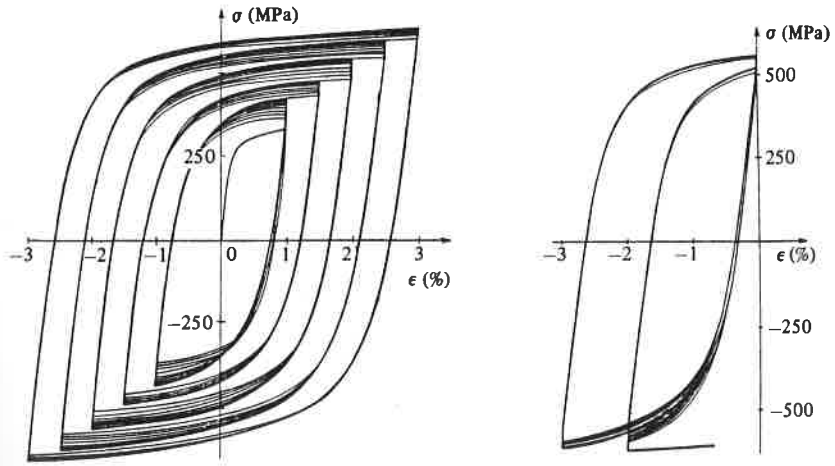

one specimen. On the other hand, when the uniqueness is not evident, the test may be used to define a more complex model which takes into account the influence of the strain path such as the one encountered in Section 5.4.4. Five increasing steps and three decreasing steps in every twenty cycles are usually sufficient.

5.2.2 *Multiaxial plasticity criteria*

The yield stress of uniaxial plasticity defines the elastic domain in uniaxial stress space (Fig. 5.10). The generalization of this concept to the multiaxial case is the yield criterion. It defines in the stress space of three or six dimensions a domain within which any stress variation generates only variations of elastic strains.

The simplest way to show the existence of this domain in a two-dimensional space is to use the results of tension (or compression)–torsion tests on thin tubes. Successive (proportionally increasing) radial loads, defined by axial force $\vec{F}$ and twisting couple $\vec{C} = \alpha\vec{F}$, are applied to a sample. Each radial loading is identified by a constant value of the scalar α ($-\infty < \alpha < +\infty$). The values of $\vec{F}$ and $\vec{C}$ at which plastic strains become noticeable are recorded; these offset strains lie between 10^{-6} and 10^{-4} depending upon the precision of the apparatus.

Fig. 5.10. One-dimensional elastic domain.

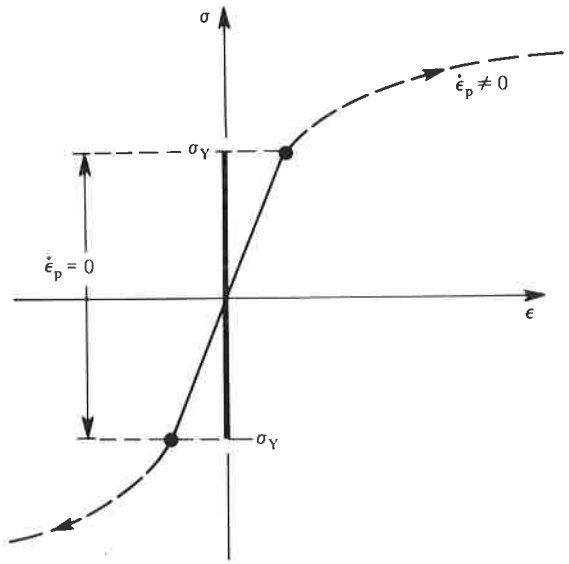

The curve obtained by plotting the normal stress σ_{11} and the corresponding tangential stress σ_{12} at plasticity thresholds then defines the boundary of the elastic domain. Fig. 5.11 shows typical test results for the same material: nonhardened (A), prehardened by a tensile load (B), and prehardened by a tensile load and a shear load (C).

The mathematical modelling of these domains and of their evolution has been the object of a number of propositions. At present we restrict ourselves to the essential concepts most commonly used; however, a more detailed discussion of the three-dimensional behaviour will be taken up in Section 5.4.

A preliminary remark must now be made regarding the terminology used in connection with isotropic or anisotropic yield and hardening criteria. In a first understanding, the terms isotropic or anisotropic yield criteria are applicable to a given state (without modification of hardening). On the other hand, hardening implies the idea of transformation. We therefore speak of isotropic hardening when the transformation is a homothetic transformation (dilatation of the criterion), of kinematic hardening for the translation of the criterion, of combined isotropic–kinematic hardening, and finally of anisotropic hardening when the transformation is arbitrary.

Fig. 5.11. Elastic domain in terms of normal and shear stresses. Tension–torsion tests on tubular specimens: 2024 aluminium alloy (after Rousset).

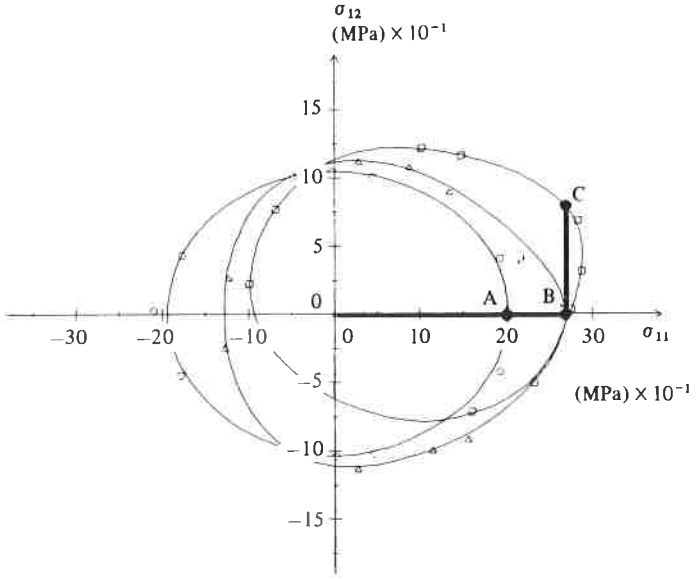

We can thus speak of 'isotropic' hardening of an initially anisotropic material.

Isotropic criteria

These criteria correspond to isotropic-hardening states. The equation of the elastic domain boundary includes, *a priori*, all the components of the stress tensor and a hardening variable which as discussed in Chapter 3 is a scalar variable in the case of isotropic hardening. Choosing this last variable to be the yield stress σ_s in simple tension, the criterion may be expressed as

$$f(\sigma_{ij}, \sigma_s) = 0.$$

Isotropy requires that the boundary of the domain be invariant under a change of axes. Therefore, the function f depends only on the three invariants of the stress tensor (invariants defined in Chapter 2):

$$f(\sigma_I, \sigma_{II}, \sigma_{III}, \sigma_s) = 0.$$

Metals generally exhibit plastic incompressibility and yield-independence with respect to hydrostatic stress. It is then sufficient to use the deviatoric stress tensor:

$$\boldsymbol{\sigma}' = \sigma - \tfrac{1}{3}\sigma_1 \mathbf{1}.$$

In the isotropic case, we may use the invariants of $\boldsymbol{\sigma}'$, namely $s_{II} = \frac{1}{2}\mathrm{Tr}(\boldsymbol{\sigma}'^2)$ and $s_{III} = \frac{1}{3}\mathrm{Tr}(\boldsymbol{\sigma}'^3)$. Therefore, the relation

$$f(s_{II}, s_{III}, \sigma_s) = 0$$

is the general expression of the isotropic criteria of incompressible plasticity. In the space of principal stresses σ_1, σ_2, σ_3, the boundary is represented by a cylinder with its axis equally inclined to the reference axes. Note that instead of the invariants s_{II} and s_{III} of the deviator, the associated homogeneous invariants can also be used.

$$J_2(\boldsymbol{\sigma}) = (3s_{II})^{1/2} = (\tfrac{2}{3}\sigma'_{ij}\sigma'_{ij})^{1/2}$$
$$J_3(\boldsymbol{\sigma}) = (\tfrac{27}{2}s_{III})^{1/3} = (\tfrac{9}{2}\sigma'_{ij}\sigma'_{jk}\sigma'_{ki})^{1/3}.$$

The von Mises criterion

Plastic deformation of metals results from slip, i.e., intercrystalline shear governed by the tangential stresses. According to the von Mises criterion, the plasticity threshold is linked to the elastic shear energy. This amounts to neglecting the influence of the third invariant and taking a linear expression for the function f.

The elastic strain energy

$$w_e = \int_0^{\boldsymbol{\varepsilon}^e} \boldsymbol{\sigma} : \mathrm{d}\boldsymbol{\varepsilon}^e$$

can be written as the sum of a shear energy w_d and an energy of volumetric deformation

$$w_e = \int_0^{\boldsymbol{\varepsilon}^e} [\boldsymbol{\sigma}' + \tfrac{1}{3}\mathrm{Tr}(\boldsymbol{\sigma})\mathbf{1}] : [\mathrm{d}\boldsymbol{\varepsilon}^e + \tfrac{1}{3}\mathrm{Tr}(\mathrm{d}\boldsymbol{\varepsilon}^e)\mathbf{1}]$$

$$w_e = \int_0^{\boldsymbol{\varepsilon}^e} \boldsymbol{\sigma}' : \mathrm{d}\boldsymbol{\varepsilon}^{e'} + \int_0^{\mathrm{Tr}(\boldsymbol{\varepsilon}^e)} \tfrac{1}{3}\mathrm{Tr}(\boldsymbol{\sigma})\,\mathrm{Tr}(\mathrm{d}\boldsymbol{\varepsilon}^e).$$

By introducing the linear elastic law

$$\mathrm{d}\boldsymbol{\varepsilon}^{e'} = (1/2\mu)\,\mathrm{d}\boldsymbol{\sigma}'$$

in the expression for shear energy $w_d = \int_0^{\boldsymbol{\varepsilon}^e} \boldsymbol{\sigma}' : \mathrm{d}\boldsymbol{\varepsilon}^{e'}$, we obtain

$$w_d = \int_0^{\boldsymbol{\sigma}'} (1/2\mu)\boldsymbol{\sigma}' : \mathrm{d}\boldsymbol{\sigma}' = (1/4\mu)\boldsymbol{\sigma}' : \boldsymbol{\sigma}'.$$

We now equate this energy of a three-dimensional state of stress to that of a one-dimensional state of stress in pure tension at the yield stress $\sigma = \sigma_s$. Since

$$[\sigma] = \begin{bmatrix} \sigma_s & 0 & 0 \\ 0 & 0 & 0 \\ 0 & 0 & 0 \end{bmatrix} \rightarrow \sigma' = \begin{bmatrix} \frac{2}{3}\sigma_s & 0 & 0 \\ 0 & -\frac{1}{3}\sigma_s & 0 \\ 0 & 0 & -\frac{1}{3}\sigma_s \end{bmatrix}$$

we obtain

$$(1/4\mu)\boldsymbol{\sigma}' : \boldsymbol{\sigma}' = (1/6\mu)\sigma_s^2$$

so that

$$\tfrac{1}{2}\boldsymbol{\sigma}' : \boldsymbol{\sigma}' - \tfrac{1}{3}\sigma_s^2 = 0.$$

The function $f(s_{II}, \sigma_s) = 0$ is therefore expressed by

$$s_{II} - \tfrac{1}{3}\sigma_s^2 = 0$$

or, with the equivalent stress $\sigma_{eq} = J_2(\boldsymbol{\sigma}) = (3s_{II})^{1/2} = (\frac{3}{2}\boldsymbol{\sigma}' : \boldsymbol{\sigma}')^{1/2}$

- $f = \sigma_{eq} - \sigma_s = 0.$

Any three-dimensional state of stress for which $\sigma_{eq} = \sigma_s$ is a state of complex stress, equivalent in the von Mises sense, to a one-dimensional state defined by the yield stress σ_s. In particular, the initial yield criterion is

expressed by

$$\sigma_{eq} - \sigma_Y = 0.$$

The expanded expressions of the von Mises yield criterion are:

in the six-dimensional stress space:

$$\tfrac{1}{2}[(\sigma_{11}-\sigma_{22})^2+(\sigma_{22}-\sigma_{33})^2+(\sigma_{33}-\sigma_{11})^2 + 6(\sigma_{12}^2+\sigma_{23}^2+\sigma_{13}^2)] - \sigma_s^2 = 0$$

in the three-dimensional principal stress space:

$$\bullet \quad \frac{1}{\sqrt{2}}[(\sigma_1-\sigma_2)^2+(\sigma_2-\sigma_3)^2+(\sigma_3-\sigma_1)^2]^{1/2} = \sigma_s.$$

This is the equation of a circular cylinder with its axis equally inclined to the three $(\sigma_1, \sigma_2, \sigma_3)$ reference axes and which has a radius $R = \sqrt{2/3}\ \sigma_s$ (Fig. 5.12).

The deviatoric plane is the plane which passes through the origin with its normal equally inclined to the three reference principal stress axes. The orthogonal projection of a point with coordinate $(\sigma_s, 0, 0)$ on this plane gives a point in Fig. 5.12 with coordinates $\sigma'_1 = \sqrt{\tfrac{2}{3}}\sigma_s$, $\sigma'_2 = \sigma'_3 = -\tfrac{1}{2}\sqrt{\tfrac{2}{3}}\sigma_s$. Conversely, the coordinates of this representative point of the uniaxial deviatoric stress tensor, are $\tfrac{2}{3}\sigma_s$, $-\tfrac{1}{3}\sigma_s$ and $-\tfrac{1}{3}\sigma_s$ with respect to the principal stress axes.

The Tresca criterion

According to this criterion, the plasticity threshold is not linked to the energy but to the shear stress: the maximum shear stress. It is expressed by:

$$\tfrac{1}{2}\operatorname*{Sup}_{i\neq j}(|\sigma_i - \sigma_j|).$$

By equating it to its value in the one-dimensional state corresponding to yielding at stress σ_s, we obtain the following expression for the criterion

$$\tfrac{1}{2}\operatorname*{Sup}_{i\neq j}(|\sigma_i - \sigma_j|) = \tfrac{1}{2}\sigma_s.$$

or

$$\bullet \quad f = \operatorname*{Sup}_{i\neq j}(|\sigma_i - \sigma_j|) - \sigma_s = 0.$$

This function can be expressed in terms of the invariants s_{II} and s_{III} of the deviatoric stress tensor. The equation below defines the set of the six planes

of the Tresca criterion.

$$f(s_{II}, s_{III}) = 4s_{II}^2 - 27s_{III}^2 - 9\sigma_s^2 s_{II}^2 + 6\sigma_s^4 s_{II} - \sigma_s^6 = 0.$$

The initial yield according to the Tresca criterion is expressed by

$$\operatorname*{Sup}_{i\neq j}(|\sigma_i - \sigma_j|) - \sigma_Y = 0.$$

Fig. 5.12. Geometric representation of the von Mises criterion on the deviatoric plane.

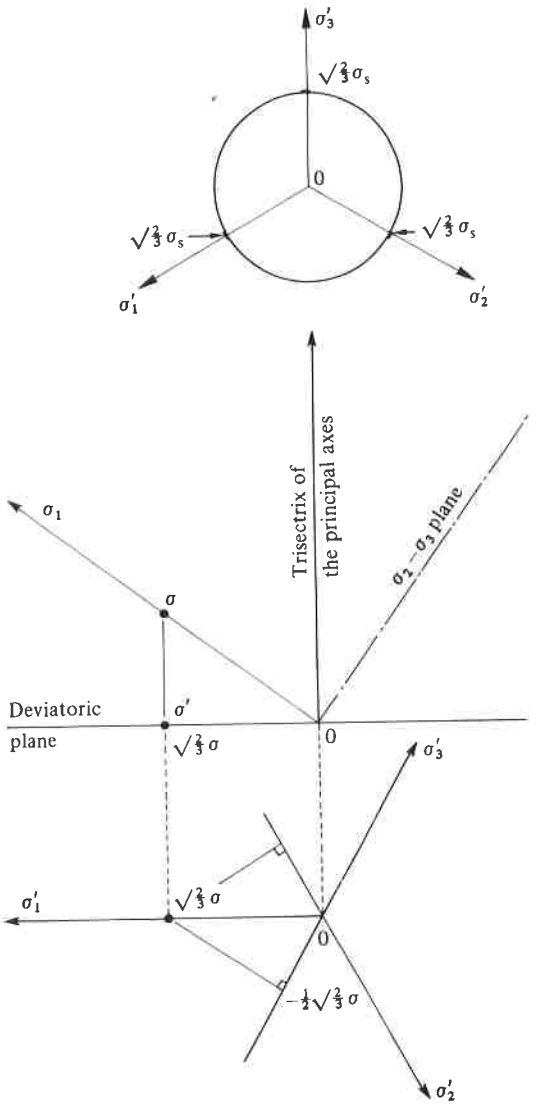

In the principal stress space, the Tresca criterion is represented by an orthogonal prism of hexagonal base with its axis equally inclined to the σ_1, σ_2, σ_3 axes (Fig. 5.13). It is inscribed within the von Mises cylinder.

Experimental validity

It is usually in the vicinity of the initial yield surface that metals are isotropic. For isotropic metals, the experimental points are situated between the von Mises and Tresca criteria, with very ductile metals closer to the Tresca criterion. An example of the yield locus determined by tension (or compression)–torsion tests is given in Fig. 5.14.

A criterion intermediary between those of von Mises and Tresca allows us to match these experimental results better. Proposed by Edelman and Drucker, it introduces a combination of the second and third invariants, J_2 and J_3, of the deviatoric stress tensor and a coefficient C dependent on the material. This criterion describes the elastic domain limit (or the yield surface) by means of the following expression:

$$f = 4s_{II}^3 - 27Cs_{III}^2 - C\sigma_s^2(3s_{II} - \sigma_s^2)^2 - \tfrac{4}{27}(1 - C)\sigma_s^6 = 0.$$

As a function of the J_2 and J_3 invariants, the above criterion is expressed by:

$$J_2^6 - \sigma_s^6 - C[J_3^6 - \sigma_s^6 + \tfrac{27}{4}\sigma_s^2(J_2^2 - \sigma_s^2)^2] = 0.$$

We recover the von Mises criterion for $C = 0$ and the Tresca criterion for $C = 1$. An example of comparison with experiments is given in Fig. 5.14 where $C = 0.384$.

In applications, however, the von Mises criterion is the one most commonly used because of its easy implementation in numerical calculations. The Tresca criterion is more difficult to use because of the

Fig. 5.13. Geometric representation of the Tresca criterion on the deviatoric plane.

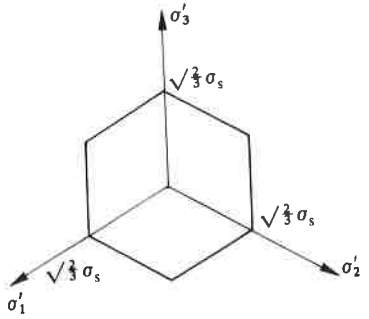

discontinuity of the normals at the corners of the yield surface (see Section 5.3.3).

Anisotropic yield criteria

These criteria cannot be expressed as functions of the stress invariants; preferred directions of anisotropy also appear. For incompressible plastic materials, the classical anisotropic criteria involve a rotation in the stress space; thus, the generalization of the von Mises criterion is of the form

$$(\mathbf{C}:\boldsymbol{\sigma}'):\boldsymbol{\sigma}' = 1$$

where $\mathbf{C}$ is a fourth order tensor dependent on the material properties, and which possesses the symmetries

$$C_{ijkl} = C_{klij} = C_{jikl} = C_{ijlk}.$$

The same criterion in terms of the components of the stress tensor $\boldsymbol{\sigma}$ is

$$(\mathbf{C}':\boldsymbol{\sigma}):\boldsymbol{\sigma} = 1$$

with $C'_{ijkk} = C'_{iikl} = 0$.

Fig. 5.14. Boundary of the elastic limit (or yield locus).

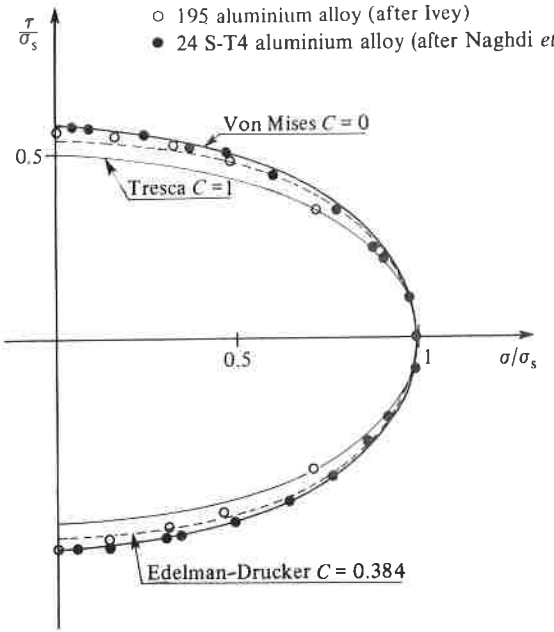

The Hill criterion

The Hill criterion corresponds to a particular kind of anisotropy in which three planes of symmetry are conserved during hardening of the material. The intersection of these three planes are the principal axes of anisotropy. The criterion is formulated with respect to these axes as the reference axes, say $(0, x_1, x_2, x_3)$. This criterion can be deduced from the general expression above with

$$\begin{aligned} C_{1111} &= F + H \quad C_{2222} = F + G \quad C_{3333} = G + H \\ C_{1122} &= -F \quad\quad C_{2233} = -G \quad\quad C_{3311} = -H \\ C_{1212} &= \tfrac{1}{2}L \quad\quad C_{2323} = \tfrac{1}{2}M \quad\quad C_{3131} = \tfrac{1}{2}N \end{aligned}$$

and the values obtained by virtue of the symmetry of C_{ijkl}, which then give

$$\bullet \quad F(\sigma_{11} - \sigma_{22})^2 + G(\sigma_{22} - \sigma_{33})^2 + H(\sigma_{33} - \sigma_{11})^2 + 2L\sigma_{12}^2 + 2M\sigma_{23}^2 + 2N\sigma_{13}^2 = 1.$$

F, G, H, L, M, N are the six scalar parameters which characterize the state of anisotropic hardening. We may determine them with the help of three experiments in simple tension and three in simple shear.

tensile yield stress σ_{s_1} in the direction $x_1 \rightarrow F + H = 1/\sigma_{s_1}^2$
tensile yield stress σ_{s_2} in the direction $x_2 \rightarrow F + G = 1/\sigma_{s_2}^2$
tensile yield stress σ_{s_3} in the direction $x_3 \rightarrow G + H = 1/\sigma_{s_3}^2$
shear yield stress $\sigma_{s_{12}}$ in the plane $(0, x_1, x_2) \rightarrow L = \frac{1}{2}\sigma_{s_{12}}^2$
shear yield stress $\sigma_{s_{23}}$ in the plane $(0, x_2, x_3) \rightarrow M = \frac{1}{2}\sigma_{s_{23}}^2$
shear yield stress $\sigma_{s_{31}}$ in the plane $(0, x_3, x_1) \rightarrow N = \frac{1}{2}\sigma_{s_{31}}^2$

Although anisotropic, this criterion does not take into account the Bauschinger effect; the yield stresses are of identical magnitude in tension and compression. However, it does take into account approximately the initial hardening of rolled sheets. An example is given in Fig. 5.15.

The Tsai criterion

The Tsai criterion allows for the eventual differences in hardening states in tension and in compression. In its most general form, it is expressed as the sum of a linear form and a quadratic form of the six stress components. Denoting the stress components by σ_α ($\sigma_1 = \sigma_{11}$, $\sigma_2 = \sigma_{22}$, $\sigma_3 = \sigma_{33}$, $\sigma_4 = \sigma_{23}$, $\sigma_5 = \sigma_{31}$, $\sigma_6 = \sigma_{12}$), the criterion can be expressed as

$$F_\alpha \sigma_\alpha + F_{\alpha\beta}\sigma_\alpha\sigma_\beta = 1.$$

The hypothesis of orthotropy and plastic incompressibility (with no hydrostatic stress influence) leads to a reduction in the number of material

coefficients F_α and $F_{\alpha\beta}$ from 27 to 8. The criterion can then be written in a form similar to that of the Hill criterion.

$$\begin{aligned} &F'(\sigma_{11} - \sigma_{22})^2 + G'(\sigma_{22} - \sigma_{33})^2 + H'(\sigma_{33} - \sigma_{11})^2 \\ &+ 2L'\sigma_{12}^2 + 2M'\sigma_{23}^2 + 2N'\sigma_{31}^2 \\ &+ P\sigma_{11} + Q\sigma_{22} - (P + Q)\sigma_{33} = 1. \end{aligned}$$

The experimental determination of the eight coefficients for a particular material is rather tricky requiring tests in tension, compression and in shear in different directions.

This criterion is quite representative of the yielding of composite fibre–resin materials and wood. As an example Fig. 5.16 gives the graph of the

Fig. 5.15. Example of a plastically anisotropic material: Hill criterion (after Lee and Zaverl).

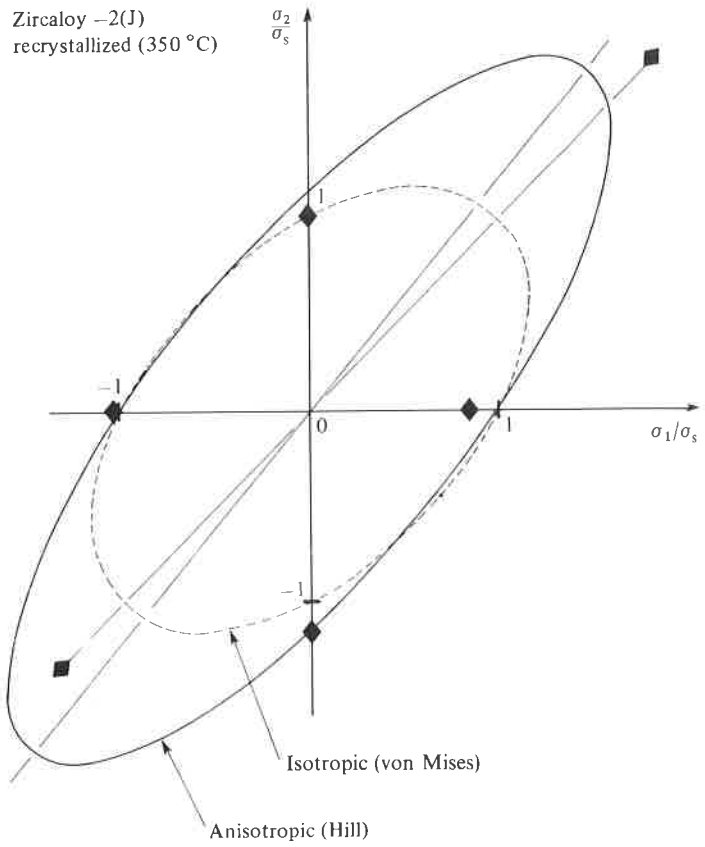

criterion in tension–compression in the L (parallel to the fibre direction) T (tangent to the growth rings) plane for the case of the massive tropical foliaceous tree 'Wana-Kouali'.

5.3 Formulation of general constitutive laws

5.3.1 *Partition hypothesis*

The partition of strains into elastic and plastic parts, already used in the preceding section, is justified by the nature of the physical phenomena. This hypothesis, which will be applied to all the theories of this chapter, is not strictly necessary for the formulation of plasticity laws; the hereditary theories based on the thermodynamics of memory processes do not use it. But, the adoption of this hypothesis greatly simplifies the problems of experimental identification and numerical calculations.

Within the framework of a general theory where large deformations are included, the hypothesis of strain partition is related to the existence of a relaxed intermediate configuration as defined in Chapter 2. The developments of the present chapter are limited to the case of small strains and linear elastic behaviour. Their generalization to the case of large deformations does not present any major problems when the elastic strains remain small. Moreover, we assume here decoupling between the elastic and plastic behaviours (Young's modulus and Poisson's ratio, for example, are supposed to be independent of hardening).

Fig. 5.16. Tsai criterion for "Wana-Kouali" wood (after Gautherin).

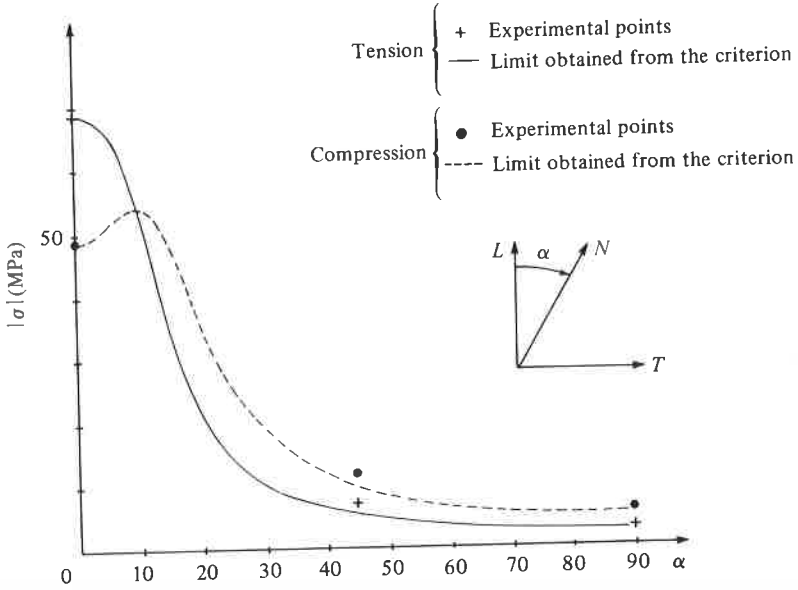

The plastic strain is defined by the difference

$$\boldsymbol{\varepsilon}^{\mathrm{p}} = \boldsymbol{\varepsilon} - \boldsymbol{\varepsilon}^{\mathrm{e}},$$

where $\boldsymbol{\varepsilon}$ is the total strain and where $\boldsymbol{\varepsilon}^{\mathrm{e}}$ is the elastic strain which is related linearly to the stress $\boldsymbol{\sigma}$ by the elasticity law. We recall here that, within the framework of a small deformation theory, the total strain is the symmetric part of the displacement gradient:

$$\boldsymbol{\varepsilon} = \tfrac{1}{2}[\operatorname{grad} \vec{u} + (\operatorname{grad} \vec{u})^{\mathrm{T}}].$$

5.3.2 *Choice of thermodynamic variables*

As mentioned in Chapter 2, the state or independent variables are the observable variables: the total strain $\boldsymbol{\varepsilon}$ and temperature T, and the internal variables $\boldsymbol{\varepsilon}^{\mathrm{p}}$, V_k. The partition hypothesis and the application of the Clausius–Duhem inequality to the case of time-independent, elastoplastic deformations allow us to write the stress tensor and the specific entropy, the thermodynamic variables associated to $\boldsymbol{\varepsilon}^{\mathrm{e}}$ and T respectively, in the form (see Chapter 2):

$$\boldsymbol{\sigma} = \rho(\partial \Psi / \partial \boldsymbol{\varepsilon}^{\mathrm{e}}), \qquad s = -\partial \Psi / \partial T$$

where ρ is the mass density and Ψ is the specific free energy, dependent on observable as well as internal variables:

$$\Psi = \Psi(\boldsymbol{\varepsilon} - \boldsymbol{\varepsilon}^{\mathrm{p}}, T, V_{\mathrm{k}}) = \Psi(\boldsymbol{\varepsilon}^{\mathrm{e}}, T, V_{\mathrm{k}}).$$

The Clausius–Duhem inequality is then reduced to

$$\boldsymbol{\sigma} : \dot{\boldsymbol{\varepsilon}}^{\mathrm{p}} - \rho(\partial \Psi / \partial V_{\mathrm{k}}) \dot{V}_k - (1/T) \vec{q} \cdot \overrightarrow{\operatorname{grad}\, T} \geqslant 0.$$

The internal variables V_{k}, of scalar or tensorial nature, represent the current state of the material, i.e., the state of hardening; classically, a scalar variable (an isotropic hardening variable) of one of the following types is used:

the accumulated plastic strain, expressed by:

$$p = \int_0^t [\tfrac{2}{3} \dot{\boldsymbol{\varepsilon}}^{\mathrm{p}}(\tau) : \dot{\boldsymbol{\varepsilon}}^{\mathrm{p}}(\tau)]^{1/2} \, \mathrm{d}\tau ;$$

the dissipated plastic work expressed by:

$$w_p = \int_0^t \boldsymbol{\sigma}(\tau):\dot{\boldsymbol{\varepsilon}}^p(\tau)\,d\tau;$$

plus one or several tensorial variables or kinematic hardening variables. In what follows, unless stated otherwise, only one kinematic variable denoted by $\boldsymbol{\alpha}$ will be used. The definitions of variables p and w_p are illustrated in Fig. 5.17(*a*) for the tension–compression case.

Very schematically, the scalar variables are associated with the density of dislocations in the current state while the kinematic variables correspond to the incompatibilities of plastic deformations within the polycrystal. Generally, unless a recovery of crystalline structure occurs which is essentially governed by time, the variables p and w_p are increasing; they do not therefore allow representation of the alternating hardening effects observed

Fig. 5.17. (*a*) Definitions of accumulated plastic strain p and dissipated plastic work w_p. (*b*) The current domain of elasticity defined by variables R and $\mathbf{X}$.

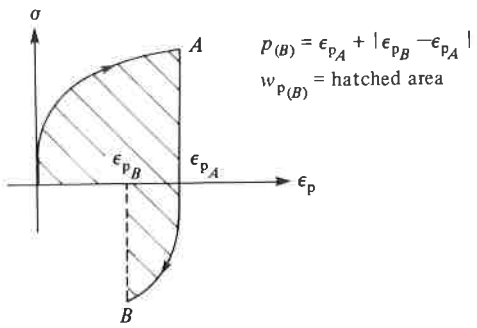

(*a*)

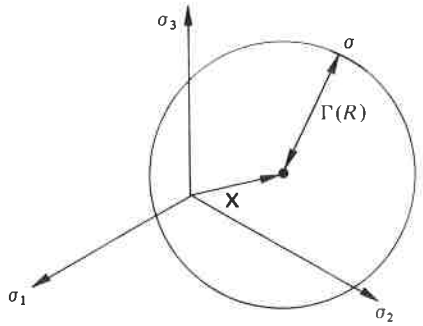

(*b*)

under cyclic loading. On the other hand, the kinematic variables are more directly related to the current state of deformation. In the case of cyclic hardening, they can represent real behaviour because of their evolution during each cycle even in a stabilized regime. A kinematic variable which is often used is the plastic strain itself ($\boldsymbol{\alpha} = \boldsymbol{\varepsilon}^p$) as for example, in Prager's hardening model (linear kinematic hardening).

The decoupling between elastic behaviour and hardening entails writing the free energy in the form

$$\Psi = \Psi_e(\boldsymbol{\varepsilon}^e, T) + \Psi_p(p, \boldsymbol{\alpha}, T).$$

The associated thermodynamic force variables can be deduced from it as

$$R = \rho(\partial\Psi/\partial p), \qquad \mathbf{X} = \rho(\partial\Psi/\partial\boldsymbol{\alpha}).$$

Figure 5.17(*b*) schematically shows the roles of these two variables in the description of the hardening state by the growth of the elastic domain; the size of the domain is a function of the isotropic variable R while its centre is identified by the kinematic variable $\mathbf{X}$.

Within the context of decoupling between intrinsic and thermal dissipations (which does not imply decoupling of the effects), and with the above variables, the Clausius–Duhem inequality expresses the positive character of these two dissipations:

$$\boldsymbol{\sigma}:\dot{\boldsymbol{\varepsilon}}_p - R\dot{p} - \mathbf{X}:\dot{\boldsymbol{\alpha}} \geqslant 0, \qquad -(1/T)\vec{q}\cdot\overrightarrow{\text{grad}}\ T \geqslant 0.$$

The intrinsic dissipation represents the difference between the energy dissipated by virtue of plastic deformations and the energy blocked within the volume element by dislocation networks for example.

5.3.3 *Loading surface and dissipation potential*

Loading surface, loading–unloading criterion

Time-independent plastic behaviour must be considered as a particular case of the more general schematic representation of viscoplasticity studied in Chapter 6. Very schematically, we may imagine, embedded in the stress space, a family of equipotential surfaces or, equivalently of surfaces of equal dissipation (Fig. 5.18). For a fixed hardening state, represented for example by the centre and the dimension of the interior surface $\Omega = 0$, the rate of flow is higher the farther the stress point is from the centre, $\mathbf{X}$. On the surface closest to the centre, $\Omega = 0$, the rate of flow is zero, whereas on the surface farthest from the centre it is infinite. The domain of viscoplasticity is

situated between the two; the domain of elasticity being represented, of course, by $\Omega < 0$.

Thus the scheme of time-independent plasticity is applicable

> either to infinitely slow loads or to the attainment of asymptotic states under fixed loads;
> or to extremely rapid loads.

The responses for these two cases differ to varying extents: for metals loaded at temperatures lower than one quarter of their absolute melting temperature, they are very close which for them justifies the use of the time-independent plasticity analysis.

In the second case of an infinitely large rate, viscous deformations can be considered negligible (as they have no time to occur!). Thus, regardless of the case under consideration, a surface, defined in the stress space exists from which plastic flow can occur. For stress states contained within this surface, the material behaviour is entirely elastic. This $f = 0$ surface is called the loading surface or the flow surface. Initially, it is identical to the initial yield surface (see Section 5.2.2).

In order to describe the possibility of plastic flow completely, it is necessary to introduce still one more criterion, that of loading–unloading.

Fig. 5.18. Equipotential flow surfaces (limiting cases of time-independent plasticity).

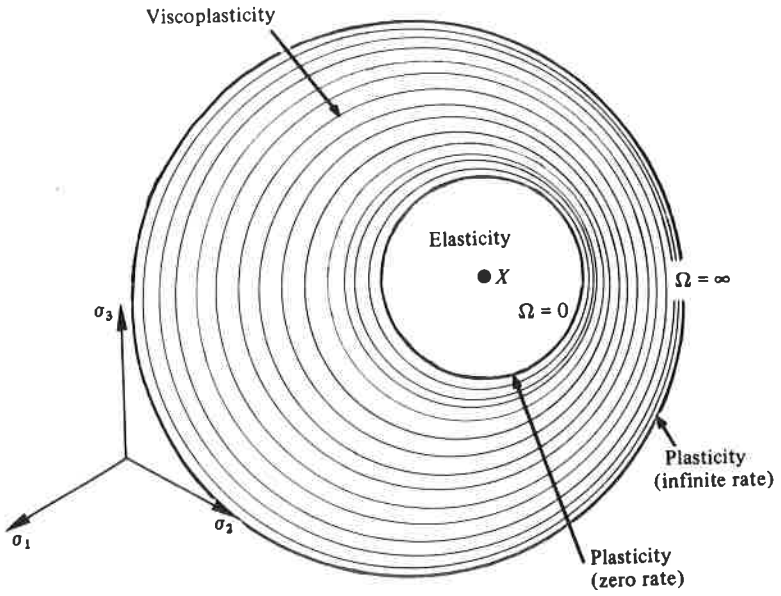

Plastic flow occurs only if the following two conditions are simultaneously satisfied (see Fig. 5.19).

(1) The representative point of the stress state is situated on the loading surface

$$f(\boldsymbol{\sigma}^*, V_k) = 0.$$

(2) The framework of classical plasticity requires that the representative point of the stress state does not leave the loading surface ($f > 0$ is impossible). During the continuous flow, the consistency condition,

$$\mathrm{d}f(\boldsymbol{\sigma}^*) = \frac{\partial f}{\partial \boldsymbol{\sigma}} : \mathrm{d}\boldsymbol{\sigma}^* + \frac{\partial f}{\partial V_k}\mathrm{d}V_k = 0$$

must be satisfied, which implies that the point representative of the stress ($\boldsymbol{\sigma}^* + \mathrm{d}\boldsymbol{\sigma}^*$) remains on the loading surface.

On the other hand, stress variation is allowed to displace the stress point towards the interior of the loading surface. This is the case of unloading characterized by

$$\mathrm{d}f(\boldsymbol{\sigma}^*) < 0.$$

According to this scheme no plastic flow can occur during unloading; the behaviour becomes elastic as soon as the unloading starts. In summary:

- $f < 0$: ⟶ elastic behaviour

Fig. 5.19. Loading–unloading criterion for a positive hardening.

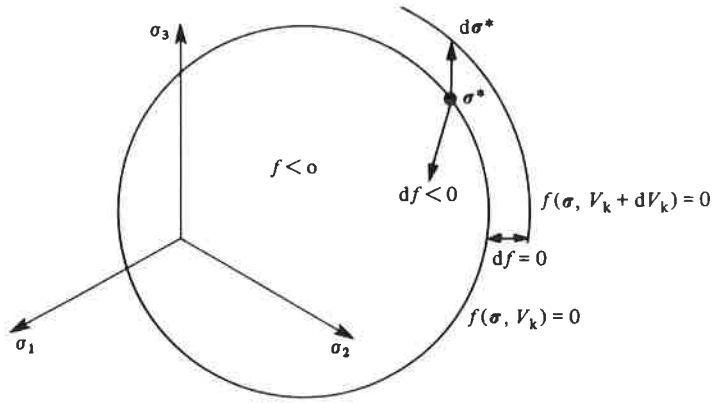

- $f = 0$ and $df = 0$: → plastic flow
- $f = 0$ and $df < 0$: → elastic unloading.

For materials with positive hardening, the loading surface is expressible as a function of the components of the stress tensor and depends on the hardening state through the internal variables. These variables are generally the thermodynamic forces $\mathbf{X}$ and R as defined previously. Eventually it also depends on the temperature:

$$f = f(\boldsymbol{\sigma}, R, \mathbf{X}, T).$$

For materials with negative hardening, it may be of more interest to use a more general formulation, in terms of strain, e.g.,

$$f' = f'(\boldsymbol{\varepsilon}, p, \boldsymbol{\alpha}, T).$$

Fig. 5.20 shows that in the case of simple tension, when the hardening is negative ($d\sigma/d\varepsilon_p < 0$), the loading condition $\dot{\sigma} > 0$ cannot be used.

Nonassociated plasticity

In the general framework of thermodynamics, the existence of a dissipation potential was postulated; its knowledge provides the laws of evolution of plastic deformation and internal variables. For plasticity, the use of this potential leads to the schematic representation of associated plasticity as will be seen in Section 5.3.3.4. This is a representation in which the yield surface (or the loading or flow surface) is assimilated with an 'equipotential surface'. A more general case is that of 'nonassociated plasticity' which is useful for describing certain materials or phenomena, and is practically

Fig. 5.20. Loading–unloading criterion in tension for positive or negative hardening.

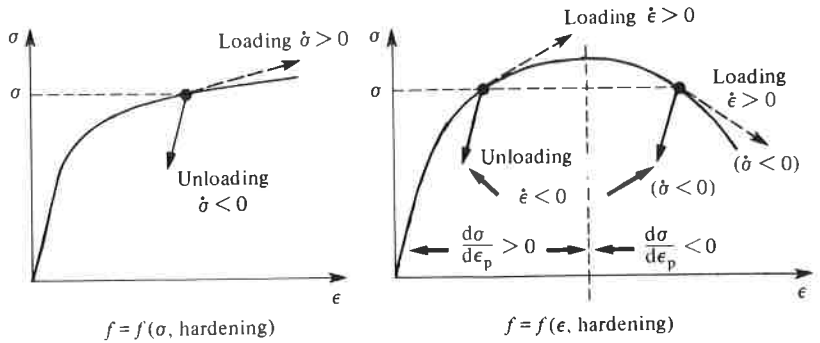

indispensible in soil mechanics. This schematic representation is not covered directly by the formalism of 'generalized standard materials' introduced in Chapter 1.

The schematic representation of nonassociated plasticity requires the use of three potentials: the free energy Ψ; the yield surface, $f = 0$; and a potential surface, F = constant, which determines the direction of plastic flow in the space of generalized force variables (it ultimately depends on the state variables, especially on the temperature);

$$F = F(\boldsymbol{\sigma}, R, \mathbf{X}, T).$$

The generalized normality hypothesis associated with the instantaneous dissipative phenomena described in Section 2.4.3 allows us to write:

$$\dot{\boldsymbol{\varepsilon}}_p = \dot{\lambda}\partial F/\partial\boldsymbol{\sigma}$$
$$-\dot{p} = \dot{\lambda}\partial F/\partial R$$
$$-\dot{\boldsymbol{\alpha}} = \dot{\lambda}\partial F/\partial\mathbf{X}$$

where $\dot{\lambda}$ is the multiplier of time-independent plasticity which is determined later. $\dot{\lambda}$ is equal to zero when there is no flow, i.e. when

$$f < 0 \quad \text{or} \quad f = 0 \quad \text{and} \quad \frac{\partial f}{\partial \boldsymbol{\sigma}} : \dot{\boldsymbol{\sigma}} \leqslant 0.$$

We may note that this concept, although it does not exactly satisfy the hypotheses of generalized standard materials, allows us to verify *a priori* the second principle of thermodynamics. The Clausius–Duhem inequality becomes:

$$\Phi = \left[\boldsymbol{\sigma} : \frac{\partial F}{\partial \boldsymbol{\sigma}} + R\frac{\partial F}{\partial R} + \mathbf{X} : \frac{\partial F}{\partial \mathbf{X}}\right]\dot{\lambda} = 0.$$

To ensure this condition, it is sufficient that F be convex, positive as soon as there is plastic flow, and include the origin ($F \geqslant f = 0$, $F(0, 0, 0; T) = 0 \forall T$). We can then easily show that

$$\Phi \geqslant F\dot{\lambda} \geqslant 0.$$

Consistency condition – expression for plasticity multiplier

We have seen that the loading–unloading criterion requires the imposition of $f = 0$ and $\dot{f} = 0$ during plastic flow. This last condition implies that

$$\frac{\partial f}{\partial \boldsymbol{\sigma}} : \dot{\boldsymbol{\sigma}} + \frac{\partial f}{\partial R}\dot{R} + \frac{\partial f}{\partial \mathbf{X}} : \dot{\mathbf{X}} + \frac{\partial f}{\partial T}\dot{T} = 0.$$

By using the relations between the internal variables and the associated thermodynamic forces, we have

$$\dot{R} = L_{pp}\dot{p} + \mathbf{L}_{\alpha p}:\dot{\boldsymbol{\alpha}} + L_{pT}\dot{T}$$
$$\dot{\mathbf{X}} = \mathbf{L}_{\alpha p}\dot{p} + \mathbf{L}_{\alpha\alpha}:\dot{\boldsymbol{\alpha}} + \mathbf{L}_{\alpha T}\dot{T}$$

where the operator $\mathbf{L}$ is derived from the free energy Ψ by:

$$L_{pp} = \frac{\partial^2\Psi}{\partial p^2} \qquad \mathbf{L}_{\alpha T} = \frac{\partial^2\Psi}{\partial\boldsymbol{\alpha}\partial T} \qquad L_{pT} = \frac{\partial^2\Psi}{\partial p\partial T}$$
$$\mathbf{L}_{\alpha p} = \frac{\partial^2\Psi}{\partial\boldsymbol{\alpha}\partial p} \qquad \mathbf{L}_{\alpha\alpha} = \frac{\partial^2\Psi}{\partial\boldsymbol{\alpha}\partial\boldsymbol{\alpha}}.$$

Substitution in $\dot{f} = 0$ and the use of normality relations leads to

$$\frac{\partial f}{\partial\boldsymbol{\sigma}}:\dot{\boldsymbol{\sigma}} + \left(\frac{\partial f}{\partial T} + \frac{\partial f}{\partial\mathbf{X}}:\mathbf{L}_{\alpha T} + \frac{\partial f}{\partial R}L_{pT}\right)\dot{T}$$
$$- \dot{\lambda}\left[\frac{\partial f}{\partial\mathbf{X}}:\mathbf{L}_{\alpha\alpha}:\frac{\partial F}{\partial\mathbf{X}} + \left(\frac{\partial f}{\partial\mathbf{X}}\frac{\partial F}{\partial R} + \frac{\partial f}{\partial R}\frac{\partial F}{\partial\mathbf{X}}\right):\mathbf{L}_{\alpha p} + \frac{\partial f}{\partial R}\frac{\partial F}{\partial R}L_{pp}\right] = 0$$

from which $\dot{\lambda}$ can be determined as a function of the different potentials, stress rate, and temperature.

Only materials with positive hardening can be covered within the context of the present formalism. For negative hardening, a flow theory dependent upon a loading function expressed in terms of strain should be developed. To say that the hardening is positive amounts to considering the hardening modulus as positive:

$$h = \frac{\partial f}{\partial\mathbf{X}}:\mathbf{L}_{\alpha\alpha}:\frac{\partial F}{\partial\mathbf{X}} + \left(\frac{\partial f}{\partial\mathbf{X}}\frac{\partial F}{\partial R} + \frac{\partial f}{\partial R}\frac{\partial F}{\partial\mathbf{X}}\right):\mathbf{L}_{\alpha p} + \frac{\partial f}{\partial R}\frac{\partial F}{\partial R}L_{pp} \geqslant 0.$$

In the present framework, if h is positive, the expression for the plasticity multiplier becomes

$$\dot{\lambda} = \frac{H(f)}{h}\left\langle\frac{\partial f}{\partial\boldsymbol{\sigma}}:\dot{\boldsymbol{\sigma}} + \left(\frac{\partial f}{\partial T} + \frac{\partial f}{\partial\mathbf{X}}:\mathbf{L}_{\alpha T} + \frac{\partial f}{\partial R}L_{pT}\right)\dot{T}\right\rangle$$

where H denotes the Heaviside step function: $H(f) = 0$ if $f < 0$, $H(f) = 1$ if $f \geqslant 0$ and the symbol $\langle\ \ \rangle$ means that $\langle u\rangle = 0$ if $u < 0$, $\langle u\rangle = u$ if $u \geqslant 0$. The introduction of these two symbols enables us directly to ensure $\dot{\lambda} = 0$ when $f < 0$ or when there is unloading ($\dot{f} < 0$).

Associated plasticity. Generalized standard materials

The theory of associated plasticity is the theory developed by identifying the function F with the loading function f. The potential φ^* then plays the role of the indicator function of the convex set defined by $f = 0$.

$$\varphi^* = \varphi^*(\boldsymbol{\sigma}, R, \mathbf{X}; T)$$

is obtained by application of the Legendre–Fenchel transformation to the dissipation potential:

$$\varphi = \varphi(\dot{\boldsymbol{\varepsilon}}^p, \dot{p}, \dot{\boldsymbol{\alpha}}; T).$$

In time-independent plasticity, the potential φ^* is equal to zero inside the elastic domain $f < 0$, and infinite outside. It is then easy to appreciate how plasticity can be considered as a particular case of viscoplasticity (see the discussion about the loading–unloading criterion, subsection 5.3.3, and Fig. 5.18).

Many classical laws follow from this specialization of the generalized standard materials. The expression for the hardening modulus becomes

$$h = \left(\frac{\partial f}{\partial R}\right)^2 L_{pp} + \frac{\partial f}{\partial\mathbf{X}}:\mathbf{L}_{\alpha\alpha}:\frac{\partial f}{\partial\mathbf{X}} + 2\frac{\partial f}{\partial R}\frac{\partial f}{\partial\mathbf{X}}:\mathbf{L}_{\alpha p}$$

and the flow law is expressed by:

$$\dot{\boldsymbol{\varepsilon}}^p = \dot{\lambda}(\partial f/\partial\boldsymbol{\sigma})$$
$$-\dot{p} = \dot{\lambda}(\partial f/\partial R)$$
$$-\dot{\boldsymbol{\alpha}} = \dot{\lambda}(\partial f/\partial\mathbf{X}).$$

The expression for the plasticity multiplier is the same as above except f replaces F.

5.4 Particular flow laws

5.4.1 *Different types of criteria and flow laws*

Before dealing with particular models, it is advisable to give definitive meanings to the terms isotropy, kinematic and anisotropy. Two aspects are distinguished: one related to flow criteria and the other to hardening, i.e., the evolution of the criterion. The words isotropic and anisotropic describe both aspects, while the term kinematic is applied only to the idea of evolution. Schematically, there are six levels of theory as illustrated below, where we have restricted ourselves to the use of the second invariant of stress (see Table 5.2).

Table 5.2. *Different plasticity criteria and flow rules*

Case	Initial criterion	Hardening variables	Transformed criterion due to hardening	
1	$f(J(\boldsymbol{\sigma}))$ isotropic	p	$f(J(\boldsymbol{\sigma}))-R(p)$	isotropic
2	$f(J(\boldsymbol{\sigma}))$ isotropic	$\mathbf{X}$	$f(J(\boldsymbol{\sigma}-\mathbf{X}))$	kinematic
3	$f(\mathbf{C}:\boldsymbol{\sigma}':\boldsymbol{\sigma}')$ anisotropic	p	$f(\mathbf{C}:\boldsymbol{\sigma}':\boldsymbol{\sigma}')-R(p)$	isotropic
4	$f(\mathbf{C}:\boldsymbol{\sigma}':\boldsymbol{\sigma}')$ anisotropic	$\mathbf{X}$	$f(\mathbf{C}:(\boldsymbol{\sigma}'-\mathbf{X}'):(\boldsymbol{\sigma}'-\mathbf{X}'))$	kinematic
5	$f(J(\boldsymbol{\sigma}))$ isotropic	$p, \mathbf{X}, \boldsymbol{\varepsilon}^p$	$f(\mathbf{C}^*:(\boldsymbol{\sigma}'-\mathbf{X}'):(\boldsymbol{\sigma}'-\mathbf{X}'))-R(p)$	isotropic + kinematic + anisotropic
6	$f(\mathbf{C}:\boldsymbol{\sigma}':\boldsymbol{\sigma}')$ anisotropic	$p, \mathbf{X}, \boldsymbol{\varepsilon}^p$	$f(\mathbf{C}^*:(\boldsymbol{\sigma}'-\mathbf{X}'):(\boldsymbol{\sigma}'-\mathbf{X}'))-R(p)$	isotropic + kinematic + anisotropic

(1) Isotropic criterion – isotropic hardening: the invariant $J(\boldsymbol{\sigma})$ and a scalar variable p are sufficient (J is, for example, the second invariant, $J = J_2$).

(2) Isotropic criterion – kinematic hardening: the translation of the criterion by a tensor $\mathbf{X}$ is used.

(3) Anisotropic criterion – isotropic hardening: the criterion is expressed in a more complex form, for example with $(\mathbf{C}:\boldsymbol{\sigma}'):\boldsymbol{\sigma}'$ where $\mathbf{C}$ depends on the material. However, this form of the criterion is retained during the hardening process by simple dilatation, and therefore, involves only a scalar variable p.

(4) Anisotropic criterion – kinematic hardening: the form of the criterion is retained during hardening but the surface is subjected to a translation represented by the tensor $\mathbf{X}$.

(5) Isotropic criterion – anisotropic hardening (nonkinematic): the invariant $J_2(\boldsymbol{\sigma})$ is transformed into a more complex expression, eventually leading to a kinematic effect in which $\mathbf{C}^*(\boldsymbol{\varepsilon}^p)$ expresses an anisotropy depending on the present state of plastic strain.

(6) Anisotropic criterion – anisotropic hardening. This is the generalization of case (5); $\mathbf{C}$ describes the initial anisotropy in a state of zero plastic strain.

Note that the distinction between the 'initial' state and 'hardened' state is subtle as any hardened state can possibly be considered as an initial state.

The anisotropy introduced by the operator $\mathbf{C}$ is not the most general one;

Fig. 5.21. Anisotropic hardening (rotation of the surface) superposed on kinematic hardening (translation) and on isotropic softening (reduction) for 1Cr–$\frac{1}{2}$Mo–$\frac{1}{4}$V steel (after Moreton *et al.*).

it only implies rotation of the criterion. For example, in the (σ_1, σ_2) plane of principal stresses it results in a change of eccentricity of the von Mises ellipse or in a rotation of the axes of this ellipse (see, e.g., Figs. 5.15 and 5.21).

Experiments show that in addition to rotation and uniform expansion or contraction of the surface, deformation of the surface can occur by the appearance of 'corners', but modelling of this kind of anisotropy is very complex. In what follows, we will deal only with cases of isotropic and kinematic hardening (cases (1)–(4)).

5.4.2 *Isotropic hardening rules*

In these rules, the evolution of the loading surface is governed only by one scalar variable, either the dissipated plastic work, or the accumulated plastic strain p, or any associated variable such as the thermodynamic force R. These rules are easily written in the general context of associated plasticity, and therefore we limit ourselves to the identity between the dissipation potential and the loading function. To simplify the presentation, the rules are developed assuming the temperature to be constant, or at least using criteria which are temperature independent. Generalization to the non-isothermal case does not present any particular problems in following the formalism given in Section 5.3.3. Thus we have

$$f = f(\boldsymbol{\sigma}, R).$$

Fig. 5.22. Isotropic hardening: representation in the stress space and in tension–compression.

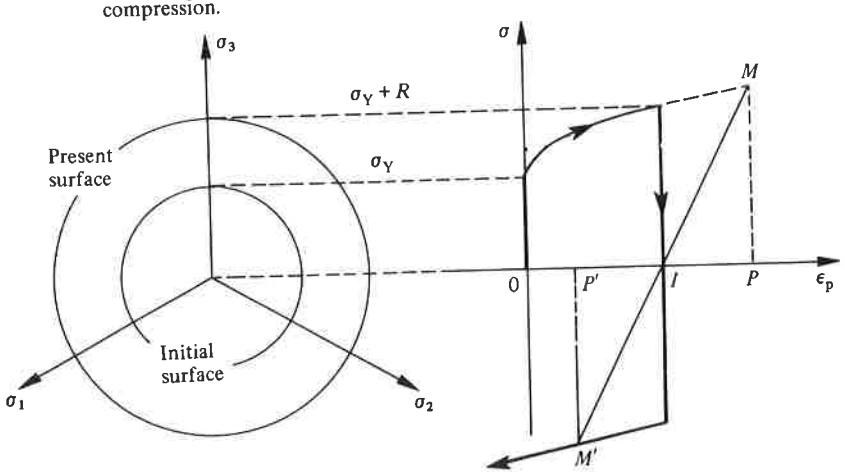

The hypothesis of isotropic hardening greatly facilitates the statement of flow equations. Whether accumulated plastic strain or accumulated plastic work is used, it is easy to identify the hardening model with any expression of the monotonic uniaxial stress–strain curve. The only differences will be in either the criterion chosen for the loading function or the dissipation expression.

The loading function is expressed in the form

$$f = f_Y(\boldsymbol{\sigma}) - \Gamma(R)$$

where the function f_Y indicates the form of the yield criterion, and the function Γ introduces hardening through the relation between the thermodynamic force R and the hardening variable chosen (p or w_p). For an isotropic material (with an initially isotropic yield surface) f_Y is a function of the stress tensor invariants.

Isotropic hardening corresponds to a uniform expansion of the initial criterion. Fig. 5.22 schematically shows the evolution of the criterion in the stress space, and the stress–plastic strain curve in tension and compression. It also shows why the accumulated plastic strain can be used as a variable of isotropic hardening: the points M and M' have the same state and the same accumulated plastic strain $0I + IP = 0I + IP'$.

Prandtl–Reuss equation

Formulation

The Prandtl–Reuss equation is a flow law in an elastoplastic regime with isotropic hardening. It is based on the following assumptions.

(1) Hypothesis of plastic incompressibility: plastic strain occurs at constant volume and flow does not depend on the hydrostatic stress $\sigma_H = \frac{1}{3}\mathrm{Tr}(\boldsymbol{\sigma})$. The loading function depends only on the deviatoric stress and the internal variables, i.e.,

$$\partial f / \partial \sigma_H = 0.$$

(2) Hypothesis of initial isotropy and isotropic hardening: the loading function depends only on the invariants J_2 and J_3 of the deviatoric stress tensor:

$$J_2(\boldsymbol{\sigma}) = \sigma_{eq} = (\tfrac{3}{2}\boldsymbol{\sigma}' : \boldsymbol{\sigma}')^{1/2}$$
$$J_3(\boldsymbol{\sigma}) = (\tfrac{9}{2}\boldsymbol{\sigma}' \cdot \boldsymbol{\sigma}' : \boldsymbol{\sigma}')^{1/3}.$$

(3) Associated plasticity and normality hypotheses:

$$d\boldsymbol{\varepsilon}^p = d\lambda(\partial f/\partial \boldsymbol{\sigma})$$
$$dp = -d\lambda(\partial f/\partial R).$$

(4) Choice of the von Mises loading function, independent of the third invariant, in the form:

$$f = \sigma_{eq} - R - \sigma_Y = 0$$

where σ_Y is the initial yield stress in tension.

The constitutive equation, in fact, the hardening curve, is expressed by the relation

$$R = k(p) = \rho(\partial \Psi/\partial p)$$

with $R(0) = k(0) = 0$.

The general procedure described in Section 5.3.3 is easily applicable. First we write

$$d\boldsymbol{\varepsilon}^p = d\lambda(\partial f/\partial \boldsymbol{\sigma}) = \tfrac{3}{2}\, d\lambda(\boldsymbol{\sigma}'/\sigma_{eq})$$
$$dp = -d\lambda(\partial f/\partial R) = d\lambda = (\tfrac{2}{3}\, d\boldsymbol{\varepsilon}^p : d\boldsymbol{\varepsilon}^p)^{1/2}$$

where we get back the definition of the accumulated strain increment. The consistency condition in the presence of flow ($f = 0$ and $df = 0$) gives

$$df = d\sigma_{eq} - k'(p)\, dp = 0$$

which can be used to express the plasticity multiplier as

$$d\lambda = dp = H(f)(d\sigma_{eq}/k'(p)).$$

For a material with positive hardening, i.e., with $k'(p) > 0$, there is no flow except when $d\sigma_{eq}$ is positive (i.e., when the equivalent stress increases). For a material with negative hardening, $d\sigma_{eq} < 0$, the plasticity multiplier must be zero, and the symbol $\langle x \rangle$ is used:

$$d\lambda = dp = H(f)(\langle d\sigma_{eq} \rangle / k'(p)).$$

The flow equation is therefore written as:

$$d\boldsymbol{\varepsilon}^p = \tfrac{3}{2} H(f) \frac{\langle d\sigma_{eq} \rangle}{k'(p)} \frac{\boldsymbol{\sigma}'}{\sigma_{eq}}.$$

It can also be expressed solely in terms of the stresses by introducing

$$p = k^{-1}(R) = k^{-1}(\sigma_{eq} - \sigma_Y)$$

and

$$g'(\sigma_{eq}) = \{k'[k^{-1}(\sigma_{eq} - \sigma_Y)]\}^{-1}.$$

Taking into account the partition of strains and the linear isotropic elasticity law, the Prandtl–Reuss equation is expressed by

- $$d\boldsymbol{\varepsilon} = d\boldsymbol{\varepsilon}^e + d\boldsymbol{\varepsilon}^p$$
- $$d\boldsymbol{\varepsilon}^e = \frac{1+\nu}{E} d\boldsymbol{\sigma} - \frac{\nu}{E} d(\mathrm{Tr}(\boldsymbol{\sigma}))\mathbf{1}$$
- $$d\boldsymbol{\varepsilon}^p = \tfrac{3}{2} H(f) g'(\sigma_{eq}) \frac{\langle d\sigma_{eq} \rangle}{\sigma_{eq}} \boldsymbol{\sigma}'$$

or

$$d\varepsilon^p_{ij} = \tfrac{3}{2} H(f) g'(\sigma_{eq}) \frac{\langle d\sigma_{eq} \rangle}{\sigma_{eq}} \sigma'_{ij}$$

while remembering that the last relation holds only when $f = 0$, i.e., when $\sigma_{eq} - R - \sigma_Y = 0$. If we neglect the elastic deformations we obtain

$$d\boldsymbol{\varepsilon} = \tfrac{3}{2} H(f) g'(\sigma_{eq}) \frac{\langle d\sigma_{eq} \rangle}{\sigma_{eq}} \boldsymbol{\sigma}'$$

which is known as the Levy–Mises relation.

Identification

A simple tension test gives meaning to the variables R and p and allows the identification of the function $g(\sigma_{eq})$ of the Prandtl–Reuss equation. In this case the sole nonzero component of stress is $\sigma_1 = \sigma$, whereas the nonzero components of the deviatoric stress tensor are $\sigma'_{11} = \frac{2}{3}\sigma$, $\sigma'_{22} = \sigma'_{33} = -\frac{1}{3}\sigma$, and we find that $p = \varepsilon_p$ and $J_2 = \sigma_{eq} = \sigma$. The flow law therefore becomes:

$$d\varepsilon_{p11} = d\varepsilon_p = g'(\sigma)\, d\sigma.$$

The function $[g'(\sigma)]^{-1}$ plays the role of the tangent modulus of the hardening curve:

$$\frac{1}{g'(\sigma)} = \frac{d\sigma}{d\varepsilon_p}$$

and indeed the variable R has the meaning:

$$R = k(p) = \int_0^{\varepsilon} k'(\varepsilon_p)\, d\varepsilon_p = \int_{\sigma_Y}^{\sigma} \frac{1}{g'(\sigma)} d\varepsilon_p(\sigma) = \int_{\sigma_Y}^{\sigma} d\sigma = \sigma - \sigma_Y$$

which is consistent with the expression of the loading function for simple

tension:

$$f = |\sigma| - R - \sigma_Y = 0.$$

Fig. 5.23 illustrates this identification, which is very simple in this case.

In the particular case where the power-law expression (see p. 169) is chosen for the hardening curve, the variable R can be written as:

$$R = \sigma_{eq} - \sigma_Y = K_Y p^{1/M_Y} = k(p)$$

with the derivative:

$$k'(p) = \frac{K_Y}{M_Y} p^{(1-M_Y)/M_Y} = \frac{K_Y}{M_Y}\left(\frac{\sigma_{eq} - \sigma_Y}{K_Y}\right)^{1-M_Y}.$$

The Prandtl–Reuss equation can then be written in one of the following forms:

$$d\boldsymbol{\varepsilon}^p = \frac{3}{2}\frac{M_Y}{K_Y} p^{(M_Y-1)/M_Y} \frac{\langle d\sigma_{eq}\rangle}{\sigma_{eq}} \boldsymbol{\sigma}'$$

$$\bullet \qquad d\boldsymbol{\varepsilon}^p = \frac{3}{2}\frac{M_Y}{K_Y}\left\langle \frac{\sigma_{eq} - \sigma_Y}{K_Y}\right\rangle^{M_Y - 1} \frac{\langle d\sigma_{eq}\rangle}{\sigma_{eq}} \boldsymbol{\sigma}'$$

or

$$d\varepsilon^p_{ij} = \frac{3}{2}\frac{M_Y}{K_Y}\left\langle \frac{\sigma_{eq} - \sigma_Y}{K_Y}\right\rangle^{M_Y - 1} \frac{\langle d\sigma_{eq}\rangle}{\sigma_{eq}} \sigma'_{ij}.$$

Fig. 5.23. Schematic representation of the tension curve and interpretation by isotropic hardening.

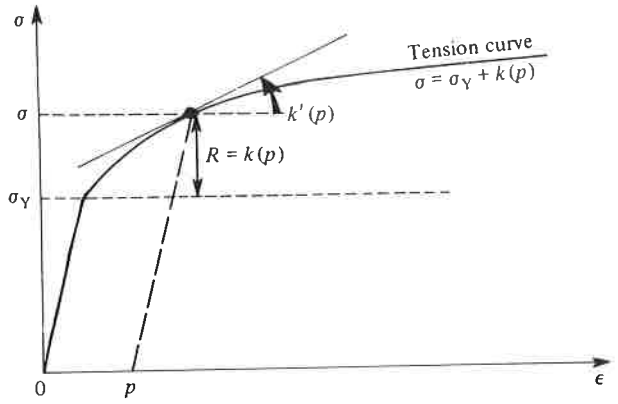

In the case of simple tension, the second expression gives:

$$d\varepsilon_p = \frac{M_Y}{K_Y}\left\langle \frac{\sigma - \sigma_Y}{K_Y}\right\rangle^{M_Y - 1} d\sigma$$

or, when integrated for $\sigma > \sigma_Y$

$$\varepsilon_p = \left\langle \frac{\sigma - \sigma_Y}{K_Y}\right\rangle^{M_Y}.$$

Case of perfect plasticity

This is the case in which there is no hardening; the variable R is zero and

$$f = \sigma_{eq} - \sigma_Y = 0.$$

The consistency condition $df = d\sigma_{eq} = 0$ cannot be used to obtain the plastic multiplier $d\lambda$. The plastic strains are now indeterminate:

$$\bullet \qquad d\boldsymbol{\varepsilon}^p = \tfrac{3}{2}\, d\lambda \frac{\boldsymbol{\sigma}'}{\sigma_{eq}}$$

where $d\lambda$ is arbitrary but positive.

Other isotropic hardening laws

By remaining within the framework of 'associated plasticity' and using the generalized normality hypothesis, it is possible to formulate more general isotropic hardening laws than the Prandtl–Reuss equation. This may be done by using the loading function which corresponds to Tresca criterion or to one of the anisotropic criteria (see Section 5.2.2).

Isotropic plasticity law using the Tresca criterion

Let us recall the normality law

$$d\boldsymbol{\varepsilon}^p = d\lambda(\partial f/\partial \boldsymbol{\sigma})$$

and for simplicity, let us study the components of $d\boldsymbol{\varepsilon}^p$ with respect to the principal stress directions with

$$\sigma_3 < \sigma_2 < \sigma_1.$$

This corresponds to the 'face' regime in the sense that the stress point is situated on one of the faces of the hexagonal prism of the Tresca criterion, which is expressed by

$$f = \mathrm{Sup}(|\sigma_i - \sigma_j|) - \sigma_s = 0$$

$$f = \sigma_1 - \sigma_3 - \sigma_s = 0.$$

We then have

$$\partial f/\partial\sigma_1 = 1, \qquad \partial f/\partial\sigma_2 = 0, \qquad \partial f/\partial\sigma_3 = -1$$

from which

$$d\varepsilon_1^p = d\lambda \qquad d\varepsilon_2^p = 0 \qquad d\varepsilon_3^p = -d\lambda.$$

In the case where two principal components are equal (e.g., $\sigma_1 = \sigma_2$) the load point is on an edge. This regime requires special handling because of the nonuniqueness of the normal to the loading surface.

The multiplier $d\lambda$ is identified from the hardening curve in simple tension as was done for the Prandtl–Reuss law:

$$d\lambda = d\varepsilon_1^p = g'(\sigma_s)\,d\sigma_s$$

from which

- $d\varepsilon_1^p = g'(\sigma_1 - \sigma_3)\,d(\sigma_1 - \sigma_3)$
- $d\varepsilon_2^p = 0$
- $d\varepsilon_3^p = -g'(\sigma_1 - \sigma_3)\,d(\sigma_1 - \sigma_3)$

} if $\sigma_1 - \sigma_3 - \sigma_s = 0$ (with $\sigma_3 < \sigma_2 < \sigma_1$).

If the hardening curve is expressed by $\varepsilon_p = (\sigma/K)^M$, then

$$g'(\sigma_1 - \sigma_3) = \frac{M}{K}\left(\frac{\sigma_1 - \sigma_3}{K}\right)^{M-1}.$$

Isotropic flow rule using anisotropic criteria
If the criterion is expressed in the form:

$$f = (\mathbf{C}:\boldsymbol{\sigma}'):\boldsymbol{\sigma}' - R - \sigma_Y = 0$$

we obtain the flow equation:

$$d\boldsymbol{\varepsilon}^p = \frac{H(f)}{k'(p)}\langle \mathbf{C}:\boldsymbol{\sigma}':d\boldsymbol{\sigma}'\rangle \frac{\mathbf{C}:\boldsymbol{\sigma}'}{R + \sigma_Y}$$

or, in index notation:

$$d\varepsilon_{ij}^p = \frac{H(f)}{k'(p)}\langle C_{pqrs}\sigma'_{pq}\,d\sigma'_{rs}\rangle \frac{C_{ijkl}\sigma'_{kl}}{R + \sigma_Y}.$$

This type of hardening rule can be used to describe materials which are strongly anisotropic in their initial state: anisotropy due to metal working, forming texture, composite materials, etc.

As was seen in Section 5.2.2, it is possible to specialize the criterion by using only six constants which describe the anisotropic state of the material. This remains fixed during the plastic flow; the principal directions of anisotropy remain unchanged.

5.4.3 *Linear kinematic hardening rules*

Prager's kinematic hardening rule

General form
Kinematic hardening corresponds to translation of the loading surface. The hardening variable $\mathbf{X}$ is of a tensorial nature; it indicates the present position of the loading surface:

$$f = f_Y(\boldsymbol{\sigma} - \mathbf{X}) - k.$$

Fig. 5.24 shows in a schematic way the movement of this surface in the stress space and the corresponding modelling in tension–compression on the stress–strain diagram. The value of the yield stress k is generally different from σ_Y used in the previous sections.

Generally, isotropy is considered to exist in the unstressed state represented by $\mathbf{X}$ and plastic deformation is supposed to take place at constant volume. Therefore, in the function f_Y only the invariants $J_2(\boldsymbol{\sigma} - \mathbf{X})$ and $J_3(\boldsymbol{\sigma} - \mathbf{X})$ of the deviatoric parts of $\boldsymbol{\sigma}$ and $\mathbf{X}$ appear. These assumptions

Fig. 5.24. Kinematic hardening: representation in stress space and in tension–compression. The scales coincide on the axes σ, σ_1, σ_2, σ_3 (but not on the axes σ'_1, σ'_2, σ'_3 of the deviatoric plane).

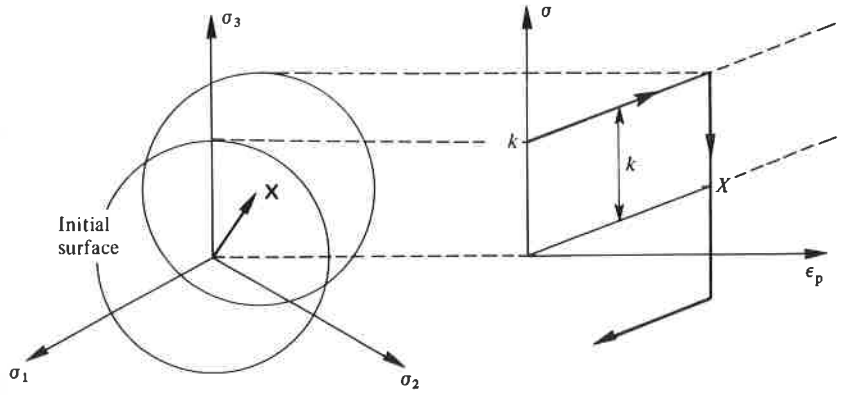

have been verified for a number of materials. Fig. 5.25 shows the example of the $2\frac{1}{4}$Cr–1 Mo steel.

The generalized normality hypothesis implies linear kinematic hardening (the hardening variable $\boldsymbol{\alpha}$ is identical to the present plastic strain):

$$d\boldsymbol{\varepsilon}^p = d\lambda(\partial f/\partial \boldsymbol{\sigma})$$
$$d\boldsymbol{\alpha} = -d\lambda(\partial f/\partial \mathbf{X}) = d\lambda(\partial f/\partial \boldsymbol{\sigma}) = d\boldsymbol{\varepsilon}^p.$$

It is difficult, even impossible, to introduce a nonlinear relation between $\boldsymbol{\alpha}$ and $\mathbf{X}$; it would lead to a one-to-one nonlinearity that would not correspond to the experimental observations under cyclic loads. (Fig. 5.26(*a*) schematically represents the nonlinearity effect that would

Fig. 5.25. Example of kinematic hardening in case of $2\frac{1}{4}$Cr–1Mo steel (after Moreton *et al.*).

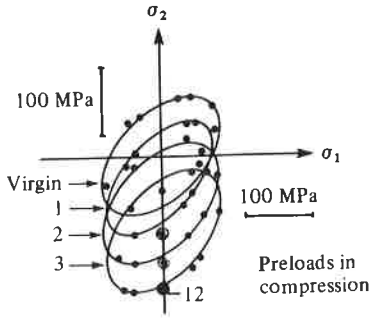

Fig. 5.26. Kinematic hardening: (*a*) nonlinear relation between $\boldsymbol{\alpha}$ and $\mathbf{X}$; (*b*) linear relation between $\boldsymbol{\alpha}$ and $\mathbf{X}$.

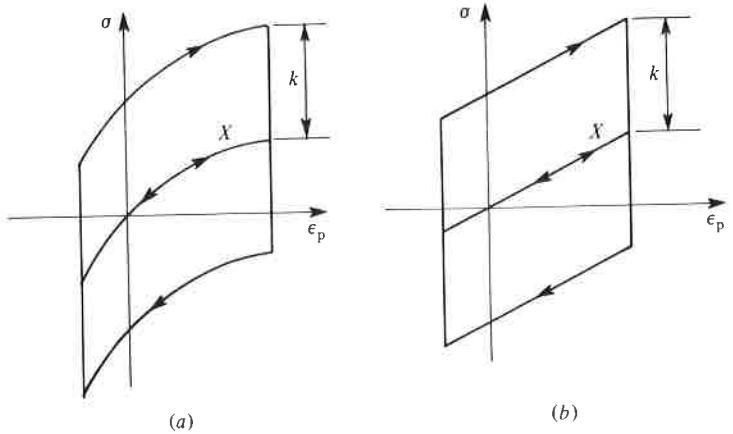

occur, for example, in a tension–compression cycle). We are led therefore to use the specific free energy in a form quadratic in $\boldsymbol{\alpha}$, which gives:

$$\mathbf{X} = \rho(\partial \Psi/\partial \boldsymbol{\alpha}) = C_0 \boldsymbol{\alpha}.$$

Prager's kinematic hardening law is based on this schematic representation:

- $$d\boldsymbol{\varepsilon}^p = d\lambda \frac{\partial f}{\partial \boldsymbol{\sigma}},$$
- $$d\mathbf{X} = C_0 d\boldsymbol{\varepsilon}^p.$$

The consistency condition when plastic flow occurs allows us to write:

$$df = \frac{\partial f}{\partial \boldsymbol{\sigma}} : d\boldsymbol{\sigma} + \frac{\partial f}{\partial \mathbf{X}} : d\mathbf{X} = \frac{\partial f}{\partial \boldsymbol{\sigma}} : d\boldsymbol{\sigma} - C_0 \frac{\partial f}{\partial \boldsymbol{\sigma}} : d\boldsymbol{\varepsilon}^p$$
$$= \frac{\partial f}{\partial \boldsymbol{\sigma}} : d\boldsymbol{\sigma} - C_0 \frac{\partial f}{\partial \boldsymbol{\sigma}} : \frac{\partial f}{\partial \boldsymbol{\sigma}} d\lambda = 0$$

which leads to the following expression for the plastic multiplier

$$d\lambda = \frac{H(f)}{C_0} \frac{\left\langle \frac{\partial f}{\partial \boldsymbol{\sigma}} : d\boldsymbol{\sigma} \right\rangle}{\frac{\partial f}{\partial \boldsymbol{\sigma}} : \frac{\partial f}{\partial \boldsymbol{\sigma}}}.$$

The plastic strain increment is:

$$d\boldsymbol{\varepsilon}^p = \frac{H(f)}{C_0} \frac{\left\langle \frac{\partial f}{\partial \boldsymbol{\sigma}} : d\boldsymbol{\sigma} \right\rangle}{\frac{\partial f}{\partial \boldsymbol{\sigma}} : \frac{\partial f}{\partial \boldsymbol{\sigma}}} \frac{\partial f}{\partial \boldsymbol{\sigma}}.$$

We note that $d\boldsymbol{\varepsilon}^p$ is equal to the projection of the increment $d\boldsymbol{\sigma}/C_0$ on the normal to the loading surface. In fact:

$$d\boldsymbol{\varepsilon}^p : \frac{\partial f}{\partial \boldsymbol{\sigma}} = \frac{1}{C_0} \left\langle \frac{\partial f}{\partial \boldsymbol{\sigma}} : d\boldsymbol{\sigma} \right\rangle.$$

Case of the von Mises criterion

In particular, if the loading surface is described by the von Mises criterion, the function f_Y depends only on the second invariant:

$$J_2(\boldsymbol{\sigma} - \mathbf{X}) = [\tfrac{3}{2}(\boldsymbol{\sigma}' - \mathbf{X}') : (\boldsymbol{\sigma}' - \mathbf{X}')]^{1/2}$$

and then it makes no difference to take f_Y as identical to the above function.

We then have

$$\frac{\partial f}{\partial \boldsymbol{\sigma}} = \frac{3}{2}\frac{\boldsymbol{\sigma}' - \mathbf{X}'}{J_2(\boldsymbol{\sigma} - \mathbf{X})}$$

with its modulus (the usual norm) equal to $\sqrt{\frac{3}{2}}$. The exterior unit normal is then:

$$\mathbf{n} = \sqrt{\frac{3}{2}}\frac{\boldsymbol{\sigma}' - \mathbf{X}'}{J_2(\boldsymbol{\sigma} - \mathbf{X})}.$$

In this particular case, we can express the kinematic hardening law in the form

$$\mathrm{d}\mathbf{X} = \tfrac{2}{3} C\, \mathrm{d}\boldsymbol{\varepsilon}^{\mathrm{p}}.$$

The plastic multiplier becomes

$$\mathrm{d}\lambda = \frac{3H(f)}{2C}\frac{\langle (\boldsymbol{\sigma}' - \mathbf{X}') : \mathrm{d}\boldsymbol{\sigma} \rangle}{J_2(\boldsymbol{\sigma} - \mathbf{X})}$$

and the increment of plastic strain

$$\mathrm{d}\boldsymbol{\varepsilon}^{\mathrm{p}} = \frac{9H(f)}{4C}\left\langle \frac{(\boldsymbol{\sigma}' - \mathbf{X}') : \mathrm{d}\boldsymbol{\sigma}}{J_2(\boldsymbol{\sigma} - \mathbf{X})} \right\rangle \frac{\boldsymbol{\sigma}' - \mathbf{X}'}{J_2(\boldsymbol{\sigma} - \mathbf{X})}.$$

We may replace $J_2(\boldsymbol{\sigma} - \mathbf{X})$ by k in view of the fact that $f = 0$. The complete law can then be written as:

- $f = J_2(\boldsymbol{\sigma} - \mathbf{X}) - k \leqslant 0$
- $\mathrm{d}\boldsymbol{\varepsilon}^{\mathrm{p}} = \dfrac{9H(f)}{4Ck^2}\langle (\sigma' - \mathbf{X}') : \mathrm{d}\boldsymbol{\sigma} \rangle (\boldsymbol{\sigma}' - \mathbf{X}')$
- $\mathrm{d}\mathbf{X} = \tfrac{2}{3} C\, \mathrm{d}\boldsymbol{\varepsilon}^{\mathrm{p}}.$

In index notation, we may write:

$$\mathrm{d}\varepsilon^{\mathrm{p}}_{ij} = \frac{9H(f)}{4Ck^2}\langle (\sigma'_{kl} - X'_{kl})\, \mathrm{d}\sigma_{kl} \rangle (\sigma'_{ij} - X'_{ij}).$$

Identification

Identification is done from simple tension tests. The matrix of plastic strain is written in the usual way while, analogous to the deviatoric stress tensor, the matrix of the deviator of internal stress is written as:

$$[X] = \begin{bmatrix} \frac{2}{3}X & 0 & 0 \\ 0 & -\frac{1}{3}X & 0 \\ 0 & 0 & -\frac{1}{3}X \end{bmatrix}.$$

The criterion and the plastic flow equation can be written in the form:

$$f = |\sigma - X| - k = 0$$
$$\mathrm{d}\varepsilon^{\mathrm{p}}_{11} = \mathrm{d}\varepsilon_{\mathrm{p}} = (1/C)\langle \mathrm{d}\sigma \rangle$$

which allows us to verify that the hardening modulus is constant and equal to C, as could be shown directly from the relation $\mathrm{d}X = C\,\mathrm{d}\varepsilon_{\mathrm{p}}$ which is illustrated in Fig. 5.26(*b*). At each instant, it is evidently possible to write:

$$\sigma = X \pm k = C\varepsilon_{\mathrm{p}} \pm k$$

where the use of + or − depends upon the direction of the plastic flow.

In principle, the determination of the kinematic hardening law of a given material is particularly simple. In practice, the choice of the straight line which best describes the tension curve depends on the field of envisaged applications and therefore on the range of strain to be encountered in the applications (Fig. 5.27). A simple rule, which allows the definition of a law from generally known characteristics of a given material, consists in using the 0.2% yield stress, the fracture stress, and the elongation at fracture:

$$C \approx \frac{\sigma_{\mathrm{u}} - \sigma_{\mathrm{Y}}}{\varepsilon_{\mathrm{u}}}.$$

The linearity of the hardening rule offers the advantage of constructing more stable and less expensive algorithms for the numerical analysis of structures. On the other hand, if in the case of cyclic loads the Bauschinger

Fig. 5.27. Identification of linear kinematic hardening in tension: A316 stainless steel.

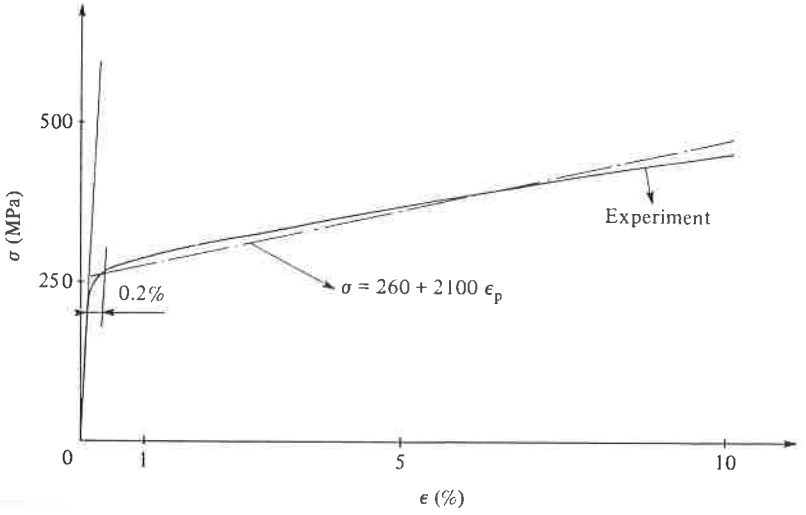

effect is qualitatively represented, ratchetting effects are not described. For any cyclic load there exists a stabilized cycle without progressive deformation as shown schematically in Fig. 5.28 for tension–compression and in Fig. 5.29 for cyclic torsion in the presence of a constant tension. In this latter case as long as the plastic strain ε_{p11} increases, the loading surface undergoes displacement in the σ_{11} direction. The stabilization occurs when $X_{11} = \sigma_{11}$, i.e., when the normal to the surface is directed along σ_{12}.

Fig. 5.28. Immediate accommodation of the linear kinematic model in tension–compression.

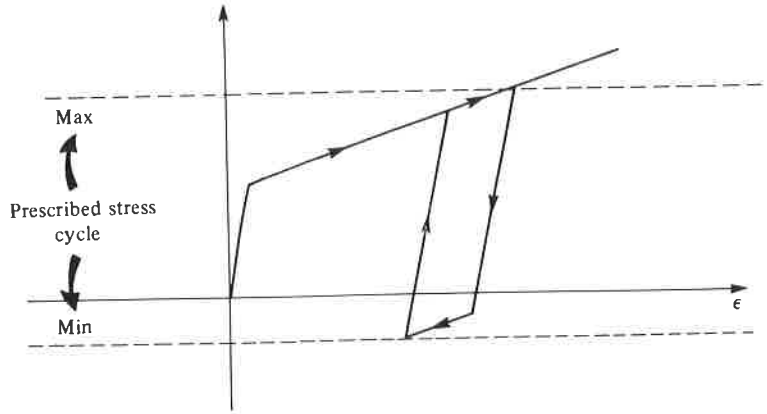

Fig. 5.29. Progressive accommodation of the linear kinematic model in cyclic torsion with constant tension.

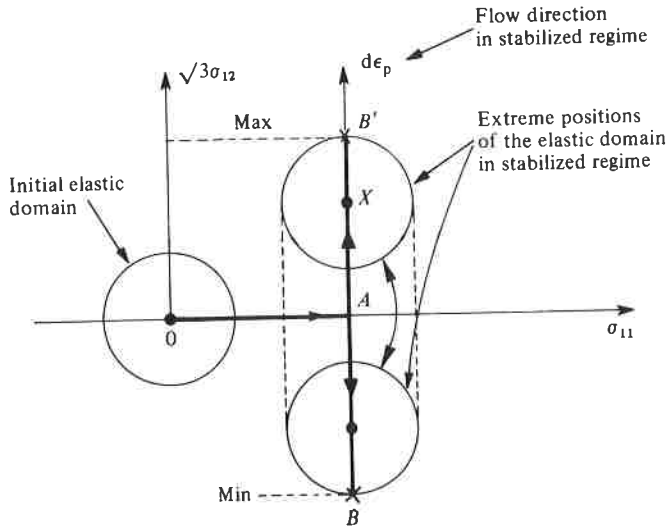

Prager–Ziegler equation and more general formulations

Ziegler's modification of Prager's rule does not come within the framework of the generalized normality hypothesis. It consists in replacing the hardening law by:

$$d\mathbf{X} = (\boldsymbol{\sigma} - \mathbf{X})\, d\mu.$$

The use of the tensor $(\boldsymbol{\sigma} - \mathbf{X})$ instead of its deviator allows us to account for the influence of hydrostatic stress on the evolution of the kinematic internal variable. Under a complex loading, therefore, we obtain flow laws different from that of Prager, but the two formulations are identical in the case of incompressible plasticity. The multiplying factor $d\mu$, determined from the consistency condition $df = 0$, is

$$d\mu = H(f)\frac{\langle (\partial f/\partial \boldsymbol{\sigma}) : d\boldsymbol{\sigma} \rangle}{(\boldsymbol{\sigma} - \mathbf{X}) : (\partial f/\partial \boldsymbol{\sigma})}$$

and the plastic multiplier $d\lambda$ can take any value depending, for example, on the invariants of $\boldsymbol{\sigma}$ or $\mathbf{X}$. This allows the introduction of a nonlinear kinematic hardening by writing for example:

$$d\lambda = \frac{H(f)}{C(\boldsymbol{\sigma})}\frac{\langle (\partial f/\partial \boldsymbol{\sigma}) : d\boldsymbol{\sigma} \rangle}{(\partial f/\partial \boldsymbol{\sigma}) : (\partial f/\partial \boldsymbol{\sigma})}$$

Fig. 5.30. Different types of kinematic hardening.

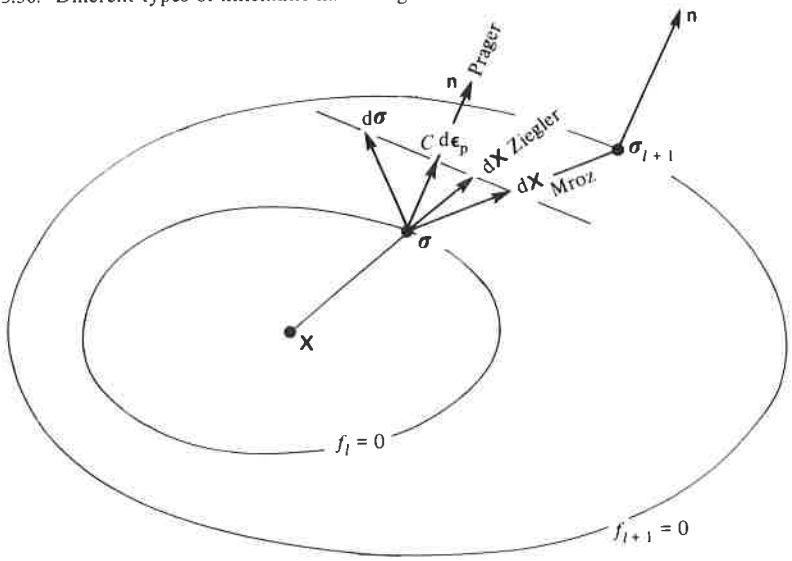

which again expresses the fact that the quantity $C(\boldsymbol{\sigma})\,d\varepsilon^p$ represents the projection of $d\boldsymbol{\sigma}$ on the normal to the loading surface. It is also the projection of $d\mathbf{X}$ on the normal (see Fig. 5.30). The choice of the function $C(\boldsymbol{\sigma})$ which specifies the evolution of the hardening modulus and therefore permits a nonlinear flow, presents some problems and leads to the prediction of abnormal behaviour in certain cyclic loading cases.

Kinematic hardening can also occur in a material which is already anisotropic in the elastic domain. Suppose that this domain is expressed in the form:

$$f = f_Y(\mathbf{C}:\boldsymbol{\sigma}':\boldsymbol{\sigma}') - k = 0.$$

A kinematic hardening in which the principal directions of anisotropy remain preserved, may be defined simply by using:

$$f = f_Y(\mathbf{C}:(\boldsymbol{\sigma}' - \mathbf{X}'):(\boldsymbol{\sigma}' - \mathbf{X}')) - k = 0.$$

The general treatment which we have already employed several times, can be used to determine explicitly the plastic multiplier $d\lambda$ of the flow law expressed by:

$$d\varepsilon^p = f'_Y\mathbf{C}:(\boldsymbol{\sigma}' - \mathbf{X}')\,d\lambda$$
$$d\mathbf{X} = Cf'_Y\mathbf{C}:(\boldsymbol{\sigma}' - \mathbf{X}')\,d\lambda.$$

Such a theory, which leads to more complex considerations, does not, however, allow us to vary the rate of anisotropy development (or the principal axes of anisotropy) as a function of the hardening.

5.4.4 *Flow rules under cyclic or arbitrary loadings*

The combination of isotropic hardening and linear kinematic hardening is quite sufficient for all cases where the load is nearly monotonic and includes the case where stresses vary almost proportionally (quasi-radial loads). However, these simple theories prove inadequate in cases of cyclic loading.

We have seen in Section 5.4.3 that linear kinematic hardening cannot be used to describe ratchetting effects correctly. It also cannot describe the relaxation effect on the average stress. Furthermore, it provides only a basic description of the Bauschinger effect and of hysteresis loops. With regard to isotropic hardening, the only stabilized cycles under prescribed stress to which this can lead are completely adapted without any plastic flow (line CC' on Fig. 5.31). Under prescribed strain, stabilization occurs according to a 'perfectly plastic' cycle (parallelogram $ABA'B'$ in Fig. 5.31).

The combination of linear kinematic hardening and isotropic hardening can be used to represent some cyclic hardening, but it does not eliminate the shortcomings mentioned above. In particular, in stabilized regimes the influence of isotropic hardening must disappear and we must again find a hysteresis cycle with the linear kinematic hardening parallelograms of Figs. 5.26 and 5.28).

The aim of this section is to show different means of improving this combination, by introducing a nonlinearity due to kinematic hardening.

Modelling with updating of characteristic coefficients

These models result directly from uniaxial models generalized by isotropic hardening, i.e., without the introduction of the tensorial variables related to the kinematic hardening. The general idea is to use the points of maximum stress (points of loading–unloading) as particular points of loading: at each point the characteristic coefficients of an isotropic hardening law are updated, e.g., the parameters of the Ramberg–Osgood relation which were discussed in Section 5.2.1:

$$\sigma = \sigma_Y + K_Y\varepsilon_p^{1/M_Y}.$$

Fig. 5.31. Cyclic behaviour with an isotropic hardening model.

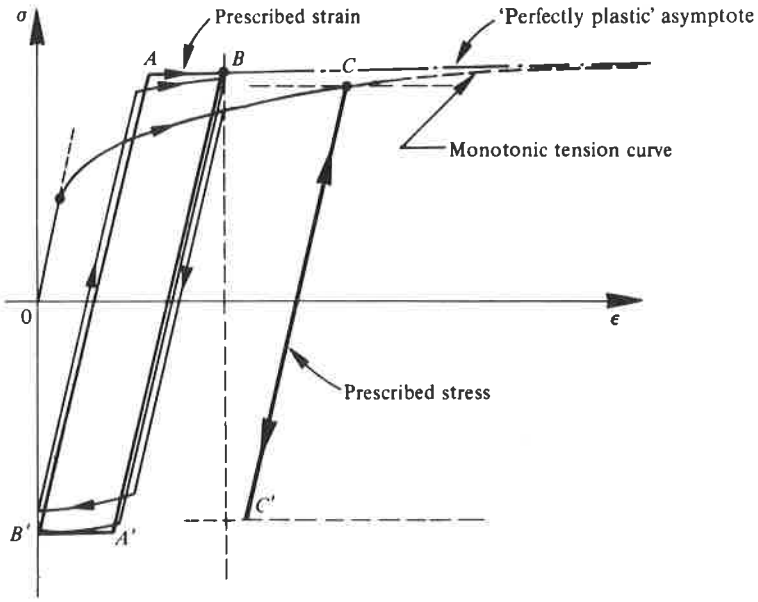

Under tension-compression, for example, with the notation of Fig. 5.32, we write that at the nth cycle (n can take the values $\frac{1}{2}$, 1, $\frac{3}{2}$, ..., k, $(2k+1)/2$, ...):

$$\sigma = \sigma_n + (-1)^{2n+1}(2\sigma_{Yn} + K_n|\varepsilon_p - \varepsilon_{pn}|^{1/M_n})$$

where the characteristic coefficients of the nth cycle (σ_{Yn}, K_n, M_n) depend on the loading history, for example the accumulated plastic strain, and on the state at the beginning of the cycle, i.e., σ_n and ε_{pn}:

$$\sigma_{Yn} = F_Y(p, \sigma_n, \varepsilon_{pn})$$
$$K_n = F_K(p, \sigma_n, \varepsilon_{pn})$$
$$M_n = F_M(p, \sigma_n, \varepsilon_{pn}).$$

We see that this type of model amounts to taking, besides the accumulated plastic strain, particular values of stress or strain states as internal variables. In fact, in this way, discrete memory variables of each stress peak are introduced, and they can actually be incorporated in the thermodynamic formalism with internal variables.

More difficulties occur when arbitrary loads are considered, even in the case of tension–compression. It is thus necessary to keep track of many previous states and to define a rule which governs the closure of each hysteresis loop and ensures that it merges with the preceding loop on return, as shown schematically in Fig. 5.33.

Fig. 5.32. Model of cyclic behaviour with updating of characteristic coefficients.

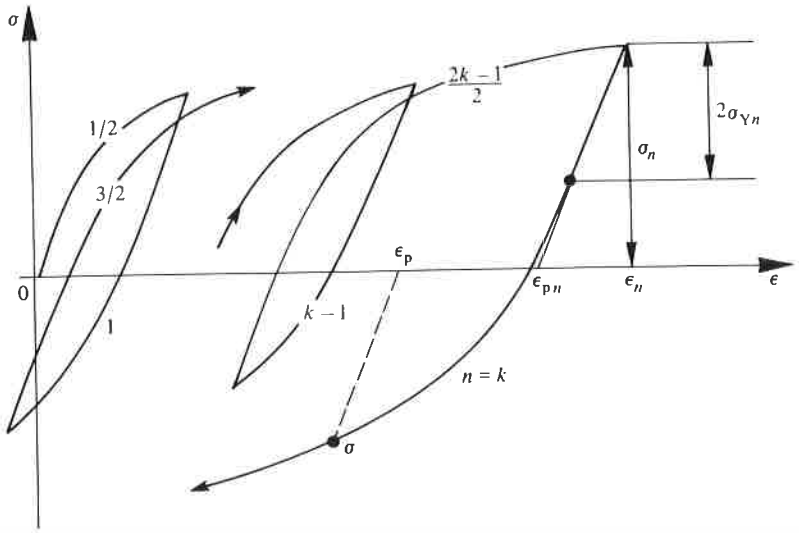

In tension–compression (or in the case of a simple load) this algorithm is quite suitable for computer calculations, but cases of nonproportional loading require much more involved considerations. Moreover, in such a theory, the points of loading–unloading play a crucial role: what would happen if cycles occurred without unloading like the 'spiraling' load shown in Fig. 5.34?

Fig. 5.33. Problem of the 'closure' of the cycle in updating rules.

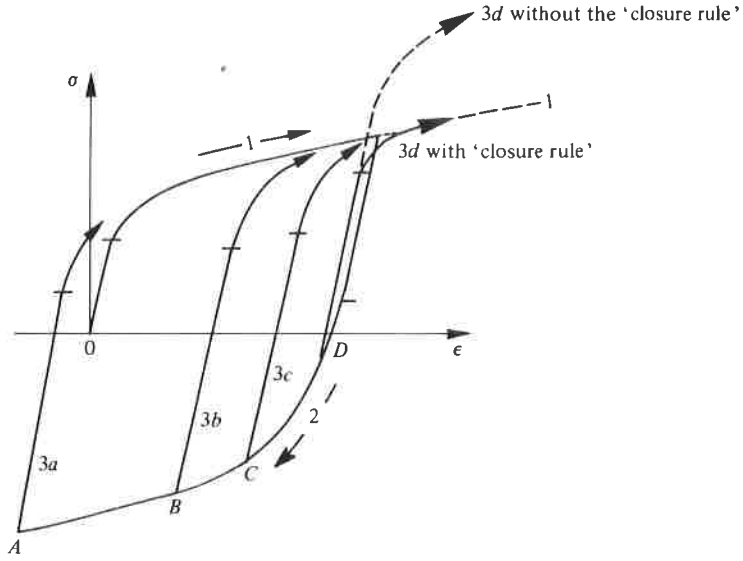

Fig. 5.34. Problem of the definition of a cycle in updating rules.

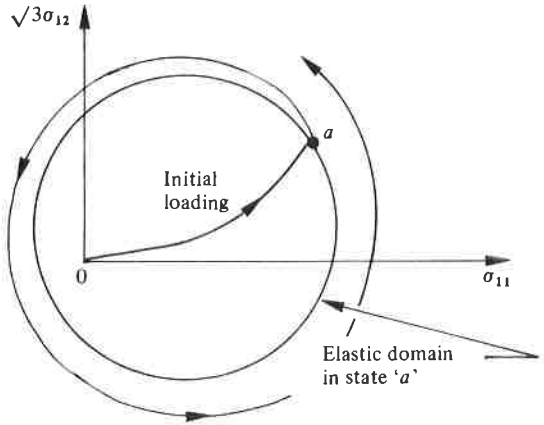

It is, however, to be noted that these concepts have been developed by several authors, including some in the field of viscoplasticity, and that the corresponding models and algorithms have been incorporated in several structural analysis computer codes.

Multilayer models and the Mroz formulation

Kinematic hardening generally corresponds to the internal stresses generated in the polycrystal by the incompatibilities of local plastic deformations from one grain to the next. It is then quite natural to improve Prager's linear hardening model by superposing several elementary models corresponding to several grains: this is the multilayer model. Work has been done on this model for a long time, and has been expanded in different ways. We have seen an example of this approach in relation to generalized St Venant model in Chapter 3: an assembly of perfectly elastoplastic elements with different moduli and yield stresses can be used to represent nonlinear kinematic hardening. Moreover (cf. Fig. 3.30) the concavity of tension and compression curves is correctly represented, as is Masing's approximation corresponding to a homothetic transformation of factor 2 between each hysteresis loop and the monotonic loading curve. Such a model can evidently be generalized by introducing isotropic and (or) linear kinematic hardening for each of the elements.

The Mroz formulation is a generalization of the multilayer model to the multiaxial case. It consists of a certain number of surfaces in the stress space, 'inserted' one into another with (linear) kinematic and (or) isotropic transformations. Denoting by $\mathbf{X}_l$ and R_l the current centre and size of the surface l (see Fig. 5.35), and assuming that it obeys the von Mises criterion, we may write,

$$f_l = J_2(\boldsymbol{\sigma} - \mathbf{X}_l) - R_l = 0.$$

Starting from a stress state located on the elastic domain (the smallest surface) successive flow will occur with each surface. Each surface is associated with a different hardening modulus which allows us to simulate the multilayer model. The last surface encountered (in loading) is the active surface and the flow direction is assumed to be normal to it:

$$\mathrm{d}\boldsymbol{\varepsilon}^{\mathrm{p}} = \mathrm{d}\lambda(\partial f_l/\partial\boldsymbol{\sigma}).$$

There is no flow ($\mathrm{d}\lambda = 0$) when the stress state is within the smallest surface: $f_l < \cdots < f_1 < f_0 < 0$. In what follows we assume that there is

flow with $f_l = 0$. The coherence of the approach requires that the surfaces $f_j = 0$ for $j < l$ 'follow' the applied stress. Thus implicitly:

$$f_0 = f_1 = \cdots = f_{l-1} = f_l = 0.$$
$$\mathrm{d}\boldsymbol{\varepsilon}^{\mathrm{p}} = \mathrm{d}\lambda_0(\partial f_0/\partial\boldsymbol{\sigma}) = \cdots = \mathrm{d}\lambda_l(\partial f_l/\partial\boldsymbol{\sigma}).$$

Fig. 5.35. Behaviour of the Mroz model: (*a*) in tension–compression; (*b*) in a biaxial stress state

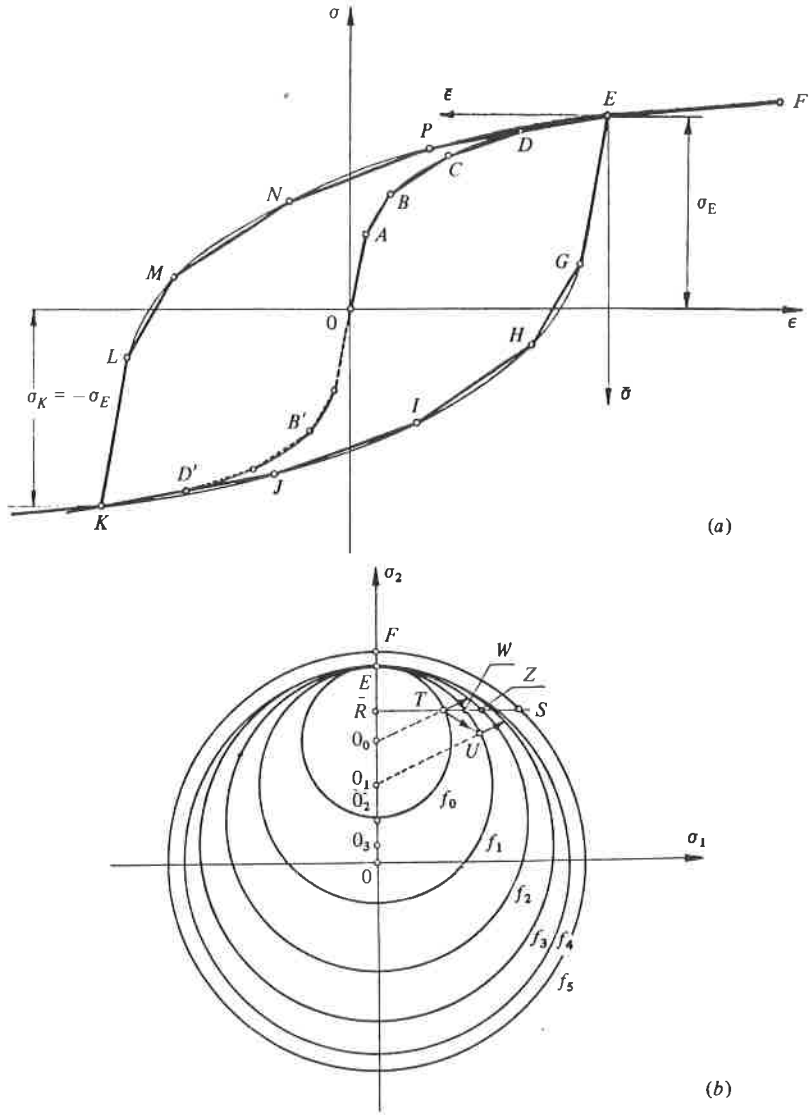

This requires the normals to the different surfaces at the point of applied stress to be identical and the plastic multipliers to be equal: $d\lambda_0 = \cdots = d\lambda_l = d\lambda$. From this it also follows (consistency conditions $df_0 = \cdots = df_l = 0$) that the movements of the centres are identical:

$$d\mathbf{X}_0 = \cdots = d\mathbf{X}_{l-1} = d\mathbf{X}_l.$$

On the other hand, the flow, and therefore the hardening between the current stress state (on surface l) and the next surface $f_{l+1} = 0$ must occur in such a way that the surfaces meet only at the point of applied stress, with identical normals. With this aim, Mroz defined the following rule: kinematic hardening occurs in the direction $\boldsymbol{\sigma}_{l+1} - \boldsymbol{\sigma}$ where $\boldsymbol{\sigma}_{l+1}$ is the stress on the surface $l+1$ such that the outward normal at this point is identical to the outward normal to the surface l at the current stress point $\boldsymbol{\sigma}$. Fig. 5.30 illustrates this hardening hypothesis which can be written in one of the following forms

$$d\mathbf{X}_l = [(R_{l+1} - R_l)\boldsymbol{\sigma} - (R_{l+1}\mathbf{X}_l - R_l\mathbf{X}_{l+1})]\frac{d\mu}{R_l}$$

or

$$\bullet \qquad d\mathbf{X}_l = (\boldsymbol{\sigma}_{l+1} - \boldsymbol{\sigma})\, d\mu.$$

Here $d\mu$ is a multiplier whose value is determined by the consistency condition $df_l = 0$:

$$d\mu = H(f_l)\frac{\langle (\partial f_l/\partial \boldsymbol{\sigma}) : d\boldsymbol{\sigma} \rangle}{\partial f_l/\partial \boldsymbol{\sigma} : (\boldsymbol{\sigma}_{l+1} - \boldsymbol{\sigma})}.$$

The multiplier $d\lambda$ of the flow relation can be an arbitrary function of $\boldsymbol{\sigma}$ or $\mathbf{X}_l$ obeying the relation

$$d\lambda = \frac{H(f_l)}{C_l(\boldsymbol{\sigma})}\frac{\langle (\partial f_l/\partial \boldsymbol{\sigma}) : d\boldsymbol{\sigma} \rangle}{(\partial f_l/\partial \boldsymbol{\sigma}) : (\partial f_l/\partial \boldsymbol{\sigma})}$$

which shows that the quantity $C_l d\boldsymbol{\varepsilon}^p$ is the projection of $d\boldsymbol{\sigma}$ on the normal to the surface $f_l = 0$. As in Ziegler's formulation, the hardening modulus may depend on $\boldsymbol{\sigma}$ or, what amounts to the same, on $\mathbf{X}_l$. However, because of the inconveniences already mentioned, it is preferable to use a constant value.

Nonlinear kinematic hardening rules

In this subsection we will limit ourselves to the use of the von Mises criterion and to one linear function f_Y of the invariant J_2. The generalization to another kind of material does not present any problem from the criterion or the plastic incompressibility point of view.

Formulation

The plasticity criterion is always expressed in the following form:

$$f = J_2(\boldsymbol{\sigma} - \mathbf{X}) - k.$$

The inconvenience of Prager's rule (proportionality between $d\boldsymbol{\varepsilon}^p$ and $\mathbf{X}$) is eliminated by a recall term which introduces a fading memory effect of the strain path

$$\bullet \qquad d\mathbf{X} = \tfrac{2}{3} C\, d\boldsymbol{\varepsilon}^p - \gamma \mathbf{X}\, dp$$

where dp is the increment of the accumulative plastic strain, and C and γ are the characteristic coefficients of the material. We generally assume the tensor $\mathbf{X}$ to be zero in the initial state. The other elements of plasticity theory are not modified. The normality hypothesis and the consistency condition $df = 0$ lead to the expression

$$\bullet \qquad d\boldsymbol{\varepsilon}^p = d\lambda \frac{\partial f}{\partial \boldsymbol{\sigma}} = \frac{H(f)}{h}\left\langle \frac{\partial f}{\partial \boldsymbol{\sigma}} : d\boldsymbol{\sigma} \right\rangle \frac{\partial f}{\partial \boldsymbol{\sigma}}$$

where the hardening modulus h now depends on the kinematic stress:

$$h = \tfrac{2}{3} C \frac{\partial f}{\partial \boldsymbol{\sigma}} : \frac{\partial f}{\partial \boldsymbol{\sigma}} - \gamma \mathbf{X} : \frac{\partial f}{\partial \boldsymbol{\sigma}} \left(\frac{2}{3}\frac{\partial f}{\partial \boldsymbol{\sigma}} : \frac{\partial f}{\partial \boldsymbol{\sigma}} \right)^{1/2}.$$

With the von Mises criterion, we have $d\lambda = dp$ and the hardening modulus becomes

$$\bullet \qquad h = C - \frac{3}{2}\gamma \mathbf{X} : \frac{\boldsymbol{\sigma}' - \mathbf{X}'}{k}.$$

It is clear that when kinematic hardening (represented by $\mathbf{X}$) increases the hardening modulus decreases. This is even more apparent in tension–compression where the hardening modulus is expressed (see the following section) by

$$h = C - \gamma X \operatorname{Sgn}(\sigma - X).$$

In pure tension, for example, this decrease in the hardening modulus induces a concavity of the stress–strain curve directed downwards. In compression the concavity is directed upwards. Thus two drawbacks of Prager's rule are eliminated: the linearity and the one-to-one correspondence between the hardening and the plastic strain (Fig. 5.36). In order

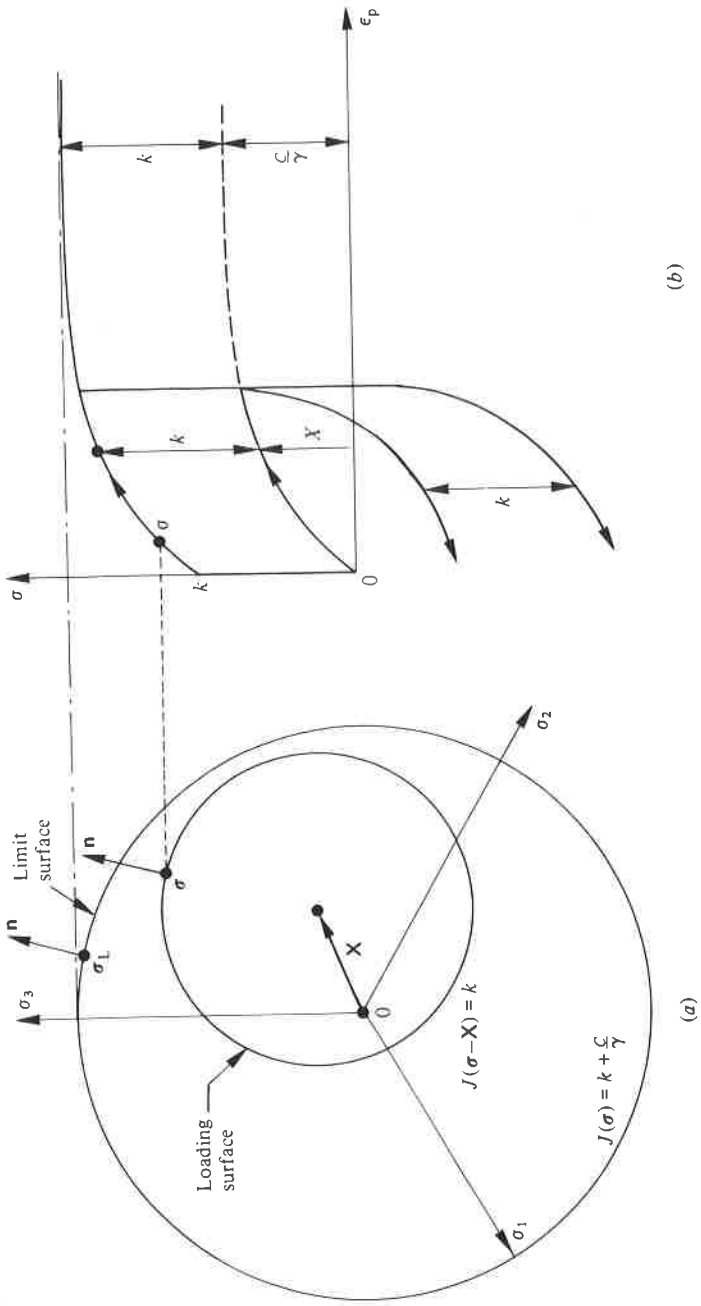

Fig. 5.36. Nonlinear kinematic hardening model: (*a*) three-dimensional, and (*b*) tension–compression.

to incorporate this nonlinear kinematic modelling in the general framework of Section 5.3.3 (generalized normality) it is necessary to abandon the associated plasticity and choose a flow potential F different from the loading surface f. Here we take

$$F = J_2(\boldsymbol{\sigma} - \mathbf{X}) + \frac{3\gamma}{4C}\mathbf{X}:\mathbf{X} - k = f + \frac{3\gamma}{4C}\mathbf{X}:\mathbf{X}.$$

The hypothesis of normal dissipativity then yields (a particular case of a von Mises type material):

$$\mathrm{d}\boldsymbol{\varepsilon}^{\mathrm{p}} = \frac{\partial F}{\partial \boldsymbol{\sigma}}\mathrm{d}\lambda = \frac{3}{2}\frac{\boldsymbol{\sigma}' - \mathbf{X}'}{J_2}\mathrm{d}p$$

$$\mathrm{d}\boldsymbol{\alpha} = -\frac{\partial F}{\partial \boldsymbol{\sigma}}\mathrm{d}\lambda = \mathrm{d}\boldsymbol{\varepsilon}^{\mathrm{p}} - \frac{3}{2}\frac{\gamma}{C}\mathbf{X}\,\mathrm{d}p.$$

By using the same thermodynamic potential as for Prager's rule, we again find:

$$\mathbf{X} = \rho\frac{\partial \Psi}{\partial \boldsymbol{\alpha}} = \tfrac{2}{3}C\boldsymbol{\alpha}$$

$$\mathrm{d}\mathbf{X} = \tfrac{2}{3}C\,\mathrm{d}\boldsymbol{\alpha} = \tfrac{2}{3}C\,\mathrm{d}\boldsymbol{\varepsilon}^{\mathrm{p}} - \gamma\mathbf{X}\,\mathrm{d}p.$$

When there is plastic flow ($f = 0$), the dissipation potential is not zero except when $\mathbf{X} = 0$:

$$F = \frac{3\gamma}{4C}\mathbf{X}:\mathbf{X}.$$

This potential always lies between 0 and $C/2\gamma$ as can easily be verified by calculating the maximum value of the modulus $J_2(\mathbf{X})$ of $\mathbf{X}$ when $\mathrm{d}\mathbf{X} = 0$ with:

$$J_2(\mathbf{X}) = (\tfrac{3}{2}\mathbf{X}':\mathbf{X}')^{1/2} \leqslant C/\gamma.$$

We note that under the initial condition $\mathbf{X}(0) = 0$, the evolution equation of $\mathbf{X}$ implies, because of the plastic incompressibility, that $\mathbf{X}$ is deviatoric: $\mathbf{X}' = \mathbf{X}$.

Tension–compression case

In the case of tension–compression, the tensors are expressed as in the case of linear kinematic hardening (Section 5.4.3). The criterion and the

equations of flow and hardening can be expressed in the form:

- $f = |\sigma - X| - \sigma_Y = 0,$
- $d\varepsilon_p = \frac{1}{h}\left\langle \frac{\sigma - X}{k} d\sigma \right\rangle \frac{\sigma - X}{k} = \frac{d\sigma}{h}$ if $(\sigma - X)\, d\sigma > 0,$
- $dX = C\, d\varepsilon_p - \gamma X |d\varepsilon_p|,$
- $h = C - \gamma X \operatorname{Sgn}(\sigma - X).$

In tension–compression, and more generally, in proportional loading, the evolution equation of hardening can be integrated analytically to give:

$$X = v\frac{C}{\gamma} + \left(X_0 - v\frac{C}{\gamma} \right) \exp\left[-v\gamma(\varepsilon_p - \varepsilon_{p0}) \right]$$

where $v = \pm 1$ according to the direction of flow, and ε_{p0} and X_0 denote the initial values, for example at the beginning of each plastic flow.

It may be remarked that here it is not necessary to use a process of updating the variables: the state (ε_{p0}, X_0) results from the previous flow, with the flow always expressed by the same evolutionary equation. At each moment the stress is given by:

$$\sigma = X + vk$$

as illustrated in Fig. 5.36(*b*).

Properties

One of the first characteristics to be noted is that the nonlinear kinematic model corresponds to a formulation of classical plasticity with two surfaces:

the yield surface coincident with the loading surface;
a limiting surface induced by virtue of the property mentioned above regarding the limit value of the modulus $J_2(\mathbf{X})$ of the kinematic variable $\mathbf{X}$. It is easily verified that this condition implies:

$$J_2(\boldsymbol{\sigma}) = J_2(\boldsymbol{\sigma} - \mathbf{X} + \mathbf{X}) \leqslant J_2(\boldsymbol{\sigma} - \mathbf{X}) + J_2(\mathbf{X}) = k + J_2(\mathbf{X})$$

from which

$$J_2(\boldsymbol{\sigma}) \leqslant k + C/\gamma.$$

This property is illustrated in Fig. 5.36, where the multiaxial situation is represented on the deviatoric stress plane, and the corresponding modelling on the stress–strain diagram. Unlike the theories which postulate *a priori* the existence of this limit surface, the present theory results directly from the choice of a kinematic evolution equation.

A second interesting property of the nonlinear kinematic hardening rule is that it agrees with the basic assumptions of the Mroz formulation. It is a particular two-surface Mroz model, but with a continuously evolving hardening modulus.

Let $\boldsymbol{\sigma}_L$ be the stress state on the limit surface with the same outward normal $\mathbf{n}$ as the direction of plastic flow at the point $\boldsymbol{\sigma}$. In the nonlinear kinematic model, the limit surface does not move. We, therefore, have

$$\frac{\boldsymbol{\sigma}'_L}{k + C/\gamma} = \frac{\boldsymbol{\sigma}' - \mathbf{X}'}{k}.$$

Replacing $d\boldsymbol{\varepsilon}^p$ in the evolution law of $\mathbf{X}$ be obtain:

$$d\mathbf{X} = \left(C\frac{\boldsymbol{\sigma}' - \mathbf{X}'}{k} - \gamma \mathbf{X}' \right) dp.$$

Or, combining the two expressions:

$$d\mathbf{X} = \gamma(\boldsymbol{\sigma}'_L - \boldsymbol{\sigma}')\, dp.$$

This last relation is identical to the Mroz hypothesis (Section 5.4.4) for a criterion of the von Mises type. The essential difference comes from the plastic multiplier which is chosen to be a constant in the Mroz theory. The advantage of the present formulation comes therefore from the fact that, with only two surfaces, it is possible to describe the nonlinearity of the hardening, and to do it in a continuous way.

The existence of a limiting surface can be used to describe the ratchetting effect either in tension–compression (nonsymmetric stress) or in tension–torsion (constant tension and cyclic torsion). Fig. 5.37 shows how these effects manifest themselves. It will be noted that the curve $X(\varepsilon_p)$ is defined to within a translation (ε_p) starting with the value X_0 (the model is insensitive to mean strains). Several consequences follow from this:

with a prescribed stress, the response of the model is stabilized after a single cycle;
the cyclic stabilization is possible only for a symmetrical stress cycle (otherwise ratchetting occurs) (Fig. 5.37(*a*));
the relation between the stress amplitude and the plastic strain amplitude for the stabilized cycle is easily obtained by integrating on two half cycles of tension and compression

$$\frac{\Delta\sigma}{2} = X_{Max} + k = \frac{C}{\gamma} \tan h\left(\gamma \frac{\Delta\varepsilon_p}{2} \right) + k;$$

Fig. 5.37. Ratchetting in (*a*) tension–compression and (*b*) tension–torsion.

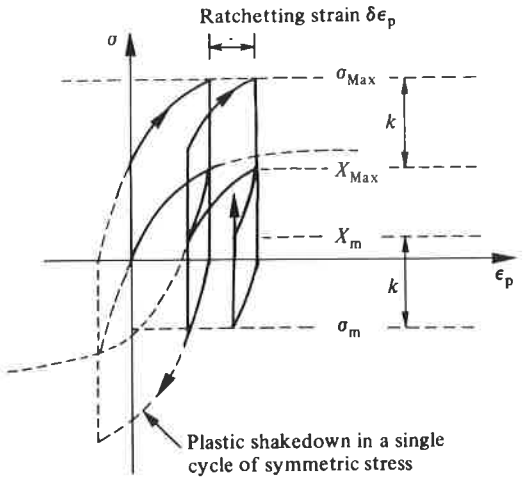

(*a*)

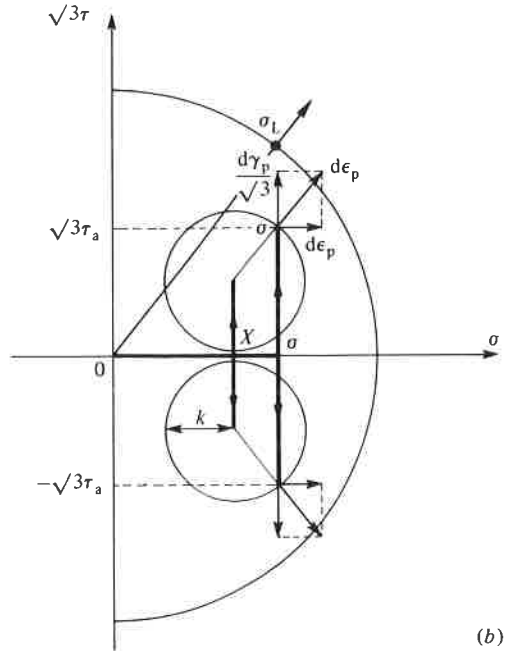

(*b*)

with controlled strain, when the mean strain is not zero, the initial asymmetry of the stresses progressively disappears: this is the mean stress relaxation effect observed in a number of materials (Fig. 5.38). In this case, however, the stabilization is slower than in the case of prescribed stress;

progressive ratchetting strain in tension–compression under prescribed stress occurs as soon as the mean stress is nonzero (and the stress range $\Delta\sigma = \sigma_{Max} - \sigma_{min}$ is more than $2k$). It is easy to show that this progressive strain per cycle is expressed by:

$$\delta\varepsilon_p = \frac{1}{\gamma}\log\left[\frac{\left(\frac{C}{\gamma}\right)^2 - (\sigma_{min}+k)^2}{\left(\frac{C}{\gamma}\right)^2 - (\sigma_{Max}-k)^2}\right]$$

at the maximum prescribed stress; the ratchetting is maximum when $\sigma_{min} = -k$ (see Fig. 5.37(*a*)).

We now reconsider the ratchetting effect in tension–torsion (Fig. 5.37(*b*)) under a constant tension and an alternating torsion of stress amplitude τ_a. Knowing that stabilization implies $dX_{11} = 0$, it can be shown that:

depending on the relative values of σ and τ_a, we will have elastic

Fig. 5.38. Mean stress relaxation

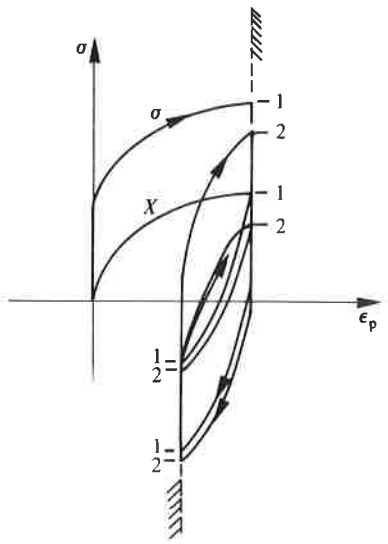

shakedown (no more flow) or ratchetting in the direction of tension (progressive strain) if:

$$\sqrt{3}\tau_a > \frac{k}{k + C/\gamma}\left[\left(k + \frac{C}{\gamma}\right)^2 - \sigma^2\right]^{1/2};$$

the ratchetting strain per cycle is proportional to the amplitude of the shear strain, with the factor of proportionality depending on the tensile stress and the dimension of the limit surface:

$$\delta\varepsilon_p = \frac{4}{\sqrt{3}} \frac{\sigma}{[(k + C/\gamma)^2 - \sigma^2]^{1/2}} \Delta\varepsilon^p_{12}.$$

Identification

The identification of characteristic coefficients k, C, γ of the material is done in tension–compression from the stabilized hysteresis loops which correspond to different strain amplitudes. For this purpose either numerical methods (see Chapter 3) or graphical methods may be used:

(1) determine k approximately from the elastic domain. This yield stress is higher than σ_Y because the initial hardening modulus C is not infinite;

(2) determine C/γ as an asymptotic value of the measure $(\Delta\sigma/2) - k$ as $\Delta\varepsilon$ increases;

(3) determine the coefficient C by fitting the results obtained by using the relation established in the previous section:

$$\frac{\Delta\sigma}{2} - k = \frac{C}{\gamma} \tanh\left(\gamma \frac{\Delta\varepsilon_p}{2}\right).$$

Figures 5.39 and 5.40 show an example of identification performed by means of three stabilized cycles on the INCO 718 alloy at 550 °C. The material is considered as plastic with the loading consisting of a prescribed plastic strain amplitude. Fig. 5.39 can be used to determine k from the experimentally obtained loops. Fig. 5.40 illustrates the determination of coefficients C and γ. The loops obtained from the calculated coefficients ($k = 520$ MPa, $C = 140\,600$ MPa, $\gamma = 380$) are shown in Fig. 5.39.

Cyclic plasticity properties

We list in Table 5.3 the coefficients of the nonlinear kinematic model which describes the material behaviour in stabilized conditions for some materials. The calculated and observed cyclic curves for some materials in Table 5.3 are shown in Fig. 5.41.

Fig. 5.39. Identification of the coefficient k from the experimental loops and verification of the model: INCO 718 alloy, $T = 550$ °C.

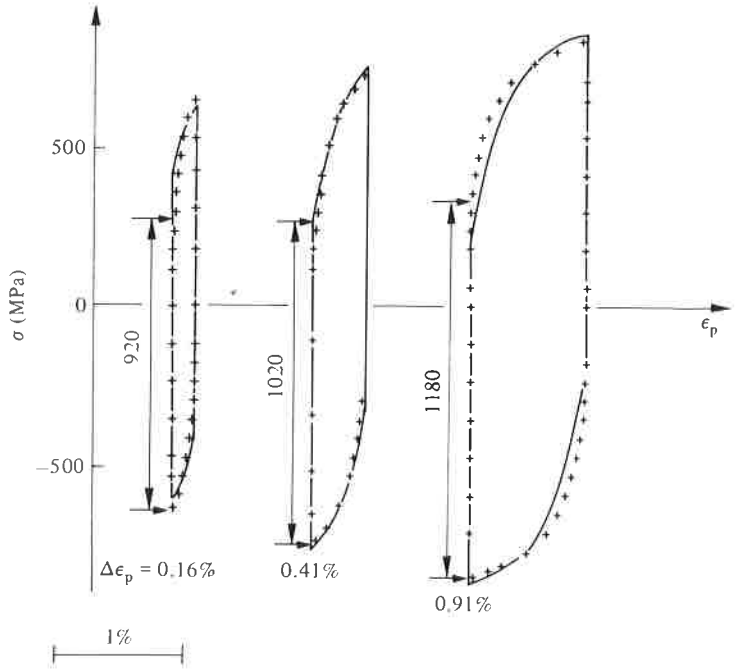

Fig. 5.40. Identification of the coefficients C and γ: INCO 718 alloy, $T = 550$ °C.

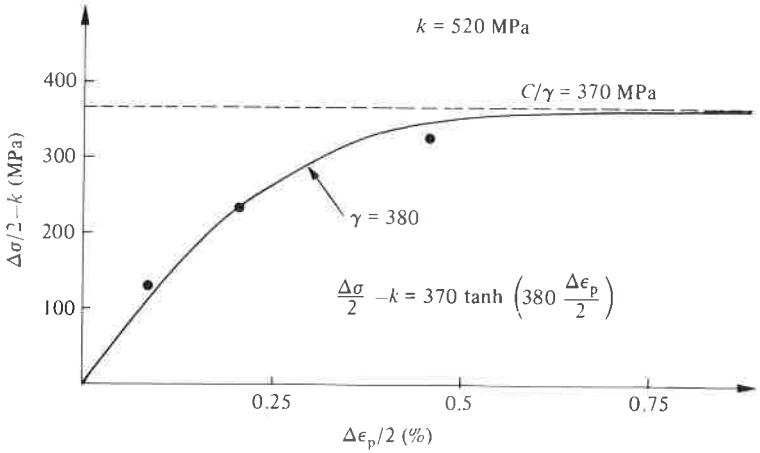

Table 5.3. *Cyclic plasticity properties*

Material	Temperature (°C)	k (MPa)	C (MPa)	γ
316L steel	20	300	30 000	60
INCO 718 alloy	550	520	140 600	380
TA6V titanium alloy	350	310	131 000	570
VO 795 cobalt	20	85	142 000	400
Structural steel	20	225	280 000	1300
NIMONIC 90 alloy	20	505	666 000	1800
TiAl 6 V4 titanium alloy	20	260	560 000	1000
35 NCD 16 nickel–chromium steel	20	980	228 000	300

Combined hardening laws

Superposition of isotropic hardening

Superposition of isotropic hardening on a nonlinear kinematic hardening results in a modification of the elastic domain by translation and uniform expansion. The state variables used in describing the isotropic hardening are the accumulated plastic strain p and the associated thermodynamic

Fig. 5.41. Cyclic curves of some materials and their interpretation by the nonlinear kinematic model.

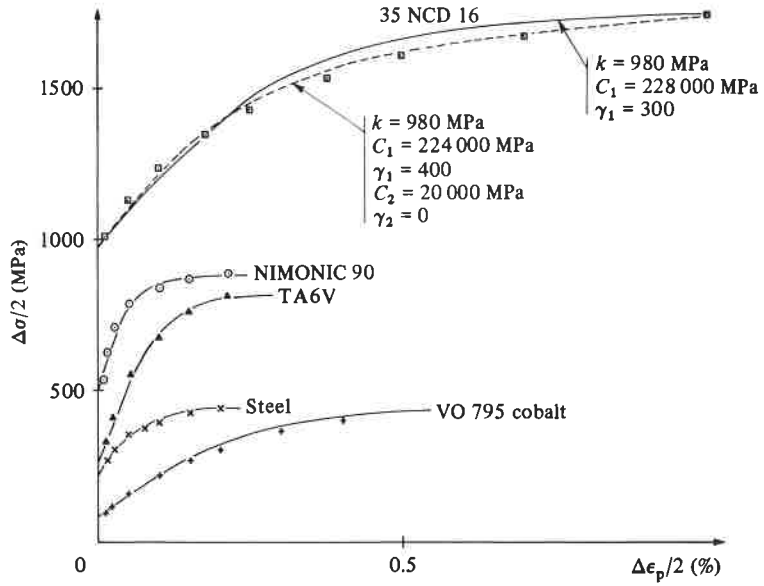

force R which represents the change in the size of the elastic domain (cf. Section 5.4.2). This domain is expressed by:

$$f = J_2(\boldsymbol{\sigma} - \mathbf{X}) - R - k \leqslant 0$$

where k represents the initial elastic limit in tension.

The evolution of R as a function of p represents the progression of hardening: for cyclic effects this evolution is slow and can occur in either an increasing fashion (cyclic hardening) or a decreasing fashion (cyclic softening). In the latter case, the formulation is valid only in the range of strain where the superposition of nonlinear kinematic hardening and isotropic softening results globally in positive hardening during each plastic flow. (Otherwise the formulation must be replaced by that in terms of strains as mentioned in Section 5.4.3).

It may prove advantageous to specialize the evolution of R by means of an equation similar to that employed for kinematic hardening:

$$\mathrm{d}R = b(Q - R)\,\mathrm{d}p$$

where b and Q are two constants. Q is the asymptotic value which corresponds to a regime of stabilized cycles, and b indicates the speed of the stabilization. The initial value of R may be taken as zero or nonzero: $R(0) = R_0$. This evolution law is quite a good representation of the cyclic hardening effects, for example in controlled strain situations. The integration of this relation and the application of the given criterion to each uniaxial cycle gives:

$$\sigma_{\mathrm{Max}} = X_{\mathrm{Max}} + k + Q[1 - \exp(-bp)].$$

Assuming X_{Max} to be a constant and the plastic strain range $\Delta\varepsilon_{\mathrm{p}}$ to be approximately constant, we obtain for the Nth cycle:

$$\frac{\sigma_{\mathrm{Max}} - \sigma_{\mathrm{Max}\,0}}{\sigma_{\mathrm{Max}\,s} - \sigma_{\mathrm{Max}\,0}} = 1 - \exp(-2b\Delta\varepsilon_{\mathrm{p}}N)$$

where $\sigma_{\mathrm{Max}0}$ and $\sigma_{\mathrm{Max}s}$ are respectively the maximum stress in the first cycle and that in the stabilized cycle. Fig. 5.42 effectively shows a very good agreement between this last relation and the experimental results on the 316 steel. (For this material the value of the coefficient Q must, however, be adjusted at each test, as mentioned later.)

Isotropic hardening, considered as a cyclic hardening effect, can also be applied to the kinematic variable by introducing functions of the ac-

Fig. 5.42. Verification of the evolution relation of the isotropic hardening. 316 steel.

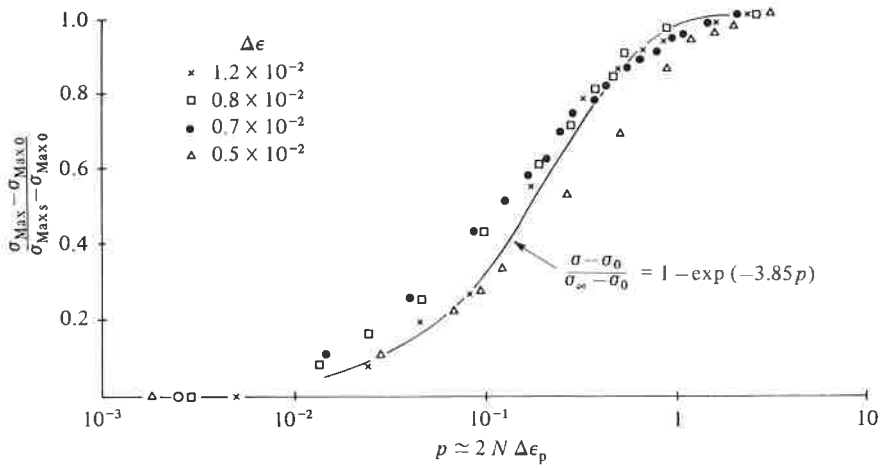

Fig. 5.43. Superposition of isotropic hardening (1) on R, (2) on C, (3) on γ.

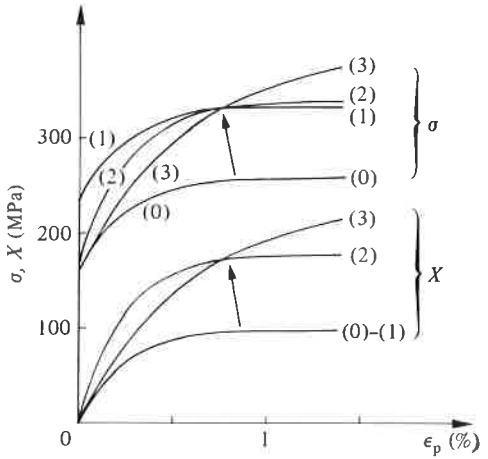

(0) R = 160 MPa, C = 40 000 MPa, γ = 400
(1) R: 160 → 229 MPa
(2) C: 40 000 → 72 000 MPa
(3) γ; 400 → 166

Fig. 5.44. Identification of the first and the stabilized cycles in a strain-controlled test on 316L steel at 20 °C (after Marquis).

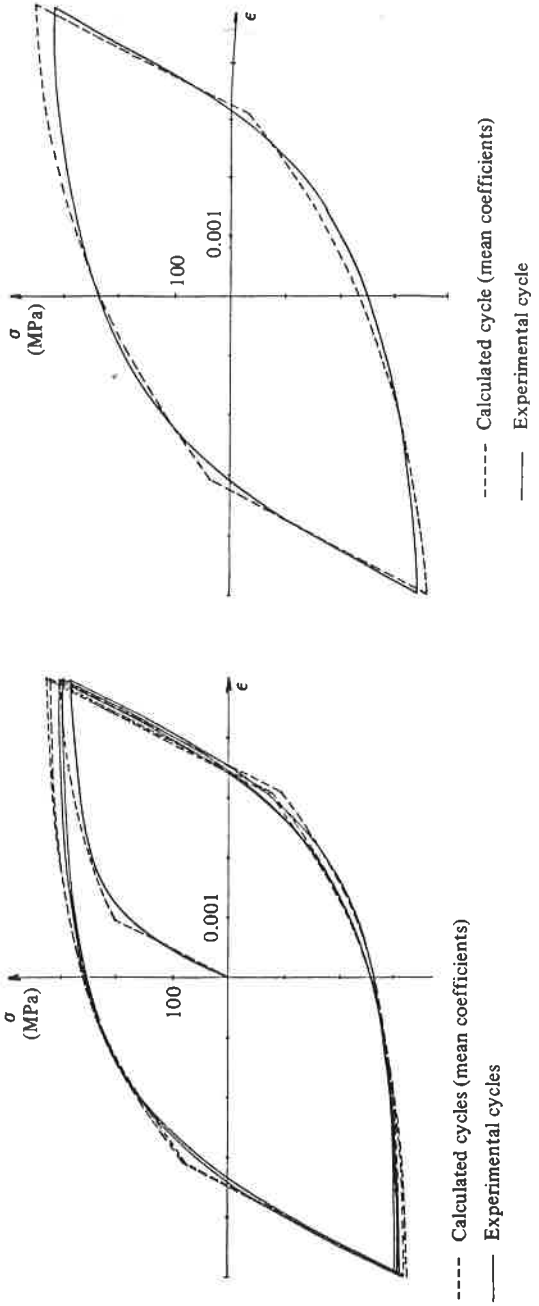

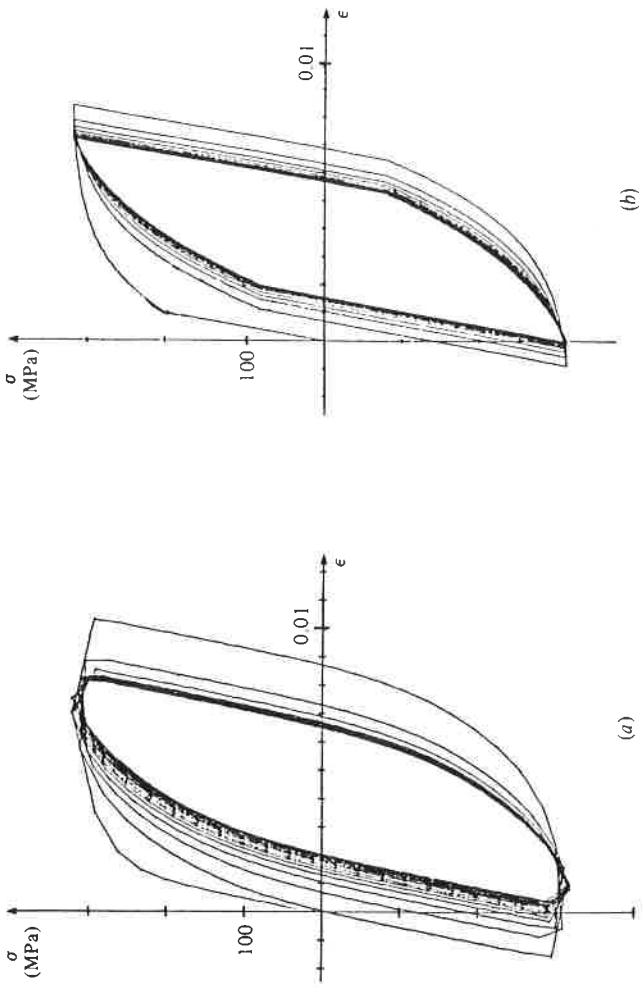

Fig. 5.45. Stress-controlled test (± 300 MPa) on 316L steel at 20 °C; (*a*) test, (*b*) numerical simulation (after Marquis).

cumulated plastic strain, for example

$$d\mathbf{X} = \tfrac{2}{3} C(p)\, d\boldsymbol{\varepsilon}^p - \gamma(p)\mathbf{X}\, dp.$$

Cyclic hardening can be represented by either an increasing function $C(p)$ or a decreasing function $\gamma(p)$. These two variations as well as the case when R is variable, are illustrated in Fig. 5.43 which can be used to judge the modelling differences by the shape of the stress-strain curve. An example of experimental simulation is given in Fig. 5.44 for the 316L stainless steel at room temperature, in the case where C is constant and γ decreases exponentially.

By comparing the first cycle and the stabilized cycle (in a strain controlled test) the effect of cyclic hardening can be observed on both the stress amplitude and the hardening modulus (i.e., the value of $d\sigma/d\varepsilon_p$) at the maximum of the hysteresis loop.

Figure 5.45 shows the comparison for a reversed stress-controlled test. There is no ratchetting effect after the stabilization of the cyclic hardening effect. The same model, with the same values of the coefficients, correctly represents the first cycle, the effect of progressive hardening, and the stabilized cycle.

In summary, the set of equations for a model with combined isotropic and kinematic hardening can be written as follows for a material obeying the von Mises criterion:

- $$d\boldsymbol{\varepsilon}_p = \tfrac{3}{2}\, d\lambda \frac{\boldsymbol{\sigma}' - \mathbf{X}'}{J_2(\boldsymbol{\sigma} - \mathbf{X})},$$
- $$d\mathbf{X} = \tfrac{2}{3} C(p)\, d\boldsymbol{\varepsilon}^p - \gamma(p)\mathbf{X}\, dp,$$
- $$dR = b(Q - R)\, dp,$$
- $$f = J_2(\boldsymbol{\sigma} - \mathbf{X}) - R - k,$$
- $$d\lambda = \frac{1}{h} H(f) \langle \tfrac{3}{2}(\boldsymbol{\sigma}' - \mathbf{X}') : d\boldsymbol{\sigma} / J_2(\boldsymbol{\sigma} - \mathbf{X}) \rangle,$$
- $$h = C - [\tfrac{3}{2}\gamma \mathbf{X} : (\boldsymbol{\sigma}' - \mathbf{X}')/J_2(\boldsymbol{\sigma} - \mathbf{X})] + b(Q - R).$$

Superposition of several kinematic models

Despite the definite improvements provided by the nonlinear kinematic hardening model over the linear one, it furnishes an inadequate description when the range of changes in strain is significant: for very low strains we recover the linear case with a poor representation of the elastoplastic transition; whereas for high strains the limiting value is reached very rapidly. It is easy to remedy such a deficiency by superposing several

analogous models. The criterion is always expressed by $f = J_2(\boldsymbol{\sigma} - \mathbf{X}) - R - k = 0$ with:

$$\mathbf{X} = \sum_l \mathbf{X}_l.$$

Each of the kinematic variables $\mathbf{X}_l$ is independent, and obeys an evolution rule such that:

$$d\mathbf{X}_l = \tfrac{2}{3} C_l \, d\boldsymbol{\varepsilon}^p - \gamma_l \mathbf{X}_l \, dp.$$

The possibility of analytical integration under proportional loading, and the principal properties remain unchanged. Additional degrees of freedom allow us to extend the domain of validity in the manner shown in Fig. 5.46. Three kinematic variables are amply sufficient to remove the deficiencies mentioned above (each one covers a range of strain). If we wish to retain a linear kinematic hardening for large deformations, it is always possible to do so (Fig. 5.46, $\gamma_3 = 0$). One of the examples of Fig. 5.41 has been recalculated with such a model.

Another advantage of this superposition is in relation to describing the ratchetting effect: the basic model leads to a ratchetting effect which is often too significant in comparison with the experimental observations. The superposition of a linear model eliminates this problem at least after a

Fig. 5.46. Superposition of several kinematic models.

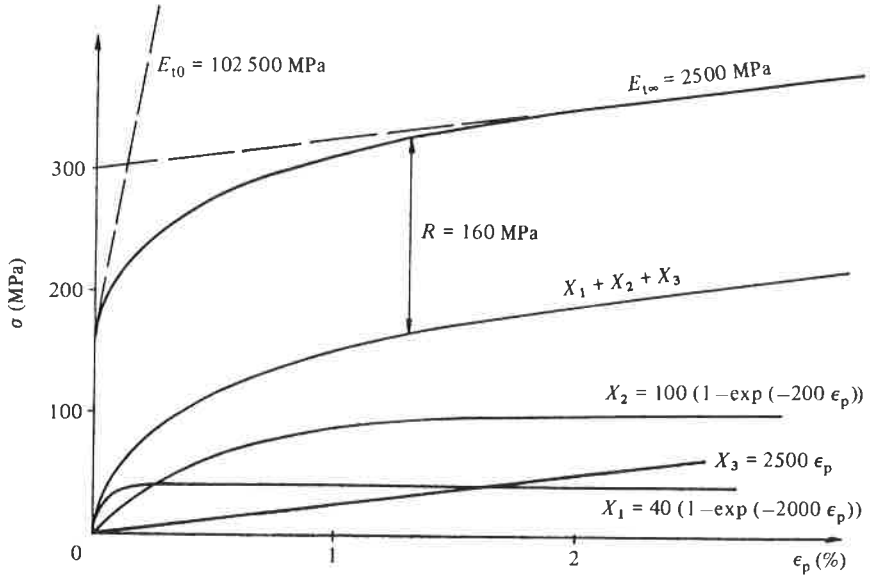

certain number of cycles. The superposition of an almost linear model ($\gamma_l \ll C_l$) leads to a less pronounced ratchetting effect.

Introduction of a hardening memory

The nonlinear kinematic model describes a hardening with fading memory (as a function of accumulated strain). Regardless of the previous history, the stabilized cycle is unique for a given cyclic load. This property is sometimes lacking, for example in some steels. To account for it, it is necessary to introduce an additional state variable (which cannot be the accumulated plastic strain as its influence becomes saturated at the stabilized cycle).

The observation of cycles under sequential loads (e.g., 316L stainless steel in Fig. 5.9) shows that in tension–compression this memory effect may be stored with the maximum plastic strain range. The comparison between the monotonic curve and the cyclic curve (Fig. 5.49) shows that cyclic hardening becomes more and more important as the amplitude of the prescribed strain increases. In other words, the asymptotic value Q of the isotropic variable R which represents the cyclic hardening (see above) is no longer a constant but depends on the strain amplitude.

The additional variable, having a memory of the maximum plastic strains can be introduced with the help of an index surface in the space of plastic strains (Fig. 5.47):

$$F = \tfrac{2}{3} J_2(\boldsymbol{\varepsilon}^p - \boldsymbol{\zeta}) - q = 0.$$

The movement of this enveloping surface of previous strains only occurs when the current state of strain is on the surface ($F = 0$) and that the flow

Fig. 5.47. Index surface defining memory in the space of plastic strains.

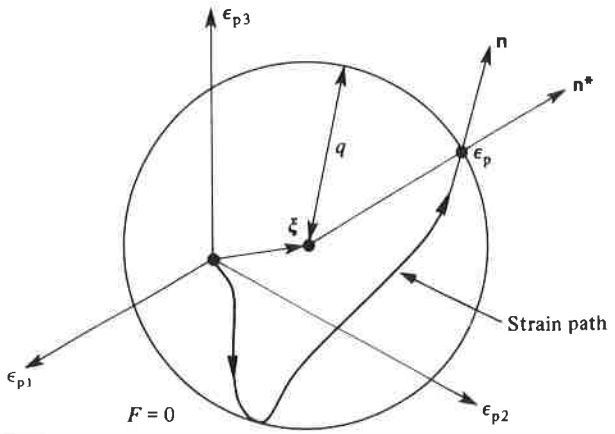

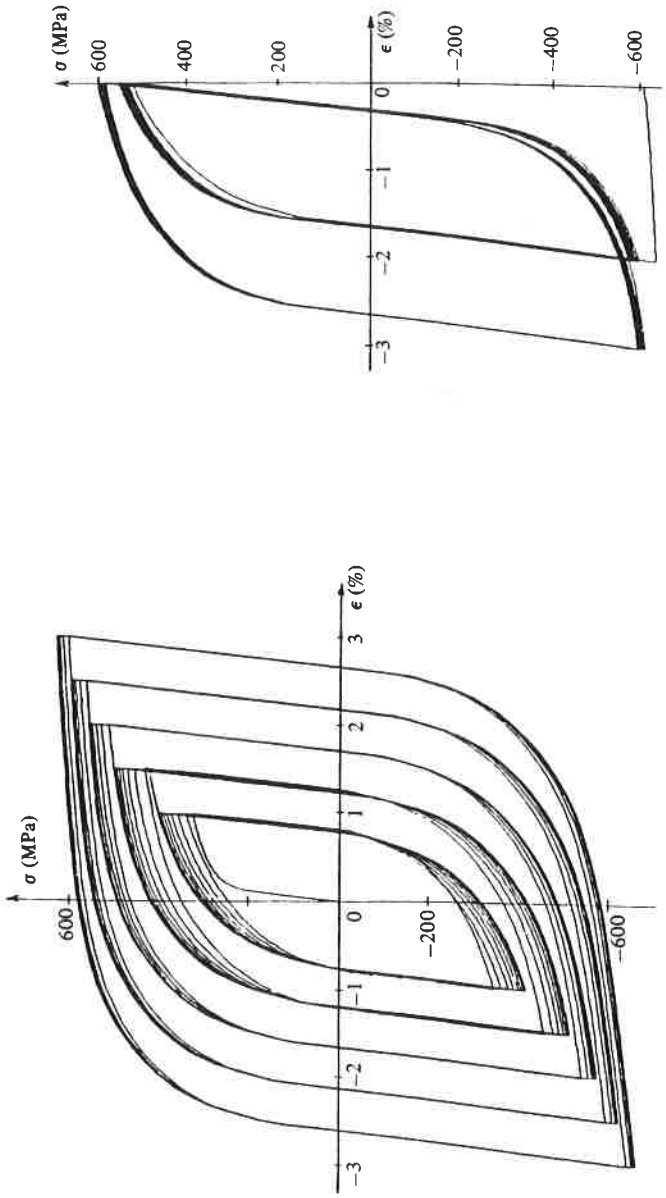

Fig. 5.48. Simulation of the test at (*a*) increasing levels, and then (*b*) decreasing levels, on 316L steel at 20 °C.

occurs in the direction external to the surface. The loading–unloading criterion used is of the same type as for classical plasticity, and the evolution equations are:

$$d\zeta = \tfrac{1}{2}(\mathbf{n}^*:d\boldsymbol{\varepsilon}^p)\mathbf{n}^* H(F)$$
$$dq = \eta\, dp\, H(F)$$

where η is determined by the consistency condition $dF = 0$:

$$\eta = \tfrac{1}{2}\langle \mathbf{n}:\mathbf{n}^* \rangle$$

where $\mathbf{n}$ and $\mathbf{n}^*$ are the unit outward normals, in $\boldsymbol{\sigma}$ and $\boldsymbol{\varepsilon}^p$ respectively, to the loading surface $f = 0$ and the index surface $F = 0$.

The size q of this enveloping surface gives the memory of deformation: in tension–compression, for example, we can easily verify that $q = \frac{1}{2}\Delta\varepsilon_{pMax}$. The choice of the dependence between the asymptotic value Q of isotropic hardening and the variable q enables us to complete the modelling process. For example, it is possible to take:

$$Q = Q_M - (Q_M - Q_0)\exp(-2\mu q)$$

where Q_0, Q_M and μ are three constants.

The superposition of this memory effect may be used to expand the modelling possibilities considerably. In the case of 316L steel, for example, (with a total of 13 coefficients) we can describe correctly:

the progressive hardening (some ten cycles) for each level of the test with increasing strain levels (compare Figs. 5.9 and 5.48);
the residual difference observed for a cycle at a lower level ($\pm 1\%$ and $\pm 1.5\%$) after one at a high level ($\pm 3\%$);
the pronounced difference between the monotonic curve and the cyclic curve (one specimen per level), the difference becoming more pronounced as the prescribed strain increases (Fig. 5.49);
the incremental cyclic tests, which for this material differ greatly depending on the strain amplitudes (Fig. 5.50).

The memory effect introduced in this way is perfect, that is permanent! However, a certain progressive fading can be observed. Thus, we may say that the reality is between the two extreme cases: permanent memory and completely faded memory. A more precise description is possible only at the expense of great complexity, and is of practical interest only for a detailed follow-up of the transient cyclic effects. In structural analysis under cyclic loads, we must often limit ourselves to analysis of the stabilized state. It is

Fig. 5.49. Simulation of monotonic and cyclic curves: 316L steel at 20 °C.

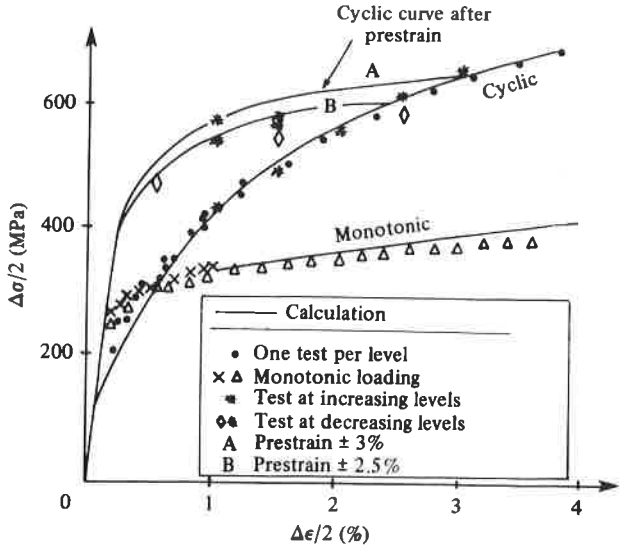

Fig. 5.50. Simulation of cyclic curves obtained by the incremental method.

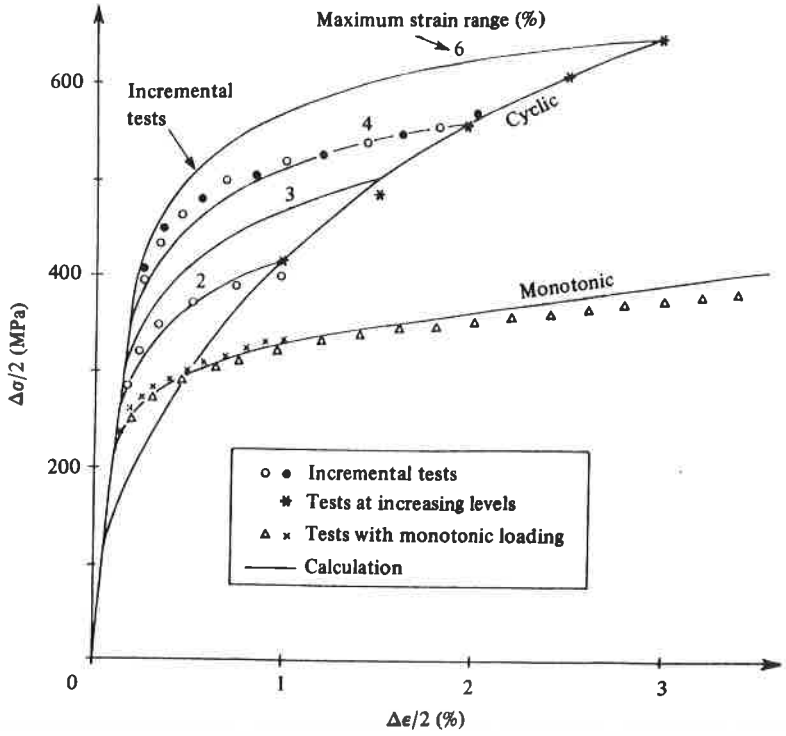

Table 5.4. *Validity of the different models.*

Models	Monotonic hardening	Bauschinger effect	Cyclic hardening or softening	Ratchetting effect	Memory effect
Prandtl–Reuss	x		x		
linear kinematic	x	x			
Mroz	x	x	x		
nonlinear kinematic	x	x		x	
kinematic + isotropic	x	x	x	x	
kinematic + isotropic + memory	x	x	x	x	x

then possible to accelerate the passage from the first cycle to the stabilized cycle by proceeding in two steps:

analysis of the first cycle to obtain an approximation (which is generally sufficient) of the value of the memory q;
saturation of the coefficients at their stabilized value $R = Q = Q(q)$ and analysis of one or more cycles under these conditions (to take into account the effects of stress redistribution).

5.4.5 *Classification of different models*

In order to define roughly the domain of validity of the different models studied, they are listed in Table 5.4 together with the phenomena they take into account.

5.5 Proportional loading

5.5.1 *Definition*

In plasticity, the current deformation of solids depends on the history of the load path. This is represented by the incremental character of the flow law which requires integration for each particular load case. An important exception is the case of proportional (or radial, or simple), loading for which the integration depends only on a scalar and can be done once and for all. These are the Hencky–Mises equations.

A loading is said to be proportional, if at any point M of the solid the stress tensor $\boldsymbol{\sigma}(M, t)$ is proportional to a tensor $\mathbf{S}(M)$, which is independent of time, the proportionality factor being a monotonic function of time $\alpha(t)$ such that $\alpha(0) = 0$:

$$\boldsymbol{\sigma}(M, t) = \alpha(t)\mathbf{S}(M).$$

During the loading the principal directions of stress remain constant.

It is easy to deduce from this that the principal directions of the stress deviator also remain constant.

$$\begin{aligned}\boldsymbol{\sigma}'(M, t) &= \boldsymbol{\sigma} - \tfrac{1}{3}\mathrm{Tr}(\boldsymbol{\sigma})\mathbf{1} \\ &= \alpha(t)[\mathbf{S} - \tfrac{1}{3}\mathrm{Tr}(\mathbf{S})\mathbf{1}] \\ \boldsymbol{\sigma}'(M, t) &= \alpha(t)\mathbf{S}'(M).\end{aligned}$$

The equivalent von Mises stress is written:

$$\sigma_{eq} = J_2(\boldsymbol{\sigma}) = (\tfrac{3}{2}\boldsymbol{\sigma}' : \boldsymbol{\sigma}')^{1/2}.$$

5.5.2 *Integrated Hencky–Mises law. Equivalent stress and strain*

The condition of proportional loading allows formal integration of the Prandtl–Reuss plasticity law by assuming the material to be nonhardened in the initial state: $\boldsymbol{\varepsilon}^p(t = 0) = 0$

$$d\boldsymbol{\varepsilon}^p = \tfrac{3}{2}g'(\sigma_{eq})\frac{d\sigma_{eq}}{\sigma_{eq}}\boldsymbol{\sigma}'$$

$$\boldsymbol{\varepsilon}^p = \int_0^t \tfrac{3}{2}g'(\sigma_{eq})\alpha(t)\mathbf{S}'\frac{d\sigma_{eq}}{\sigma_{eq}}.$$

To integrate with respect to the variable σ_{eq}, we need to express α as a function of σ_{eq}:

$$\alpha = \frac{\sigma_{eq}}{(\tfrac{3}{2}\mathbf{S}' : \mathbf{S}')^{1/2}} = \frac{\sigma_{eq}}{J_2(\mathbf{S})}$$

$$\boldsymbol{\varepsilon}^p = \frac{\mathbf{S}'}{J_2(\mathbf{S})}\int_0^t \tfrac{3}{2}g'(\sigma_{eq})\,d\sigma_{eq}.$$

After integration and multiplication of numerator and denominator by α we obtain the Hencky–Mises relation:

$$\boldsymbol{\varepsilon}^p = \tfrac{3}{2}g(\sigma_{eq})\frac{\boldsymbol{\sigma}'}{\sigma_{eq}}.$$

This relation leads to the concept of equivalent stress and strain, equivalence with respect to the uniaxial case of tension–compression.

The expression for the von Mises criterion:

$$\sigma_{eq} - \sigma_s = 0$$

already shows that any multiaxial state represented by σ_{eq} can be compared to the uniaxial case represented by σ_s. This is why σ_{eq} is called the equivalent stress in the von Mises sense. A similar concept can be defined for strain by expression the Hencky–Mises equation in a scalar form, by calculating the second invariant of the strain tensor:

$$(\tfrac{2}{3}\boldsymbol{\varepsilon}^p : \boldsymbol{\varepsilon}^p)^{1/2} = \frac{3}{2}\frac{g(\sigma_{eq})}{\sigma_{eq}}(\tfrac{2}{3}\boldsymbol{\sigma}' : \boldsymbol{\sigma}')^{1/2} = g(\sigma_{eq}).$$

The quantity $\varepsilon_{eq}^p = (\tfrac{2}{3}\boldsymbol{\varepsilon}^p : \boldsymbol{\varepsilon}^p)^{1/2}$ can be used to express any multiaxial evolution (under proportional loading) in a manner equivalent to the uniaxial hardening law, and is called the equivalent strain in the sense of

von Mises:

- $\varepsilon_{peq} = g(\sigma_{eq})$

with

- $\varepsilon_{peq} = (\frac{2}{3}\boldsymbol{\varepsilon}^p : \boldsymbol{\varepsilon}^p)^{1/2}$ and $\sigma_{eq} = (\frac{3}{2}\boldsymbol{\sigma}' : \boldsymbol{\sigma}')^{1/2}$.

All multiaxial states under proportional loading are represented by a unique graph in the space of equivalent stress and equivalent strain.

5.5.3 *Existence theorem for proportional loading*

Sufficient conditions for the existence of a proportional loading, for a given structure and load, are as follows:

The external forces increase proportionally with a single parameter.
The initial state is an undeformed, nonhardened state.
The material obeys the Prandtl–Reuss law.
The hardening law is expressed in the form of a power function.
Elastic deformations are negligible.

Let a solid $\mathscr{S}$ be loaded by

body forces of density $\vec{f}(M,t)$ per unit volume in $\mathscr{S}$,
surface forces of intensity $\vec{F}(M,t)$ per unit area on the outer surface of $\mathscr{S}$.

We seek conditions under which at any instant the solution of the problem in terms of stress, i.e., $\boldsymbol{\sigma}(M,t)$, can be expressed as a scalar function of the solution $\boldsymbol{\sigma}^*(M,t^*)$ at a particular instant t^*. Thus, supposing $\boldsymbol{\sigma}^*(M,t^*)$ to be known

$$\boldsymbol{\sigma}(M,\, t) = (\alpha(t)/\alpha^*)\boldsymbol{\sigma}^*(M,\, t^*)$$

where $\alpha(t)$ is a scalar function of time such that:

$$\alpha(0) = 0, \qquad \dot{\alpha} \geqslant 0 \qquad \text{and} \qquad \alpha(t^*) = \alpha^*.$$

The equations of static equilibrium and the boundary conditions at the instant t^*

$$\operatorname{div} \boldsymbol{\sigma} + \vec{f} = 0$$
$$\boldsymbol{\sigma} \cdot \vec{n} = \vec{F}$$

will be satisfied, independent of time, if

$$\vec{f} = (\alpha/\alpha^*)\vec{f}^*(t^*) \qquad \vec{F} = (\alpha/\alpha^*)\vec{F}^*(t^*)$$
$$(\alpha/\alpha^*)\operatorname{div}\boldsymbol{\sigma} + (\alpha/\alpha^*)\vec{f}^* = 0$$
$$(\alpha/\alpha^*)\boldsymbol{\sigma}\cdot\vec{n} = (\alpha/\alpha^*)\vec{F}^*.$$

Choosing the Prandtl–Reuss equation, the plasticity relations can be integrated to give the Hencky–Mises relation if:

$$\boldsymbol{\varepsilon}^p(t=0) = 0.$$

Under this condition

$$\boldsymbol{\varepsilon}^p = \frac{3}{2} g\left(\frac{\alpha}{\alpha^*}\sigma^*_{eq}\right)\frac{\boldsymbol{\sigma}^*}{\sigma^*_{eq}}.$$

If g is of the form $g(\sigma_{eq}) = [\sigma_{eq}/K]^M$, then

$$\boldsymbol{\varepsilon}^p = (\alpha/\alpha^*)^M \boldsymbol{\varepsilon}^{p^*}(t^*).$$

The elasticity law shows that

$$\boldsymbol{\varepsilon}^e = (\alpha/\alpha^*)\boldsymbol{\varepsilon}^{e^*}(t^*).$$

The strain–displacement relations have still to be satisfied, but

$$\boldsymbol{\varepsilon}^* = \tfrac{1}{2}[\operatorname{grad}\vec{u}^* + (\operatorname{grad}\vec{u}^*)^T]$$

formally leads to

$$\boldsymbol{\varepsilon} = \boldsymbol{\varepsilon}^e + \boldsymbol{\varepsilon}^p = \tfrac{1}{2}[\operatorname{grad}\vec{u} + (\operatorname{grad}\vec{u})^T]$$

for arbitrary t only if $\boldsymbol{\varepsilon}^e = 0$.

From these equations we obtain the set of conditions stated before the proof. These conditions are rather restrictive, but, in practice, we very often meet conditions of almost proportional (i.e., almost radial) loading.

5.6 Elements of computational methods in plasticity

The aim of this Section is to give only a few indications of how to use the models and plasticity properties in the traditional computational methods described in some of the works cited as references.

5.6.1 *Structural analysis*

Analysis of stress concentration by Neuber's method

This is an approximate technique that can be used to take into account the redistribution of stress caused by plastic flow in a zone of stress concentration, a case often met in practice. The conditions of validity of this method are that the plastic zone must remain sufficiently contained (surrounded by an elastic zone) and that the loading must be radial. The elastic solution of the problem under the action of the external forces is assumed to be known: let $\boldsymbol{\sigma}_E$ be the elastically computed stress at the most stressed point.

Plane stress

For plane structures, of small thickness, we may consider the stress state at the root of a notch to be uniaxial. Neuber's method assumes that the product of the stress and the local strain is independent of the plastic flow. In other words, we write:

$$\sigma\varepsilon = \sigma_E\varepsilon_E = \sigma_E^2/E$$

where σ_E and ε_E are the local stress and strain calculated on the basis of

Fig. 5.51. Application of Neuber's method for a monotonic loading.

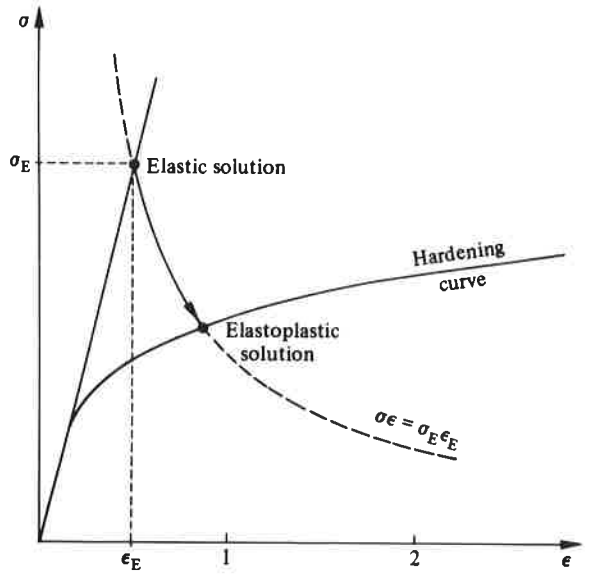

elasticity (E is Young's modulus). We then have a graphical construction (Fig. 5.51) using the hardening curve of the material. The (approximate) local elastoplastic solution is given by the intersection of this curve with the hyperbola corresponding to the elastic solution (σ_E, ε_E).

For cyclic loading, the method can be generalized branch by branch. Since the unloading is elastic, the same construction is repeated from the last loading point (e.g., Fig. 5.52) by writing:

$$\sigma'\varepsilon' = (\sigma - \sigma_0)(\varepsilon - \varepsilon_0) = (\sigma_E - \sigma_{E0})(\varepsilon_E - \varepsilon_{E0}) = (\sigma_E - \sigma_{E0})^2/E$$

and by using a change of axes. This requires knowledge of the constitutive equation for each reversal. We may also use the cyclic curve of the material

Fig. 5.52. Application of Neuber's method to a cyclic loading case.

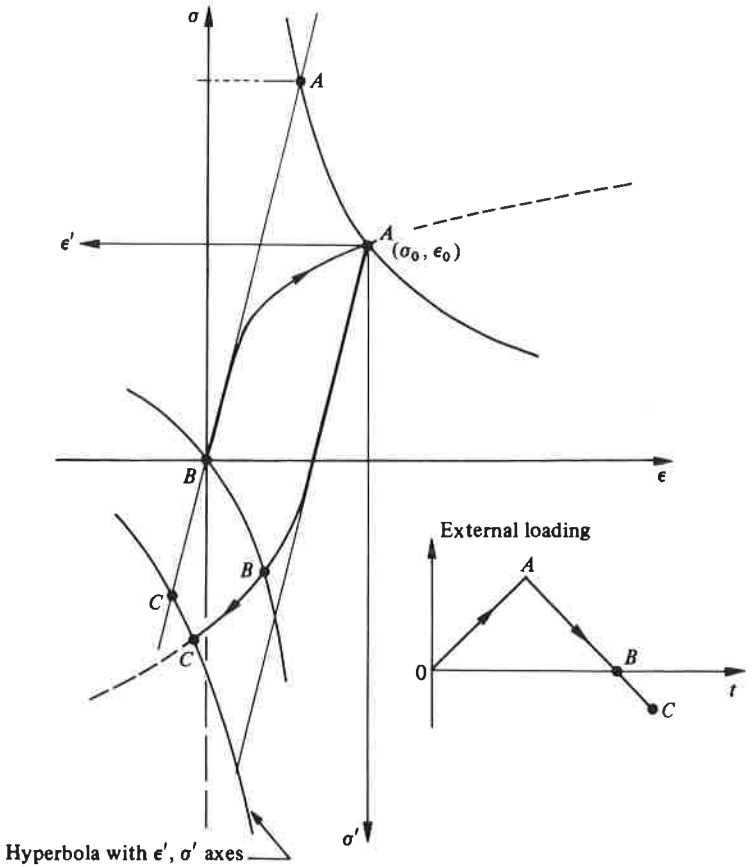

directly and think in terms of amplitudes:

$$\Delta\sigma\Delta\varepsilon = \Delta\sigma_E\Delta\varepsilon_E = (\Delta\sigma_E)^2/E.$$

More general case

When the local stress is not uniaxial, several hypotheses can be proposed to generalize the method. Elementary invariants such as the von Mises equivalent stress and equivalent strain, or the maximum principal stress and maximum principal strain can be used. The most direct generalization, which is satisfactory because it is based on an energy concept, can be written:

$$(\boldsymbol{\sigma} - \boldsymbol{\sigma}_0):(\boldsymbol{\varepsilon} - \boldsymbol{\varepsilon}_0) = (\boldsymbol{\sigma}_E - \boldsymbol{\sigma}_{E0}):(\boldsymbol{\varepsilon}_E - \boldsymbol{\varepsilon}_{E0}).$$

Few results are available that could be used to validate or invalidate one or the other of these generalizations, bearing in mind the fact that these are approximate methods.

Finite element methods in elastoplasticity

In Chapter 4, we outlined the application of the finite element method within the framework of linear elasticity. We will limit ourselves here to showing briefly how this method can be generalized to the case of plasticity by solving in a step-by-step fashion a succession of elasticity problems.

For an elastic material without initial stress, the formulation leads to the linear problem[†]

$$Kq = Q$$

where K is the stiffness matrix of the structure, obtained by assembling the stiffness matrices of each element, q is the column of nodal unknowns, i.e., nodal displacements, and Q is the column of nodal forces equivalent to the external forces.

The initial stress σ_0, assumed known, can be taken into account in the constitutive law, by writing, in the notation of Chapter 4:

$$\sigma = a\varepsilon + \sigma_0.$$

The above system is then transformed into:

$$Kq = Q + Q_0$$

[†] The brackets of matrix symbols have been omitted in this section.

where Q_0 is the column of nodal forces equivalent to the initial stress:

$$Q_0 = -\int_V B^T\sigma_0\,dV.$$

The simplest method of solving an elastoplastic problem incrementally is the method of 'initial strain' in which the existing plastic strain is treated as the initial strain:

$$\sigma = a\varepsilon_e = a\varepsilon - \underbrace{a\varepsilon_p}_{\sigma_0}.$$

The solution for the load F being known, we write the preceding system in incremental form

$$K\Delta q = \Delta Q + \Delta Q_0$$

Fig. 5.53. Iterative integration schemes: (*a*) initial strain method; (*b*) variable stiffness method; (*c*) initial stress method; (*d*) mixed method (variable stiffness + initial stress).

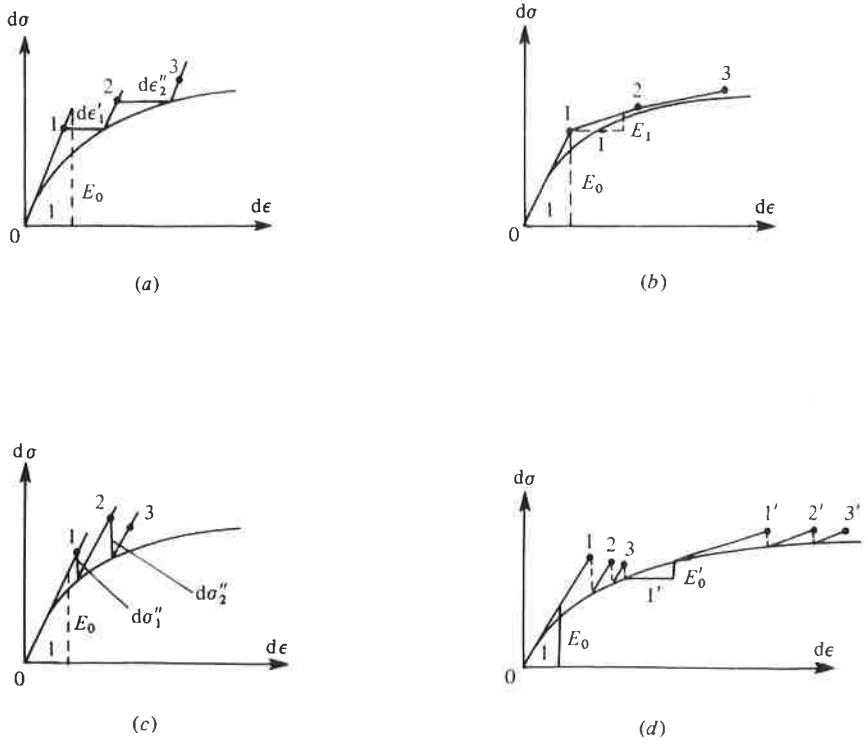

with

$$\Delta Q_0 = \int_{\mathscr{S}} B^T a \Delta\varepsilon_p \, dV.$$

The iterative scheme for progressing from load level F to the following level $F + \Delta F$ is now apparent, and is illustrated in Fig. 5.53(*a*).

(i) Start with $\Delta\varepsilon_p = 0$.
(ii) Solve the linear system to find Δq, $\Delta\sigma$.
(iii) Use the constitutive equation to obtain the new increments $\Delta\varepsilon_p$ in plastic strain. This step may require one or more internal iterations to satisfy the hardening law correctly (requiring intermediate steps).
(iv) Repeat the procedure starting from (ii).

This method converges but sometimes with difficulty, particularly when the hardening moduli are low. We are then led to modify it by varying the stiffness of the structure. The plasticity law can be written in the form:

$$d\varepsilon_p = a_p^{-1} \, d\sigma$$

where a_p denotes the hardening moduli matrix which depends on the current state (and therefore on the unknown qs).

The constitutive equation may be written as

$$d\sigma = a \, d\varepsilon - a \, d\varepsilon_p = a \, d\varepsilon - a \cdot a_p^{-1} \, d\sigma$$

from which it is easy to obtain

$$d\sigma = a_{ep} \, d\varepsilon$$

with

$$a_{ep} = (a^{-1} + a_p^{-1})^{-1}.$$

In fact, the stiffness is not varied at each iteration (see Fig. 5.53(*b*)). We then write

$$d\sigma = a_{ep0} \, d\varepsilon - a_{ep0} \, d\varepsilon^*$$

with

$$d\varepsilon^* = (a_p^{-1} - a_{p0}^{-1}) \, d\sigma^*$$

where $d\sigma^*$ is the value of $d\sigma$ in the preceding iteration.

The 'variable stiffness' method consists in using the following linear system

$$K(q)\Delta q = \Delta Q + \Delta Q^*$$

where $K(q)$ is the tangent stiffness matrix for the load F:

$$K(q) = \int_{\mathscr{S}} B^T a_{ep} B \, dV$$

and ΔQ^* corresponds to the initial stresses induced by the strain increments $d\varepsilon^*$. The stiffness matrix $K(q)$ is constant during iterations in going from F to $F + \Delta F$. The iteration procedure is the same as before. This method performs much better although at the cost of requiring extra computations in the reevaluation and reduction of the stiffness matrix. A number of variants can be developed.

5.6.2 *Limit analysis*

Two limit theorems are given here without proof. They enable us to bound, in the energy sense, the solution of a given plasticity problem by choosing in a class of particular stress and strain fields those that are closest to the solution.

Admissible fields

The particular fields used, called admissible fields, must satisfy a number of conditions.

Admissible stress field

A stress field is an admissible field for a given problem if it is

statically admissible:

the functions $\sigma_{ij}(x_1, x_2, x_3)$ are continuous and piecewise continuously differentiable in the domain under consideration;

they satisfy the static equilibrium equation

$$\operatorname{div} \boldsymbol{\sigma} + \vec{f} = 0;$$

they satisfy the given boundary conditions

$$\boldsymbol{\sigma} \cdot \vec{n} = \vec{F}^d;$$

plastically admissible: the plasticity criterion is satisfied at all points of the domain:

$$f(\boldsymbol{\sigma}) \leqslant 0.$$

Admissible rate of displacement field

A velocity field is an admissible field for a given problem if it is

kinematically admissible:
the functions $v_i(x_1, x_2, x_3)$ are continuous and piecewise continuously differentiable in the domain under consideration;

they satisfy the boundary conditions

$$\vec{v} = \vec{v}^{\,d};$$

plastically admissible: the functions v_i satisfy the condition of incompressibility of total strain:

$$\dot{\boldsymbol{\varepsilon}} = \tfrac{1}{2}[\operatorname{grad}\vec{v} + (\operatorname{grad}\vec{v})^{T}], \quad \operatorname{Tr}(\dot{\boldsymbol{\varepsilon}}) = 0$$

which implies that the elastic deformations are negligible.

Limit theorems

The principle of virtual work, the convexity of the plasticity criterion, and the normality law can be used to prove the following two theorems.

The lower bound theorem

In a class of admissible stress fields for a given problem, the field closest to the solution in the sense of total energy is that which maximizes the functional of the power of external forces.

If $\vec{F}^*$ and $\vec{F}$ are respectively the surface intensities of forces of the admissible field and the real field, where the velocities $\vec{v}^{\,d}$ are the given velocities, then

$$\int_{\partial\mathscr{V}_v} \vec{F}^* \cdot \vec{v}^{\,d}\, dS \leqslant \int_{\partial\mathscr{V}_v} \vec{F} \cdot \vec{v}^{\,d}\, dS.$$

The upper bound theorem

In a class of admissible velocity fields for a given problem, the field closest to the solution in the sense of total energy is the field that minimizes the functional difference between the power of the internal forces and that part of the power of the external forces which corresponds only to the given forces.

With asterisks denoting the admissible field:

$$\int_{\mathscr{V}} \boldsymbol{\sigma} : \dot{\boldsymbol{\varepsilon}}\, dV - \int_{\partial\mathscr{V}_F} \vec{F}^{d} \cdot \vec{v}\, dS \leqslant \int_{\mathscr{V}} \boldsymbol{\sigma}^* \cdot \dot{\boldsymbol{\varepsilon}}^*\, dV - \int_{\partial\mathscr{V}_F} \vec{F}^{d} \cdot \vec{v}^*\, dS$$

where $\boldsymbol{\sigma}^*$ is related to $\dot{\boldsymbol{\varepsilon}}^*$ by the constitutive equation.

These theorems, which are usually used with the assumption of rigid perfectly plastic solids, require the choice of the yield stress value to be made in a manner consistent with the approximation of the theorems:

$\sigma_s = \sigma_Y$ for the lower bound theorem (σ_Y = elastic limit)

$\sigma_s = \sigma_u$ for the upper bound theorem (σ_u = ultimate strength).

5.6.3 *Approximate global method of uniform energy*

In the problems of metal forming (rolling, spinning, forging, die stamping, embossing, etc.) the unknowns are the external forces necessary to transform a given initial geometry into a specified final geometry. These problems may be solved by the methods of limit analysis. From a number of approximate methods (the method of slices, the method of characteristics, etc.) we mention the uniform energy method as the one which is especially easy to use.

Its basis lies in the gross assumption that the energy density or the power of deformation is uniform in the zone of the solid which is undergoing plastic deformations. Under radial load, neglecting elastic strains, and using the concept of equivalent stress and strain, this power density is expressed by:

$$\dot{w} = \boldsymbol{\sigma} : \dot{\boldsymbol{\varepsilon}} = \sigma_{eq}\dot{\varepsilon}_{eq}.$$

By considering the material to be rigid-perfectly plastic with a yield stress σ_s in the deformed zone of volume V_p, the total power of the internal stress is

$$\dot{W} = \sigma_s \dot{\varepsilon}_{eq} V_p.$$

We calculate the 'mean' $\dot{\varepsilon}_{eq}$ according to the final and the initial geometries. This deformation is assumed to have occurred at a constant rate during a time Δt which is expressed as a function of the geometry and of the velocity v at the point of application of the unknown force F. By equating the power of the internal forces to that of the external forces i.e.,

$$\sigma_s \dot{\varepsilon}_{eq} V_p = Fv$$

we can easily determine F.

This method gives results which are either too high or too low, depending on the particular case, but usually too low: the material being characterized by σ_s, it is advisable to take

$$\sigma_s = \sigma_u.$$

Bibliography

Hill R. *The mathematical theory of plasticity.* The Clarendon Press, Oxford (1950–71).
Kachanov L. M. *Foundations of the theory of plasticity.* North-Holland Publication Company, Amsterdam (1971).
Argon A. S. *Constitutive equations in plasticity.* M.I.T. Press, Cambridge, Mass. (1975).
Mandel J. *Plasticité et viscoplasticité.* Cours C.I.S.M. Udine. Springer-Verlag, Berlin (1971).
Prager W. *Problèmes de plasticité théorique.* Dunod, Paris (1958).
Zyckowski M. *Combined loading in the theory of plasticity.* Polish Scientific Publishers, Varsovie (1981).
Salençon *Calcul à la rupture et analyse limite.* Presses de l'ENPC, Paris (1983).
Hult J. & Lemaitre J. *Physical non-linearities in structural analysis.* I.U.T.A.M. Symposium Springer-Verlag, Berlin (1981).
Sawczuk A. & Bianchi G. *Plasticity today.* (Conf. C.I.S.M. Udine). Elsevier Applied Sciences Publisher (1985).
Baque P., Felder E., Hyafil J. & Descatha. *Mise en forme des métaux.* Dunod, Paris (1973).
CNRS. *Mise en forme des métaux et alliages.* Edition du C.N.R.S., Paris (1976).
Szczepinski W. *Introduction to the mechanics of plastic forming of metals.* Sijthoff and Noordhoff, Groningen (1979).

6

VISCOPLASTICITY

Tout solide est un fluide qui s'ignore.

With this Chapter, we come to problems related to the temporal growth of permanent deformations, i.e., to the study of the perfectly viscoplastic, perfectly elastic viscoplastic, and hardening elastoviscoplastic solids, described schematically in Chapter 3.

The important dates in the development of the mathematical modelling of viscoplasticity are:

1910, with the representation of primary creep by Andrade's law;
1929, with Norton's law which links the rate of secondary creep to the stress;
1934, with Odqvist's generalization of Norton's law to the multiaxial case.

The first IUTAM Symposium 'Creep in Structures' organized by Hoff took place in 1960. It became the starting point of a great development in viscoplasticity with the works of Hoff, Rabotnov, Perzyna, Hult and Lemaitre for the isotropic hardening laws, and those of Kratochvil, Malinin and Khadjinsky, Ponter and Leckie, and Chaboche for the kinematic hardening laws.

These works are now realizing their full potential in view of the possibilities offered by modern computers for analysing structures subjected to high temperature creep. Some of the basic principles of these methods are given at the end of this Chapter, which is essentially devoted to the formulation and identification of constitutive laws.

The formalism used is that of the thermodynamics of irreversible processes, guided by the phenomenological aspects described at the beginning of the chapter. Particular multiaxial constitutive laws are presented in detail in terms of modelling, identification and particular material